Utilisation des modèles NTCP et de carcinogenèse pour les choix balistiques et de particules en hadronthérapie de l'adulte et de l'enfant

Yasid Boudam

UNIVERSITE GRENOBLE I – JOSEPH FOURIER

ECOLE DOCTORALE
Ingénierie pour la Santé, la Cognition et l'Environnement

Doctorat

Physique Radiologique et Médicale

Yasid BENHACENE BOUDAM

Utilisation des modèles NTCP et de carcinogenèse pour les choix balistiques et de particules en hadronthérapie de l'adulte et de l'enfant

Thèse dirigée par le Pr Jacques BALOSSO

Soutenue le 21 novembre 2008 à Grenoble

Jury :

Georges NOËL, PUPH HDR	**Président**
Olivier CASELLES, HDR	**Rapporteur**
Christian CARRIE, MD HDR	**Rapporteur**
Jean-Louis HABRAND, PUPH HDR	**Examinateur**
Régis FERRAND, Ing DR	**Examinateur**
Jacques BALOSSO, PUPH HDR	**Directeur de thèse**

Remerciements

A toute ma famille je dédie ce travail, de tout cœur merci de votre soutien.

Je remercie aussi le Pr Jacques Balosso de son soutien et sans qui rien n'aurait été possible. Merci de toute son aide et de ses conseils avisés (qui furent bien nombreux).

Merci à toute l'équipe du CPO (qui devint par la suite ICPO). Merci enfin à l'équipe du GSI – Darmstadt pour l'accueil et l'ambiance instructive que j'y ai trouvée.

Chapitre liminaire des résumés anglais et français

<u>Résumé en français</u> :

Certains problèmes scientifiques et techniques, imparfaitement résolus dans la mise en œuvre des traitements par ions légers ont été étudiés. La thèse développe successivement les trois approches suivantes :

1) La première partie de cette thèse travaille sur la définition de l'équipement (faisceaux fixes *versus* gantry) pour un centre de traitement et ainsi traiter la plus large variété possible de tumeurs pour un spectre élargi de situations cliniques caractéristiques chez l'adulte. Les tumeurs étudiées sont des tumeurs de la base du crâne, du rachis cervical haut, bronchiques, ganglionnaires thoraciques, ganglionnaires abdominales et de la prostate, l'on obtient ainsi un éventail assez large d'indications thérapeutiques.
2) La seconde partie met à contribution une partie des outils développés dans la première phase (traitement chez l'adulte). Le même design de salle de traitement est utilisé mais pour un ensemble de tumeurs intracrâniennes de la base du crâne et de la sphère ORL chez l'enfant et l'adulte jeune.
   Il peut être conclu que l'étude de multiples situations anatomo-pathologiques en thérapie protons n'a pas permis de dégager d'incidences bialistiques originales et particulières à la gantry.
3) La dernière phase donne lieu à l'étude des caractéristiques physiques propres aux faisceaux d'ions carbone. Une comparaison est menée sur la base de simulations de données par l'utilisation de modèles de calcul du risque d'induction néoplasique après traitement chez l'adulte et plus spécifiquement chez l'enfant. La simulation semble indiquer que les ions carbone induiraient un phénomène de stérilisation cellulaire à doses *intermédiaires* & *hautes* dans les tissus & organes chez l'adulte et l'enfant.

- **<u>Titre anglais</u> :**

Dosimetric evaluation of the usefulness of different beam line equipments in term of deterministic and stochastic effects for particle therapy for adults and children.

- **<u>Résumé en anglais</u> :**

The question of the protontherapy is seen through a purely dosimetric aspect. The main question is to know if the multiplication of beam incidences thanks to a gantry allows obtaining an increase of the therapeutic benefit for the patient. These results suggest that a facility equipped with at least three fixed incidences of beam (horizontal, vertical from above and oblique around 50°) could probably treat properly most of the tumor locations.The second part focus on the pediatric cases in protontherapy. The protons as effective inducer of deterministic and stochastic effects in the pediatric tissues are gauged in the discussion. A

thorough investigation on the limits and the possibilities offered by the protons for children is proposed. The third part introduces the study of the carbon-ions treatment. Their carcinogenic action is evaluated and compared against the photons, with consideration to the pediatric tissues and organs. The goal is to estimate by simulation if the carbon-ions bring a therapeutic advantage against the photon or proton treatments. The set of complex interactions within the tissues and organs are precisely explained and a simplified approach is brought. In conclusion, the set of complex radiobiological effects acting within tissues to induce different dose-responses of neoplasic risk can have contradictory actions. The *standard* and the *repopulation* models provide a comprehensive insight in spite of their purely theoretical aspect. They reveal some encouraging possibilities for the treatment of children by carbon-ions, especially when the choice of hypofractionation will be possible.

– **Mots clés en français :**

Radiothérapie, protons, ions carbone, hadronthérapie, gantry, probabilité de complication, inter-comparaison de plans de traitement, risque déterministe, risque stochastique, onco-pédiatrie, effet carcinogène, tumeur secondaire radio-induite.

– **Mots clés en anglais :**

Radiotherapy, protons, carbon-ions, hadrontherapy, gantry, complication probability, treatment plan inter-comparison, deterministic risk, stochastic risk, onco-paediatry, carcinogenic effect, second malignant neoplasia.

– **Intitulé et l'adresse de l'unité où la thèse a été préparée :**

Service de Cancérologie-Radiothérapie
Hôpital Albert MICHALLON
CHU de Grenoble
BP 217
F-38043 Grenoble Cedex 09

Table des Matières

Organisation du mémoire

Le mémoire est structuré suivant trois grands chapitres associés à trois articles scientifiques originaux qui sont introduits par des pages liminaires. Publications scientifiques *ad hoc*, ces chapitres répondent à un souci d'exposé clair, synthétique, facilement exploitable dont l'œil du lecteur reconnaît facilement (par habitude) les codes usuels. A noter que les articles sont en cours de soumission pour publication (le choix de la langue est donc l'anglais).

A cela s'ajoute les pages liminaires qui résument succinctement ces articles pour orienter et accompagner plus facilement le lecteur. Adjonctions introductives, elles ouvrent le sujet et parlent de certains aspects peu (ou non) développés dans le chapitre d'étude et apportent nos observations et suggestions personnelles.

I - Introduction

I – 1. Une collaboration du programme ETOILE et du Centre de Protonthérapie d'Orsay – Institut Curie

Le Projet ETOILE se développe depuis 1997 (l'autorisation ministérielle est venue par la suite en février 2007) pour mettre en place à Lyon un centre de traitement par faisceaux d'ions légers (protons et ions carbone) [1]. Ce centre d'*hadronthérapie* mettra en œuvre le traitement par irradiation de cancers radiorésistants pour les patients français et sud européens. ETOILE se développe dans un réseau de centres similaires en élaboration en Europe : le centre allemand HIT de *Heidelberg* (Baden-Württemberg) [2] est en cours de démarrage de traitement, celui de l'Italie CNAO à Pavie [3] est en cours de finition, et bien d'autres projets se développent en parallèle (des centres sont à venir à *Munich* où un centre de protonthérapie privé est en attente d'ouverture ; *Essen* le WPE en cours d'achèvement (Rhénanie du Nord Westphalie) ; *Marburg* en construction (Hesse) ; *Kiel* contrat signé (Schleswig-Holstein) et *Wiener Neustadt* appel d'offre en cours (Autriche) …).

En France, les responsables des centres d'hadronthérapie actuels et futurs – Orsay, Nice et Lyon – ont décidé de coopérer, en particulier en matière de projet médical et de développement de recherches. L'optimisation des modalités de traitement et des outils technologiques dont la gantry (bras isocentrique), prévue, au moins à terme, dans l'équipement d'ETOILE, est notamment un sujet de coopération qui intéresse concrètement l'ensemble des centres de traitement. L'Institut Curie, responsable du Centre de Protonthérapie d'Orsay, supervise son extension et sa modernisation en s'équipant d'une gantry proton (bras isocentrique rotatif). L'une de ses questions a alors été de demander l'exposé clair d'un choix de protocoles balistiques *vs* l'équipement (gantry ou non) pour une liste détaillée de pathologies tumorales pour différentes localisations anatomiques (intracrânienne, thoracique, abdominale, pelvienne) chez l'adulte et l'enfant (*cf* résultats des tableaux 1 & 2 de la partie *II - pages liminaires du premier & second article*).

Fruit de cette collaboration, la présente investigation a bénéficié des moyens de planification utilisés en protonthérapie à l'ICPO, de même que l'usage des données et des compétences cliniques dans la préparation des traitements. Certains problèmes scientifiques et techniques, imparfaitement résolus dans la mise en œuvre des traitements par ions légers, ont pu ainsi être étudiés : à savoir,

- identifier les situations anatomo-cliniques dont le traitement serait significativement amélioré par la disponibilité d'une gantry ;
- définir des protocoles balistiques et dosimétriques standardisés, prenant notamment en compte les différents niveaux d'équipements des centres (faisceaux fixes – horizontal, vertical, oblique ; gantry) ;
- établir une typologie de ces situations par la définition d'outils objectifs et de bases quantitatives indispensables à toute prise de décision concernant un choix balistique, dosimétrique et d'équipement ;
- évaluer l'impact à long terme de ces traitements chez les patients particulièrement jeunes qui pourraient être amenés à les recevoir (tumeurs pédiatriques, sarcomes de l'adulte jeune, …).

Ce faisant, la thèse développe successivement les trois approches suivantes :

1) l'étude dans le cadre des protons d'un spectre élargi de situations cliniques caractéristiques chez l'adulte. Il s'agit à terme d'aboutir à un protocole précis d'utilisation des incidences selon le volume anatomique à traiter et la position qui peut être donnée au patient. Il sera finalement proposé un choix d'utilisation des incidences et des positions pour chaque type de situation clinique. Cette phase a été réalisée à l'ICPO.
2) Cette seconde partie met à contribution une partie des outils développés dans la première phase (traitement chez l'adulte) et en introduit d'autres pour développer de nouvelles approches balistiques soumises cette fois-ci aux contraintes spécifiques du traitement pédiatrique. Il s'agit notamment d'évaluer l'impact en terme de risque stochastique de tumeurs radio-induites selon les choix balistiques propres à chaque salle de traitement. Toute une discussion sera alors développée et il sera proposé là encore une table d'utilisation des incidences et positions de traitement chez l'enfant, de même qu'une discussion sur les avantages et limites d'un traitement par protons.
3) Cette dernière phase donne lieu à l'étude des caractéristiques physiques propres aux faisceaux d'ions carbone. Elle a été permise par la coopération avec l'équipe du GSI (*Gesellschaft für Schwerionenforschung mbH*) de Darmstadt en Allemagne. Dans le contexte de la planification des traitements par ions carbone, les données radiobiologiques de radiosensibilité intrinsèque et mutationnelle propre au faisceau de carbone permettent par simulation d'évaluer le risque de carcinogénèse et de le comparer à celui du rayonnement photon. Une attention particulière est portée ici au cas de l'enfant et de l'adulte jeune.

Les travaux objets de cette thèse ont tout d'abord été amorcés dans le Centre de Protonthérapie d'Orsay. Un apprentissage de base a été acquis au sein de l'équipe de l'ICPO sur les stations de travail de logiciels ISIS et ISOGRAY produits par DOSIsoft Corp. (DOSIsoft SA, 45/47 av. Carnot – F-94230 Cachan, France). Le travail sur ces consoles et logiciels de plan de traitement a permis le développement des deux premières phases de la thèse. La dernière phase s'est faite en Allemagne à Darmstadt au GSI, spécialisé dans la recherche et le traitement de tumeurs intracrâniennes et sarcomes prostatiques par ions carbone.

Il convient maintenant d'introduire et de décrire succinctement le fonctionnement du centre français de protonthérapie (l'ICPO). Les caractéristiques physiques et radiobiologiques des protons y seront mentionnées, de même qu'une description des caractéristiques des ions carbone en dernière partie d'*introduction.*

I – 2. Historique et présentation du Centre de Protonthérapie d'Orsay

1954 : Sur l'initiative d'Irène Joliot-Curie, la Faculté des Sciences de Paris commande pour l'université Paris-Sud un accélérateur de particules, le synchrocyclotron. Cet accélérateur commandé à la société Philips (Pays-Bas) est utilisé pour la recherche fondamentale en physique nucléaire et physique des particules.

1977 : Le synchrocyclotron est complètement rénové par l'Institut de Physique Nucléaire d'Orsay (IN2P3/CNRS). Son énergie, initialement de 156 MeV, est alors portée à 201 MeV, ce qui permet d'élargir les champs d'action et de recherche. A la fin des années 1980 cette installation est dépassée sur le plan scientifique.

1987 : Le démantèlement de l'installation est prévue par l'IN2P3 mais le Dr Jean Marc Lhoste alors directeur de la section de recherche biologique de l'Institut Curie en propose la médicalisation (communication personnelle du Dr Jacques Balosso). Premières expérimentations sur le faisceau dans l'optique d'utiliser le rayonnement à des fins médicales.

1989 : Fin des recherches en physique nucléaire et des particules.

1991 : Création du Centre de Protonthérapie d'Orsay (CPO) ; le synchrocyclotron est utilisé à des fins exclusivement médicales dans le cadre d'un syndicat inter hospitalier rassemblant l'Institut Curie (Paris), l'Institut Gustave Roussy (IGR Villejuif), le Centre René Huguenin (Saint Cloud) et les Hôpitaux de l'Assistance Publique de Paris (AP-HP) qui a acquis le centre pour un franc symbolique.

1991 : Premier traitement ophtalmologique au CPO

1994 : Premier traitement intracrânien au CPO

2003 : Avec plus de 3000 patients traités, le CPO s'inscrit au troisième rang mondial des centres de protonthérapie et au premier rang européen (aux côtés du PSI – Suisse).

2004 : Rattachement du CPO à l'Institut Curie (d'où l'acronyme *ICPO*).

Le personnel

Le centre est une structure réunissant une vingtaine de personnes de compétences diverses. L'équipe médicale et paramédicale conjugue les compétences de médecins, de physiciens, de dosimétristes et de manipulateurs en électroradiologie. A cela s'ajoutent les techniciens chargés de la surveillance et de la maintenance de l'accélérateur, ainsi que de la fabrication d'accessoires (collimateurs, compensateurs) indispensables à la réalisation des traitements.

I – 3. La protonthérapie

I - 3.1. Le synchrocyclotron d'Orsay

Du nom éponyme de synchro(ne) et cyclotron, le synchrocyclotron est un accélérateur circulaire. La source de protons, un plasma d'hydrogène, se situe au centre de la chambre d'accélération. Les protons tirés du plasma sont accélérés par un champ électrique dont la fréquence se synchronise avec la fréquence d'accélération de la particule ; il s'agit en effet de compenser la variation relativiste de la masse du proton accéléré. Parallèlement, elles sont soumises à un champ magnétique qui permet de courber la trajectoire et de les faire (re)passer dans la zone accélératrice (à travers le champ électrique). L'énergie atteinte en fin d'accélération est de 201 millions d'électronvolts (201 MeV), les protons sont alors dirigés vers les deux salles de traitement existantes (design du centre d'Orsay de la période 2006 - 2007). Le faisceau d'énergie maximale de 201 MeV est utilisé dans la salle de traitement des tumeurs intracrâniennes. Le second faisceau est dégradé à 73 MeV pour la salle de traitement des tumeurs oculaires.

I - 3.2. Avantages balistiques des protons

La Protonthérapie est une radiothérapie de haute précision, dite *millimétrique*. Son profil de dose inversé et sa faible diffusion latérale en font un outil de prédilection pour le traitement des cancers par rayonnement ionisant, en particulier chez l'enfant et l'adulte jeune. La courbe de dépôt de dose en profondeur des protons (courbe bleue, figure 1) montre comment le faisceau cède la majeure partie de son énergie en fin de parcours pour s'arrêter brusquement (Pic de Bragg). Cette très faible diffusion distale des protons est à comparer au profil de dose des photons (courbe orange, figure 1) et prouve définitivement la supériorité balistique des protons par rapport aux techniques conventionnelles d'irradiation photon. On peut voir en particulier la différence de dose atteinte à l'entrée (dose à la peau) à l'avantage des protons pour une dose identique photons *vs* protons en milieu de plateau de modulation du pic de Bragg (acronyme anglais *SOBP* pour *Spread Out Bragg Peak*).

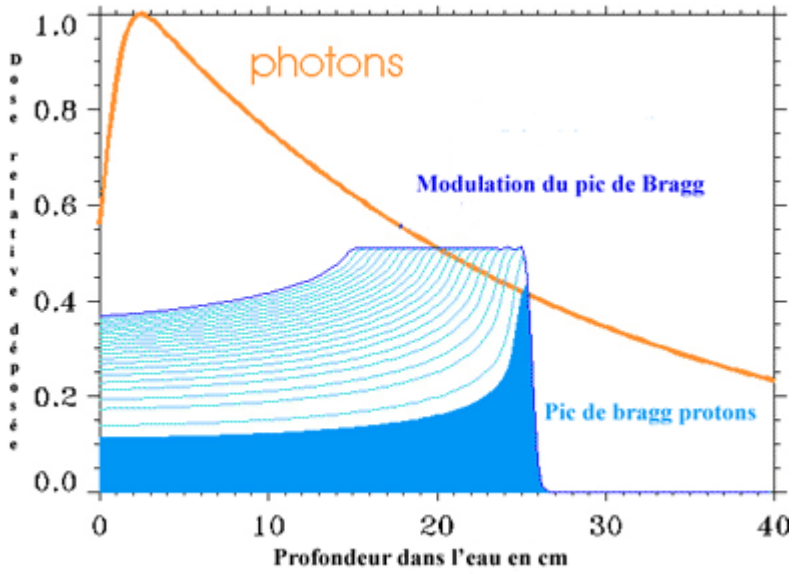

Figure 1 : courbes de rendement en profondeur d'un faisceau de photons (d'environ 10 MeV d'énergie maximale) et protons (d'énergie voisine de 200 MeV pour le pic le plus profond)

Ce plateau de modulation est obtenu par *modulation* de l'énergie du faisceau, *énergie* et *longueur du parcours moyen de la trajectoire* étant deux paramètres liés. Les protons de 200 MeV parcourent ainsi 26 cm dans l'eau avant de s'arrêter alors que les protons 60 MeV parcourent 3 cm d'eau [4]. La modulation de l'énergie est obtenue par l'utilisation d'une roue rotative en aluminium constituée de segments d'épaisseur variable (voir figure 2) que le faisceau traverse (parmi d'autres éléments encore) en sortie du synchrocyclotron.

Un inconvénient majeur de la protonthérapie est sa mise en œuvre par une technologie lourde et sophistiquée, ce qui naturellement ne facilite pas sa diffusion. Elle inclut en effet un accélérateur de particules particulièrement complexe et onéreux tel qu'un synchrocyclotron, une enceinte de radioprotection, des systèmes de conformation du faisceau et de positionnement, et surtout un personnel technique hautement qualifié, etc.

I - 3.3 Déroulement du traitement intracrânien

I – 3.3.1. La dosimétrie

La balistique d'irradiation est définie lors de la dosimétrie prévisionnelle. Elle est réalisée par les dosimétristes sous la supervision des radiothérapeutes et radiophysiciens. Grâce à une modélisation informatique, ils établissent le meilleur plan de traitement et s'attachent à délivrer notamment, selon un protocole d'irradiation strict, 95% de la dose de prescription de référence à au moins 95% du volume tumoral (Clinical Target Volume) tout en limitant au minimum les doses aux organes à risque environnants.

Les caractéristiques balistiques des protons permettent de réaliser des escalades de doses pour la tumeur. La précision atteinte permet aussi de protéger relativement les structures critiques avoisinantes et de réduire les volumes d'isodose aux tissus sains irradiés, le but étant de diminuer d'autant les risques de complications à court, moyen et long terme. Ceci apporte un avantage décisif à la protonthérapie en termes de traitement de tumeurs radiorésistantes telles les chordomes et chondrosarcomes.

I – 3.3.2. Mise en forme du faisceau d'irradiation

Une fois les plans de traitement établis sur ordinateur, il s'agit de conformer réellement le faisceau à la tumeur tel que voulu par les plans de calcul et de le projeter à la bonne profondeur à travers les structures anatomiques. La protonthérapie met en œuvre une irradiation conformationnelle avec précision millimétrique. Pour cela, il est placé sur la trajectoire du faisceau proton différents éléments (voir figure 2), à savoir : i) un ***absorbeur*** (ou filtre binaire) pour adapter la profondeur de pénétration du faisceau ; ii) un ***modulateur*** pour étaler le dépôt d'énergie et pouvoir traiter toute la tumeur dans son épaisseur ; iii) un ***collimateur*** pour conformer dans le plan orthogonal à l'axe du faisceau la forme de dépôt d'énergie; iv) un ***compensateur*** pour modifier la conformation de la dose en profondeur.

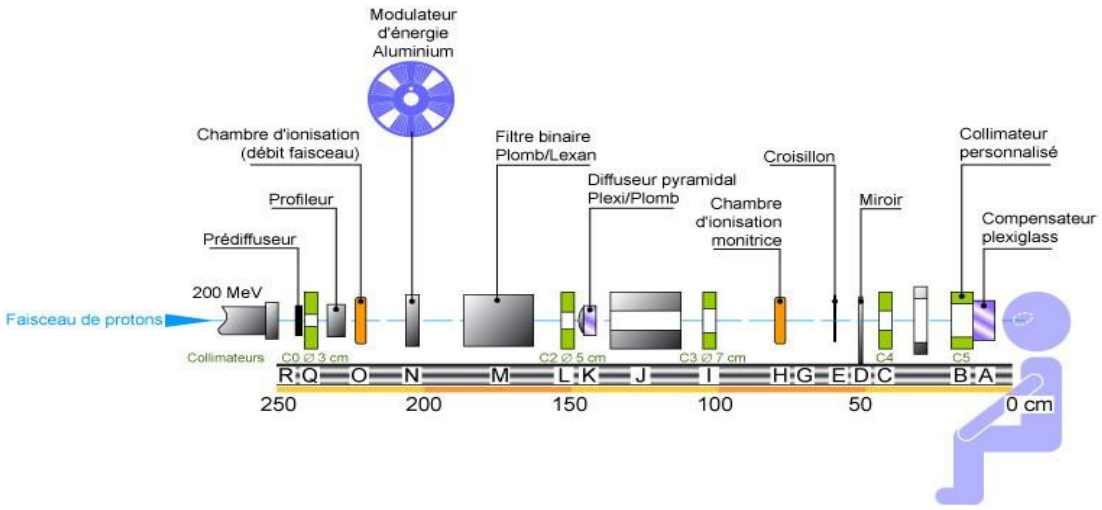

Figure 2 : ligne de faisceau thérapeutique de protons à l'ICPO

Le jeu d'articulation de ces quatre éléments permet d'adapter et sculpter physiquement le faisceau d'irradiation à la forme exacte de la tumeur tout en appliquant le strict cahier des charges de radioprotection des organes et structures à risques environnants voulu par le protocole d'irradiation.

Le collimateur et le compensateur sont en particulier des accessoires personnalisés pour chaque patient et sont réalisés par l'équipe mécanique d'usinage des pièces.

Le collimateur : est réalisé en cuivre et permet de protéger les tissus situés latéralement par rapport à la tumeur. Chaque collimateur est unique, usiné en fonction de la forme de la lésion sous une incidence donnée de faisceau. Il est identifié et contrôlé à plusieurs étapes (fabrication, contrôle de qualité du faisceau, traitement) pour chaque champ.

Figure 3 : le collimateur, il conforme la dose au profil tumoral.

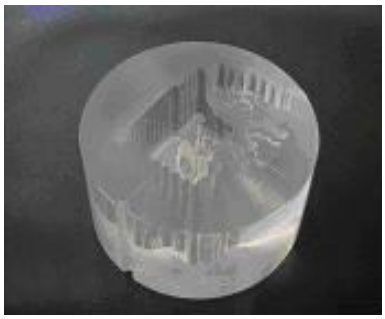

Figure 4 : le compensateur, il modifie la dose en profondeur.

Le compensateur : usiné dans un matériau polymère équivalent-tissu, permet d'ajuster la profondeur de pénétration des protons en chaque point de la tumeur. Il est unique, identifié et contrôlé pour chaque champ.

I – 3.3.3. Le positionnement du patient

Le positionnement patient est un aspect important du traitement car il est partie prenante de la précision dite millimétrique du traitement. La ligne de faisceau proton est fixe et c'est le patient qui est placé en fonction des incidences de faisceaux voulues par la balistique de traitement planifiée par le dosimétriste. Or séance, la précision et la reproductibilité de la mise en place du patient doivent être assurées. Pour cela, il est nécessaire d'utiliser :

- un système de contention i.e. un masque thermoformé qui permet l'immobilisation et la reproductibilité quotidienne de la mise en place du patient.
- des repères anatomiques visibles radiologiquement, implantés sous anesthésie locale dans la boîte crânienne pour les tumeurs intracrâniennes. Il s'agit de billes en or d'environ 1 mm de diamètre qui permettent un repositionnement millimétrique.

Le manipulateur installe le patient avec la contention fixée à la table ou à la chaise robotisée. Des clichés radiographiques orthogonaux permettent à chaque séance de traitement d'identifier ces repères anatomiques radio-opaques. Un traitement informatique compare ensuite leurs positions dans l'espace par rapport aux données de l'imagerie de référence et calcule les corrections nécessaires. Elles sont traduites alors par le système de pilotage du robot en coordonnées au $10^{ème}$ de mm près qui permettent de replacer le patient avec une précision opérationnelle au millimètre près.

I – 3.3.4. Le traitement

Chaque temps d'irradiation est précédé du positionnement patient – série de clichés radiologiques et corrections apportées par l'informatique et la robotique. Lorsque le patient est bien positionné, un dernier contrôle des accessoires et des paramètres du faisceau est effectué, le faisceau peut enfin être débloqué. Concrètement la mise en place dure en moyenne 30 minutes et le temps d'irradiation, 1 minute.

I – 4. Le faisceau d'ions carbone

Le faisceau d'ions carbone présente la caractéristique du profil de dose inversé (pic de Bragg) tout comme le faisceau protons (voir figure 5). Il a l'avantage d'un dépôt de dose plus faible que celui des protons en amont du pic de Bragg mais l'inconvénient d'une queue de fragmentation, visible en aval du pic.

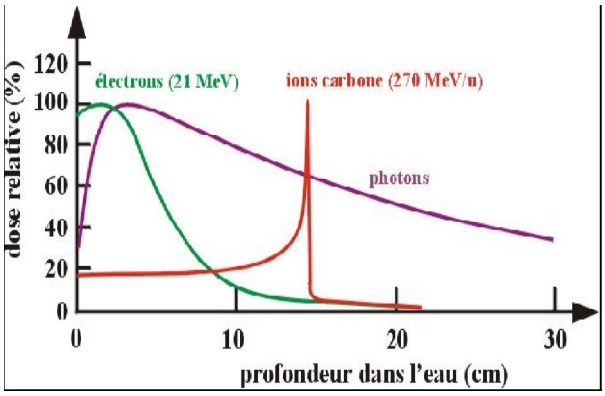

Figure 5 : comparaison des dépôts de doses pour des photons, des électrons et des ions carbone avec son dépôt en profondeur caractéristique en pic de Bragg.

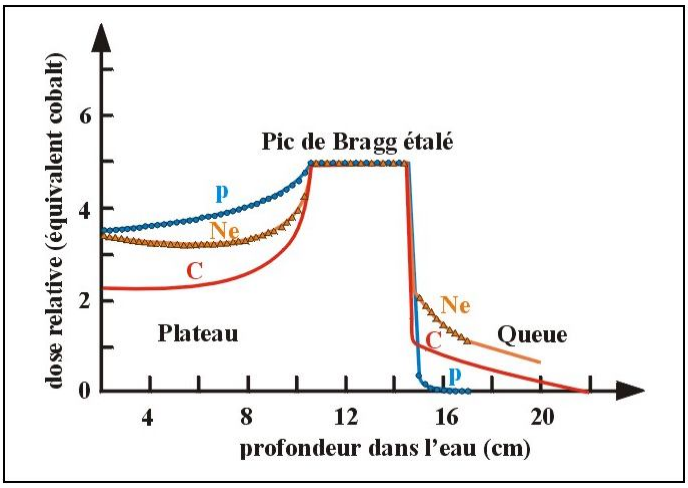

Figure 6 : dépôt de dose sur une cible pour des protons, des néons et des ions carbone. Les néons et carbones montrent une fragmentation en aval du pic de Bragg étalé.

En effet le dépôt de dose dans une cible consiste en l'ionisation des atomes de la matière traversée. On voit que l'utilisation d'ions légers tels le carbone (ou d'ions plus lourds tels le néon, voir figure 6) génère en plus des réactions nucléaires qui vont créer des fragments. Ces fragments élargissent le pic de Bragg de manière notable.

Le traitement en profondeur de tumeurs de grand volume oblige à superposer des pics de Bragg de différentes énergies et de moduler leur intensité pour avoir une répartition homogène du dépôt de dose tout comme le rayonnement proton. Pour une même dose déposée en amont de la tumeur, l'effet biologique sur la tumeur est plus important pour les ions carbone (voir figure 7), ceci permet alors un meilleur contrôle des tumeurs radiorésitantes.

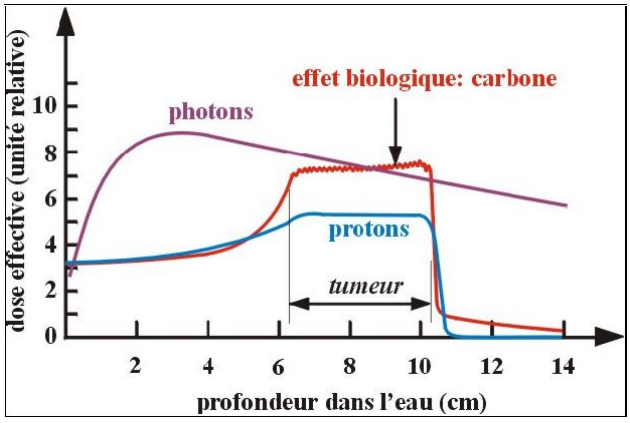

Figure 7 : comparaison de l'effet biologique des photons, protons et ions carbone.

Le carbone a un transfert d'énergie linéique (TEL) dans la matière supérieur à celui des protons et photons (TEL moyen carbone environ 90 à 100 keV/µm, celui des protons est voisin de 1 keV/µm et celui des photons du cobalt de 0,3 keV/µm). Il crée ainsi des radiolésions cellulaires (cassures du brin d'ADN) plus difficilement réparables, ce qui lui confère une plus grande efficacité biologique relative en fin de parcours de l'ordre de 3 (celui du proton en milieu de SOBP est considéré égal à 1,1).

Les propriétés balistiques des ions carbone sont supérieures (hors fragmentation) à celles des protons. Ils présentent en effet une moindre diffusion latérale (voir figure 8) et distale. La chute de dose en distale (90% - 20%) est 3-4 fois plus accentuée en carbone qu'en protons.

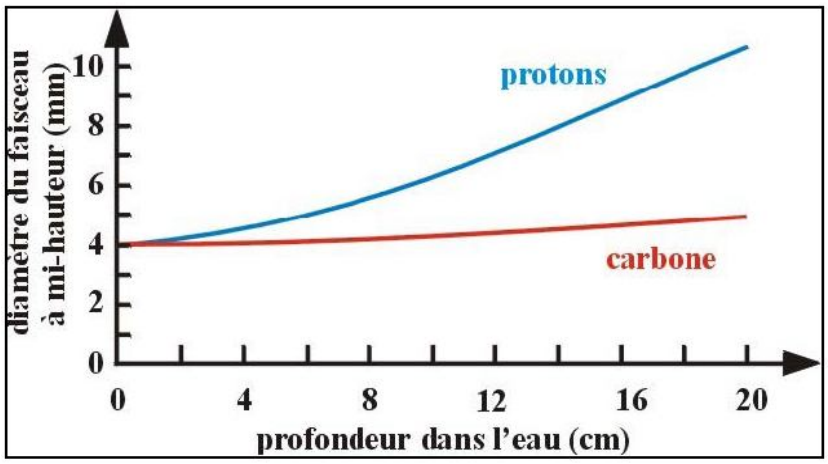

Figure 8 : comparaison de la diffusion latérale des ions carbone et des protons.

Les caractéristiques physiques et radiobiologiques des ions légers protons et carbones permettent l'atteinte de tumeurs radiorésistantes (échec local de la radiothérapie conventionnelle), proches d'organes vitaux ou sensibles. L'hadronthérapie permet grâce à ses qualités balistiques de mieux épargner les tissus et organes sains. La thérapie par ions légers a pu faire ses preuves dans le traitement de chordomes et sarcomes de la base du crâne, de tumeurs dites radiorésistantes à proximité de la moelle épinière, des tumeurs des sinus de la face, de cancers du poumon, du foie et de la prostate[1]. Leurs caractéristiques physiques et biologiques se révèlent ainsi très prometteuses d'un point de vue balistique de traitement et de leur impact en termes de contrôle tumoral et de tolérance de traitement, particulièrement chez l'enfant. Par contre, chacune de ces caractéristiques *avantageuses* ne sera pleinement efficiente, dans le cadre de la thérapie, que par une démarche de justification de chacun des actes de traitement dirigée et constamment améliorée par une recherche de pointe.

Quel serait en effet le sens d'une telle précision si l'absence d'investigation clinique entraînait une méconnaissance des structures anatomiques à éviter prioritairement ? Sans croisement des compétences technologiques et techniques à la recherche clinique, comment tout simplement établir une thérapie *sur mesure* dite millimétrique vis à vis de zones ou structures (exemple des réseaux neuronaux responsables des capacités neurocognitives en évolution chez l'enfant) que l'on ne saurait correctement localiser et par suite éviter ? L'objet technologique oblige à ce travail de recoupement des disciplines et les investigations futures

[1] Cf publications : Schulz-Ertner D, et al. Carbon ion radiation therapy for chordomas and low grade chondrosarcomas—current status of the clinical trials at GSI. Radiother Oncol. 2004 Dec;73 Suppl 2:S53-6. OU Tsujii H, et al. Overview of clinical experiences on carbon ion radiotherapy at NIRS. Radiother Oncol. 2004 Dec;73 Suppl 2:S41-9.

devraient prioritairement s'attacher, sans doute par un travail bibliographique approfondi, à croiser données épidémiologiques, physiologiques, anatomiques et biologiques. Tout ceci permettrait la création de protocoles d'irradiation dont la démarche thérapeutique serait beaucoup plus détaillée qu'actuellement.

L'une des dimensions de ce travail s'attache entre *autres* à ouvrir quelques voies et poser quelques jalons dans l'optique d'une meilleure réalisation des procédures thérapeutiques pour les ions légers chez l'adulte, l'adulte jeune et l'enfant.

II - Pages liminaires du premier & du second article:

Dans le cadre d'un projet de coopération scientifique et technique entre ETOILE et l'ICPO, des actions de recherche préfigurant une partie du programme national de recherche sur l'hadronthérapie (protons et carbones) ont été entreprises. Certaines de ces recherches portent notamment sur l'optimisation des modalités de traitement et des outils technologiques dont la gantry – objet de recherche technologique prévu dans l'équipement d'ETOILE.
La première phase de recherche du présent travail a été réalisée au centre de protonthérapie d'Orsay, riche de compétences dans la préparation des traitements intracrâniens. Au delà des consoles et logiciels de plan de traitement que le centre d'Orsay possède, les données accumulées de cas cliniques concrets sont autant d'informations et d'exemples indispensables à l'acquisition des connaissances de base et au lancement de travaux de recherche dans le domaine.

Pour le travail qui nous intéresse ici, il a été choisi différents cas anatomo-pathologiques de tumeurs difficiles et radiorésistantes. Les dosimétries optimales par faisceaux de protons fixes sont comparées pour chacune des pathologies aux dosimétries établies pour la configuration de type gantry. Le design des salles avec faisceaux fixes varie selon divers modèles de centres existants (centre de traitement de l'ICPO, du N.A.C. (Afrique du sud), du NIRS (Japon), etc.). L'évaluation du plan de traitement pour chacune de ces salles s'accompagne de l'étude du gain en matière de faisabilité, de gain potentiel en matière de tolérance à long terme ou de risque carcinogène (second cancer radio-induit). Le but est de reconnaître si la gantry apporte un bénéfice du strict point de vue dosimétrique et d'énoncer alors, s'il y a lieu, tous les avantages (qualitatifs et quantitatifs) qu'elle peut fournir.

II – 1. Premier article – utilisation et intérêt(s) de la gantry en protonthérapie chez l'adulte

La première partie de cette thèse a un aspect assez pratique et technique. Il s'agit de la définition de l'équipement (faisceaux fixes *versus* gantry) pour un centre de traitement et ainsi traiter la plus large variété possible de tumeurs. La gantry isocentrique offre-t-elle un avantage dosimétrique par rapport à un traitement avec faisceaux fixes *i.e.* une salle avec 1 faisceau horizontal *versus* une salle à 2 faisceaux : 1 horizontal + 1 vertical (venu d'en haut) *versus* une salle à 3 faisceaux : 1 horizontal + 1 vertical + 1 oblique. La référence est la situation où le patient est soit traité en position assise, soit en décubitus étant entendu qu'un patient donné doit avoir une seule position par rapport à son support quelques soient les incidences utilisées (en d'autres termes, il ne peut pas être à plat pour un faisceau et incliné en roulis ou en tangage pour un autres faisceau à cause du déplacement interne des organes entre les différentes positions).

La problématique posée est ainsi la suivante : la balistique permise par une gantry offre-t-elle certaines incidences originales de faisceaux que la configuration d'une salle à

faisceaux fixes interdirait ? La multiplicité des incidences offerte par la gantry induit-t-elle un bénéfice thérapeutique (et si oui de quel ordre et pour quels organes) pour le patient par le design dosimétrique original qu'elle proposerait ?

Les tumeurs étudiées sont des tumeurs de la base du crâne, du rachis cervical haut, bronchiques, ganglionnaires thoraciques, ganglionnaires abdominales et de la prostate ; l'on obtient ainsi un éventail assez large d'indications thérapeutiques. Des doses de prescription dans le volume tumoral macroscopique (GTV) et des contraintes de dose pour chaque organe à risque (OAR) proche des tumeurs ont été définies et strictement imposées. Les doses prescrites sont données telles que définies dans les centres les plus avancés dans le traitement de ces tumeurs. Enfin la comparaison des différentes dosimétries est basée sur les histogrammes dose-volume (HDV) cumulatifs & différentiels, des index de conformation (détaillés dans l'article 1 & 2) et le calcul du NTCP (Normal Tissue Complication Probability).

II – 2. Second article – intérêt de la gantry chez l'enfant

Reprenant la même problématique et les mêmes possibilités de traitement offertes par le design des salles du premier article, un ensemble de tumeurs intracrâniennes de la base du crâne et de la sphère ORL sont comparées chez l'enfant et l'adulte jeune.
La même méthode d'analyse est appliquée (le protocole pédiatrique d'irradiation étant différent de l'adulte) en incluant à la discussion le risque de carcinogénèse radio-induit.

II – 3. Schémas d'irradiation des différents sièges tumoraux chez l'enfant et l'adulte et leur répartition par salle de traitement

Les schémas standards d'irradiation (obtenus de l'article 1 & 2 par l'étude des plans de traitement) sont le résultat d'un difficile compromis entre l'occurrence de complications aiguës, chroniques et néoplasiques. Ces résultats sont dépendants de l'âge du patient lors du traitement, de la localisation tumorale et des organes à risques à proximité. Le tout peut être résumé brièvement par les tableaux qui suivent :

Adultes:

Siège	Incidences standards d'irradiation[2]	Salle de traitement
Prostate	Latéraux	Ligne horizontale (table)
Rétropéritonéal	Obliques	Salle double (table)
Paravertébral		
Abdominal	Latérale et cranio-obliques	Salle double (table)
Pulmonaire	Latérale et obliques	Salle double (table)
Médiastinal	Caudo-obliques	Salle double (table)
Intracrânien	Coplanaires + non-coplanaires	Ligne horizontale (table + chaise)

Tableau 1 : Répartition des patients adultes selon le siège tumoral par salle de traitement avec incidence d'irradiation. (Salle double : pour salle équipée de deux lignes de faisceau d'incidences différentes)

[2] Le terme « coplanaire » désigne tout faisceau coplainaire au plan transverse anatomique ; toute autre orientation est appelée « non-coplanaire ».

Il semble qu'un partage se dessine entre *(i)* le cancer de la prostate et la tumeur intracrânienne qui requièrent une ligne horizontale *(ii)* les tumeurs extra-crâniennes (hors prostate) qui requièrent une ligne oblique. Il est intéressant de voir que d'un strict point de vue dosimétrique la gantry ne fait aucune différence avec une salle avec faisceaux horizontal et oblique (avec chaise et/ou table).

Enfants:

Anatomopathologie	Siège	Incidences standards d'irradiation	Salle de traitement
Rhabdomyosarcome embryonnaire	Ethmoïde+orbite int+sinus max+intra crânien (sus orbitaire)	Caudale Oblique-antéro-caudale Latérale Oblique-latéro-craniale	Ligne horizontale (table + chaise) Gantry (si anesthésie)
Rhabdomyosarcome embryonnaire	Région parapharyngée	Coplanaires ipsilatéraux	Ligne horizontale (chaise) Gantry (si anesthésie)
Médulloblastome	Fosse postérieure exclusive[3]	Coplanaires postérieures	Ligne horizontale (chaise) Gantry (si anesthésie)
Dysgerminome	Ventricules cérébraux	Obliques latéraux en plan frontal	Ligne horizontale (table)
PNET	Thalamo-pédonculaire	Coplanaires ipsilatéraux	Ligne horizontale (chaise) Gantry (si anesthésie)

Tableau 2 : Répartition en condition pédiatrique selon le siège tumoral par salle de traitement avec incidences d'irradiation.

Les plans de traitement des tumeurs intracrâniennes et de la sphère ORL peuvent tous être réalisés par un design de salle à faisceaux fixes. D'un strict point de vue dosimétrique, la salle à faisceau fixe horizontal (avec chaise et/ou table) permet en effet toutes les incidences souhaitées pour le traitement. Par contre si l'anesthésie générale s'impose (d'un point de vue pratique) pour le traitement de l'enfant et l'oblige à la position en décubitus, alors la gantry se révèle indispensable pour la réalisation de la quasi-totalité des plans de traitement.

En résumé, avancer que la gantry permet par ses incidences une construction balistique originale et apporte un bénéfice thérapeutique pour le patient (permettant une distribution de dose particulière) ne se vérifie pas. Par contre le bénéfice apporté par la gantry hors justification dosimétrique peut apparaître à bien d'autres niveaux d'appréciation.

II – 4. Justifications de la gantry – que nous dit l'expérience d'autres centres ?

Une discussion avec le Dr De Laney (***Massachusetts General Hospital*** - Boston) a permis de connaître son avis concernant l'usage et l'utilité de la gantry [communication

[3] Pour l'irradiation totale du névraxe, la moelle épinière est irradiée par un faisceau verticale et oblige sous anesthésie générale à une gantry.

personnelle au Centre Léon Bérard le 29 juillet 2005]. Le bras isocentrique est utilisé à Boston ainsi qu'un fauteuil de traitement inclinable avec un contrôle de faisceau de type passif. Il n'a pas été fait d'étude comparative entre bras isocentrique et faisceau fixe. Dr De Laney, par sa propre expérience, nous a confirmé ne pas avoir de réponse formelle au principe spécifique d'utilisation du bras isocentrique à Boston pour certains traitements i.e. une construction balistique originale propre à la gantry, mais il fait remarquer que les traitements de Boston recourent abondamment à des faisceaux obliques.

L'*article 1* confirme l'incidence d'obliquité autour de 50° (à l'axe vertical) comme indispensable à la balistique des plans de traitement. L'obliquité est en effet nécessaire pour les localisations tumorales profondes du tronc, intrathoraciques ou abdominales lorsqu'elles se situent contre le rachis (tumeurs bronchiques périphérique, sarcomes rétropéritonéaux…). Cette situation nécessite des faisceaux obliques en décubitus. Une situation similaire peut se retrouver pour des tumeurs sus-mésocoliques (comme les tumeurs du pancréas) à cause de la proximité de la moelle épinière et des deux reins. Le cas de tumeurs abdominales en situation prévertébrale médiane (comme les tumeurs sus mésocoliques) avec GTV proche de la moelle épinière interdirait l'utilisation de faisceaux antérieurs selon le critère de fin de parcours d'un faisceau de protons, et les entrées latérales seraient limitées par la dose aux reins. Dans tous ces cas, la proximité du GTV par rapport aux organes à risque (OAR) peut imposer des incidences obliques.

A noter aussi qu'en utilisant seulement des faisceaux verticaux et horizontaux, les doses à la peau, en latéral et antérieur, atteignent des valeurs bien supérieures à celles rencontrées habituellement avec les photons (bien qu'en deçà des limites imposées par le protocole d'irradiation) du fait de l'absence de phénomène de « build up » avec les protons. L'expérience de Boston enseigne que la dose à la peau est importante (voire même dépasse celle des photons) et qu'au moins deux portes d'entrées sont nécessaires lors d'un plan de traitement. Pour exemple, bien qu'il soit parfaitement possible de traiter les prostates en protons par deux faisceaux latéraux issus d'un faisceau horizontal fixe (comme il est fait au *Loma Linda University Medical Center*), l'avis du Dr De Laney est que le traitement doit inclure des faisceaux obliques d'où l'avantage du bras lors de telles irradiations, notamment en termes de gain de temps.

Que nous dit encore l'expérience de Boston sur la nécessité d'usage du bras isocentrique ? Elle est entre *autres* jugée nécessaire dans les situations suivantes:

- Pour les traitements qui se feraient sous anesthésie générale chez l'enfant, la position en décubitus est obligatoire y compris pour les tumeurs de la tête, et l'usage d'un bras isocentrique sera seul à même d'offrir à la fois l'usage de plusieurs incidences et une durée des séances compatible avec la situation de ces patients.
- Un faisceau postérieur nécessite de placer le patient en procubitus, ce qui est une position très inconfortable voir impossible pour un insuffisant respiratoire et une position qui ne permet pas l'utilisation du gating respiratoire selon les techniques spirométriques.
- Pour les traitements complexes nécessitant plusieurs incidences non limitées au plan horizontal, y compris les cas de tumeurs intracrâniennes, le bras isocentrique permet un gain de temps de traitement et un positionnement plus facile et plus rapide du patient.
- Les irradiations intéressant la région interne de la racine des membres, notamment au niveau de la cuisse sont des zones très difficiles d'accès qui nécessitent au moins des faisceaux verticaux, la disponibilité d'incidences obliques ou la combinaison dans la

même position de faisceaux verticaux opposés seraient certainement utiles et seulement disponible grâce à un bras isocentrique.

De l'expérience acquise à Boston, l'équipe du MGH signale en définitif qu'il est plus facile de traiter avec une gantry qu'avec des faisceaux fixes. Les situations qui étaient antérieurement traitées en position assise avec le cyclotron d'Harvard sont maintenant traitées en position couchée avec le bras isocentrique. L'utilité du bras isocentrique en proton peut être par certains côtés comparée à l'utilité du bras en photons : c'est celle d'un **positionnement unique du patient** à l'isocentre du système avec un **gain de temps** très important dès qu'il y a plusieurs faisceaux à traiter. Ainsi l'utilité de la gantry ne se réduit pas à son seul aspect dosimétrique mais se joue plus au niveau de l'ergonomie, du traitement sous anesthésie, et de l'efficience économique du centre de traitement.

III - Premier Article

III – 1. Dosimetric evaluation of the usefulness of different beam line equipments for protontherapy centers

Yasid BOUDAM[1], Georges NOEL[2], Régis FERRAND[2], Christine GAUTIER[2], Jean-Louis HABRAND[2,3], Jean-Jacques MAZERON[2,4], Jacques BALOSSO[1] and the ETOILE program

1 : University Joseph Fourier, Grenoble, France ; 2 : Protontherapy Center of Orsay - CPO, BP65, F-91402 Orsay cedex, France; 3: Gustave Roussy Institut, Villejuif, France; 4: Tumors Centre, Pitié-Salpétrière Hospital, F-75651 Paris cedex 13, France.

Corresponding author: Pr Jacques BALOSSO
Department of Radiotherapy
Hôpital Michallon
BP 217
F-38043 GRENOBLE cedex 09
France
tel: +33 4 76 76 54 35
fax: + 33 4 76 76 56 29
JBalosso@chu-grenoble.fr

Key words: Radiotherapy, protons, hadrontherapy, gantry, complication probability, treatment plan inter-comparison.

Acknowledgments:
We are grateful to Dr Pascal Pommier and Dr David Sarrut for helpful discussion of this work.

III – 1.i. Summary

Dosimetric distributions for protons have been calculated for different tumor sites (tumors of the skull base; tumors of the upper cervical spine; pulmonary tumors; thoracic lymph nodes and lymphomas; abdominal lymph nodes; pancreatic cancer; prostate cancers) and several treatment room configurations. The set of tumors has been selected taking into consideration both requirements for useful local regional treatment (i.e. low metastatic risk and/or high local risk), and the need of representative conditions that could be treated in the future by protons or carbon ions. Five virtual treatment rooms have been designed to compare their respective possibilities. Four had fixed beams (horizontal, vertical from above, oblique) and one was a mobile gantry. The patient lies on a couch and/or sits in a chair. The treatment dosimetric quality indexes, the dose constrains for the organs at risk, the DVH assessment and the normal tissue complication probability (NTCP) calculations have been used to segregate the alternative treatment plans. The treatment dosimetric quality indexes presented very little interest to rank treatment plans established with proton techniques. Conversely, the cumulative DVH and the NTCP assessments provided powerful tools to establish the best treatment plans for the different tumor locations. These results suggest that a facility equipped with at least three fixed incidences of beam (horizontal, vertical from above and oblique around 50°) could probably treat properly most of the tumor locations.

III – 1.1. Introduction :

Protontherapy is presently used only in a few highly specialized centres for the treatment of very selected conditions [1]. At the present time the technological progress and the acceptation of more expensive treatments for cancer patients are able to produce the economical conditions of a wider spread of this type of radiotherapy throughout the world. Moreover, the availability of an increased health care-offer of protontherapy will probably open the medical indication spectrum. Thus a raising question is the definition of the minimal equipment for a protontherapy centre able to treat the largest variety of tumor conditions. More precisely, the question of the usefulness of an expensive equipment as an isocentric gantry is raised.
The isocentric gantry compared to a set of fixed beam lines may open the ballistic possibilities for hadrontherapy and seems to become systematically included in the design of the new proton facilities. However, for more heavy charged particles, the weight and the cost of such a piece of equipment remains an important drawback [2, 3]. Considering the very closed ballistic characteristics of any charged particle and the well-mastered dosimetry of protons, we proposed to compare through a protontherapy approach the different qualities of treatment made with or without the use of a mobile isocentric gantry. Different configurations of treatment rooms have been defined, either one or two orthogonal fixed beams with a sitting or a lying patient, or one oblique fixed beam with a lying patient, or a mobile isocentric gantry with a lying patient.
In this paper are reported the objective values of conformal indexes and the doses delivered to the organs at risk along with the analysis of the different dose volume histograms (DVH) for a set of representative tumors chosen in the different parts of the body. For this study, the normal tissue complication probability (NTCP) [4] through the dose volume histogram reduction scheme [5] will also be used. That will enable us to propose a powerful multiparameter comparative method of the treatment rooms above-referenced. This work shows that the contribution to the dosimetric quality of a mobile gantry is very limited compared to the set-up of three fixed beams (horizontal-vertical-oblique). Such a room equipped with three fixed beams might treat properly tumors in thoracic, abdominal and pelvic areas.

III – 1.2. Material and methods :

III – 1.2.1. Dose expression and dose prescription according to ICRU target volumes

Dose is reported in CGE (Cobalt Gray Equivalent) which is obtained by multiplying the physical dose in Gy by the proton relative biological effectiveness - RBE - relative to ^{60}Co. Proton RBE is estimated to be 1.1 in ICPO. It has been assessed with survival curves of rodent cells and was found consistent with previous reports of proton beams RBE in other clinical centers [6, 7, 8]. Prescribed doses were from 50 CGE up to 74 CGE according to tumor locations for the CTV defined with a 5 mm margin around the GTV. For fixed targets, the PTV has a 3 mm margin around the CTV for a typical prescribed dose of 55 CGE for intra cranial tumors. The treatment volumes were defined according to the recommendations of ICRU report n°50 and 62 [9, 10], organs at risk as well as the GTV are outlined by the radiation oncologist. From this information a virtual treatment plan with beam arrangement is generated in the ISIS or ISOGRAY TPS workstations and evaluation criteria are applied to check its quality.

III – 1.2.2. Tumors sites

Height different types of clinico-anatomical conditions have been used: tumors of the skull base & tumors of the high cervical spine (n = 7); pulmonary tumors (n = 2); thoracic lymph nodes and lymphomas (n = 2); abdominal lymph nodes (n = 2); pancreatic cancer (n = 1); and prostate cancers (n = 1). This set of tumors has been selected taking into consideration both requirements for useful local regional treatment, (i.e. low metastatic risk and/or high local risk), and for having valid sample of the conditions that could be treated in the future by protons or carbon ions.

III – 1.2.3. Treatment room configuration

Five different treatment rooms have been designed to compare their respective possibilities.
Room A has a fixed horizontal beam with a horizontal mobile couch (CPO design); Room B has two fixed isocentric beams, one horizontal and one vertical coming from the ceiling with and a horizontal mobile couch (N.A.C., South Africa design); Room C has a fixed horizontal beam with a robotised mobile chair (CPO design); Room D has an isocentric mobile gantry with a horizontal mobile couch (Boston, Loma Linda, Kashiwa, Hyogo design); Room E has an oblique 50 to 55° fixed beam coming from the ceiling and a horizontal mobile couch inspired from the design for carbon ions in Hyogo (Hyogo design).

III – 1.2.4. Qualitative criteria studied

Treatment dosimetric quality indexes have been taken from the RTOG [11, 12]. Two different indexes for dosimetric quality have been used: i) the homogeneity index (HI) defined as Imax/IR (Imax is the highest isodose, RI is the reference isodose chosen as the 95% of the prescribed dose); ii) the coverage index (Coverage-RTOG) defined as Imin/IR (Imin is the lowest isodose included in the tumor volume).
Treatment conformal quality indexes are the following: i) the conformity index defined by the RTOG (CI RTOG) as VIR/VT [11, 12] (VIR is the volume encompassed by the reference isodose, VT is the tumor volume equal to the GTV defined in the ICRU 50 report [9, 10]); ii) the target coverage (TC) defined as VTIR/VT [13, 14, 15] (VTIR is the volume of the tumor that is encompassed by the reference isodose, VTIR = VIR ∩ VT); iii) the conformity index (CI) defined as VTIR/VIR by Lomax et al. [15].
The cumulative DVH have been established for each dosimetric project to check the following data: the dosimetric constrains of healthy tissues (dose-volume relation and maximal doses), the assessment of the prescribed dose.
The portal skin doses have been reported as at least 60% of the average dose obtained in the spread out Bragg peak (SOBP), and at the most 100% of that dose. The volume encompassed by the lowest isodoses between 5 to 20% of the prescribed dose were also measured and reported. These doses are expressed in CGE.
The use of the "normal tissue complication probability (NTCP)" approach is also performed to rank alternative treatment plans. The investigation of the NTCP has been done according to the Lyman-model [4], which relies on a sigmoid dose response relationship (Figures 1 to 4). To assess each treatment plan in the frame of iso-NTCP chart (Figure 5 "didactic n°1"), the effective volume (Veff) of each organ at risk must be obtained and plot in the iso-NTCP chart [16]. The Veff are retrieved from the differential DVHs, obtained through the dose volume histogram reduction scheme method [5]. The Veff plot will enable us to segregate alternative treatment plans according to there relative positions in the iso-NTCP chart [16]. It has been advised, using this method, to judge the respective quality of treatment plans mainly in relative terms taking into account the present lack of comprehensive clinical and radiobiological data, in particular about fractionation alteration. This empirical model can be

applied to any organ through parameters summarized by Burman (fitting the summarized tolerance data from the Photon Treatment Planning Collaborative Working Group [17]).

III – 1.2.5. Equipment used for the study

The dosimetry and HDV have been computed with either an ISIS or an ISOGRAY treatment planning software produced by the DOSIsoft Corp. (DOSIsoft SA, 45/47 av. Carnot – F-94230 Cachan, France) routinely used for the protontherapy planning at the ICPO.

III – 1.3. Results :

The quality indexes have been established for each treatment proposition and are shown in Table 1. More specifically for the high dose conformation (shadowed areas in the Table 1) the indexes yield similar results whatever the treatment setting. However, this is only a physical assessment that is unable to discriminate treatment plan at the point of view of the tissue tolerance according to different biological characteristics of the organ at risk. Therefore the comparison of the treatment propositions have been further studied according to the NTCP concept and are hereby presented according to the different anatomical situations.

For intracranial and skull base tumors, target volume and organs at risk such as brainstem, upper spinal cord, pituitary gland, optic nerves and chiasm, and internal ears were delineated. Treatment plans of 7 patients have been generated using the ISIS three-dimensional treatment planning system. The respected dose constraints were <56 CGE to the optic nerves and optic chiasm, <63 CGE to the anterior aspect of the brainstem, and <56 CGE to the middle of the brainstem. Due to the proximity of critical normal structures and their low tolerance thresholds to irradiation, beam orientations possibilities are rather reduced. The "ICRU" volumes for these tumor sites are defined as following: i) a PTV1 is considered as a "PTV55Gy" defined as the "CTV55Gy" plus 2 mm margin for positioning uncertainty and proton diffusion; ii) a reduced PTV2 is defined as "CTV71Gy", which is taken as the GTV (gross target volume according to ICRU definition) expanded to the nearby anatomical structure suspected to be involved by the tumor process (clivus, cavernous sinus…) with no additional margin. The prescribed dose to PTV1 is up to 55 CGE by large fields (2 coplanar beams and 3 non-coplanar); the reduced PTV2 is then irradiated up to 71 CGE, using opposed-lateral, posterior, antero-oblique and sometimes antero-lateral oblique beams. All these irradiation modalities may be delivered in sitting position in treatment room C without necessity of a gantry.

For prostate, a single representative CT scan has been used with a prescribed treatment dose of 74 CGE. Rectum, bladder and femoral head and neck are the organs at risks. For this tumor location, taking into account the dosimetric constrains of healthy tissues, the optimal dose distributions to the tumor were obtained with technique of opposed lateral portals in room A, as well as with lateral and antero oblique coplanar beams in room D (or E).

At first sight, the cumulative DVH assessment indicates in room A a better protection for low and intermediate doses to the bladder and the rectum although a mildly higher dose to femoral heads. So according to this DVH study, the room A seems to be optimal for healthy tissue sparing. However, the comparison of the different room-related treatment plans carried on iso NTCP chart revel an opposite situation. Indeed the parameters, introduced by Burman [17] for bladder and rectum response, express a high tolerance dose (80 CGE) and only a minor risk of complications for low and intermediate doses. Therefore, the low doses part of the DVH is of minor relative contribution compared to the high doses part, very similar among the different rooms, to assess the relative quality of treatments. Thus few differences for bladder and rectum tolerance can be expected between rooms A, E (or D). Actually the plots of the

treatment associated effective volumes of femoral heads on the iso-NTCP graph indicate an obvious difference of the rooms for the bone necrosis risk. The best results are obtained in rooms D or E. So for prostate tumors a dose distribution through multiple ports (lateral and oblique) appears better than an irradiation limited to lateral ports.

For lung tumors, two peripheral tumors and two central tumors have been studied. The dose of 70 CGE was prescribed along with 56 CGE to mediastinal nodes if necessary. The organs at risk are brachial plexus, lung, oesophagus, heart and spinal cord. For distant peripheral lung tumors, coplanar beams (Figures 6 A), anterior and lateral ports in the treatment room B, offer the optimal irradiation. For proximal and median lung tumors, non-coplanar beams including an antero-medial foot-oriented oblique beam (with different table positions) seem the most suitable and is available in room E (Figures 6 B). The cumulative DVH assessment, relative to lungs and heart, indicates a real advantage in the use of room E with a 50° non coplanar beam for these two organs at risk. Iso-NTCP chart confirms this advantage of room E for lungs and shows no difference for the heart.

In abdominal locations a single case of locally advanced pancreatic tumor has been studied. The organs at risk considered are spinal cord, kidney, liver, stomach, small intestine and spleen, all of them surrounding the target lesion. The prescribed dose was 60 CGE. Due to the high radiosensitivity of kidney, an accepted constrain for any ballistic solution will be to avoid posterior ports. Therefore principal organ at risk are reduce to liver, stomach and small intestine. Some more concern could be raised from the movement of the targeted pancreatic tumor and the variations of intestinal air contain and body weight that could modify the beam range for successive treatment sessions. These latter parameters are not taken into account in the present study, but would worth specific analysis.
The studied possibilities are (Figures 6 C & D): i) the use of coplanar beams in rooms A and E with anterior, lateral and oblique ports and without posterior ports; ii) the use of a non-coplanar configuration with an antero-medial head-oriented oblique beam as available in room E. The optimal obliqueness is 55° with table position between 80° and 100°. These two solutions have been assessed by comparison of their respective cumulative DVH and iso-NTCP chart. Regarding cumulative DVH the non-coplanar solution seems better for sparing liver, stomach and spleen. However, the iso-NTCP chart comparison give a different figure: i) no significant difference appears for these latter organs at risks for the coplanar and non-coplanar settings, probably because the cumulative DVH differences are for low and medium doses, which have less impact on the toxicity of these organs as measured by iso-NTCP charts; ii) for small intestine Iso-NTCP chart and cumulative DVH show a better protection of small intestine by coplanar setting. Noteworthy, differences appear for the kidneys in favour of the non-coplanar solution. However, kidney irradiation is, in any case, very weak thanks to the constraint of non posterior ports, so this difference has no incidence on decision making. Combine solutions associating coplanar and non coplanar beams could be studied in particular cases where liver sparing would demand more attention than intestinal one.

III – 1.4. Discussion :

III – 1.4.1. Usefulness of the gantry

The viewpoint of this work is to provide dosimetric data and validate a comparison tool specifically for the dosimetric aspects of the assessment of the usefulness of a rotating isocentric gantry for hadrontherapy. However, beside dosimetric considerations, many other lines of arguments are to be taken into account for the practical decision-making. For

instance: i) a lying position for all patients, made possible by a gantry, allows a more comfortable position for head & neck treatments in adults and any possibility of treatment for children especially when general anesthesia is needed; ii) the application of the isocentric principle for the treatment, made possible by the gantry and its associated isocentric table, should enable a reduce number of patient position with consequently less controls and time saving; iii) the cost effectiveness and the technical reliability of this large piece of equipment are also important points, etc.

III – 1.4.2. No statistical assessment

The interest of a statistical approach by multiplying the number of cases for each tumor location is questionable. In fact a statistical method could assess the NTCP differences between various treatment plans and provide objective conclusions about the best irradiation ballistic with a confidence interval. However, as few differences of organ locations and volume exist among human adult patients and as tumor locations amenable to hadrontherapy are rather uniform for a given type, the choice of representative typical situations should be an acceptable approach.

III – 1.4.3. Choice of the reference isodose

The calculation of dosimetric quality indexes is based on ratio between a tumor volume and the volumes given by a reference isodose (see Material and Method section). Due to the steepness of the dose gradient at the edge of the volume irradiated by a proton beam, the value of the volumes encompassed by the 95% isodose is "unstable" i.e. could change in a very large extend for a very small variation of the position of the isodose toward the tumor volume. For this reason the use of the 95% isodose as reference, often produces very poor values of dosimetric quality indexes although obviously very good dose distribution as shown by the cumulative DVH. Therefore, the use of a slightly more "internal" isodose as the 90% one restores consistent indexes. For homogeneity, this choice has been extended to all location even if the 95% isodose was less misleading for the intracranial lesions.

III – 1.4.4. Other studies and discussion of the comparison approach for proton set-up

Quantitative models for comparisons of treatment planning of classical photontherapy *vs* IMRT *vs* proton have been largely published [18, 19]. In particular very fine studies have been made for specific tissues as optic tract for instance [20]. In more recent studies ranking IMRT plans, attempts are made to implement accurate biological models for the establishment of absolute NTCP and to assess their validity to distinguish different treatment plan [21, 22].
So far however there is no publication of a specific comparison of the impact of the availability of a rotating gantry *vs* fixed beams in protontherapy centers upon treatment dosimetric quality. In fact, the present study relies principally on the relative comparison of treatment plan's NTCP obtained through a well recognized model [23, 17] without trying to estimate an absolute NTCP through original biological models.

More precisely, the NTCP values, DVH calculations and mean doses to organs at risk are often used to compare the proton *vs* photon treatment techniques. For instance, Fuss *et al.* in their work [20] comparing for optic nerve gliomas, standard photon irradiation *vs* IMRT and *vs* protontherapy made the very interesting observation that different dose/volume domains of the DVH (low, mid and high-dose domains) have different predictive weight for the risk of complication of a specific organ. Namely for optic tract, only the high dose/volume domain of the DVH is predictive for the relative risk of complication for the compared treatment plans. Conversely, these treatment plans are not discriminated according to the sole difference of

their low-mid dose/volume DVH parts. The practical consequence to treat optic gliomas is the favorable effect of treatment set-up using numerous contributing beams instead of a reduce number of high dose ports. Interestingly enough, this principle can be generalized in the sense that the different parts of a given DVH are not equally predictive for a given tissue, and, for different tissues it is different parts of their respective DVH that are actually predictive of their complication risk. For instance lungs and rectum are opposite examples at the point of view of their tolerance parameters, according to Burman et al. [17], which are also the characteristics of the position and the slope of their respective sigmoid curves NTCP *vs* dose or volume relationship. Lung is characterized by TD50 = 24.5Gy; m = 0.18; n = 0.87 (Figure 1) for clinical pneumonitis end-point and consequently the predictive part of lung DVH is the low-dose domain, moreover its high volume dependence given by "n" indicates to reduce as much as possible the number of beams; the rectum parameters are TD50 = 80Gy; m = 0.15; n = 0.12 (Figure 1) for severe proctitis / necrosis / stenosis / fistula end points, indicating that the predictive part of rectum DVH is the high-dose domain, and its low volume dependence given by "n" indicates additionally to the high TD50 the possibility to increase the number of beams.

The proton-to-proton treatment comparison developed in the work needs the same approach because of the following reasons:
i) the good conformity obtain by any proton set-up for the high-dose part of the treatment minimize the usefulness of any comparison solely based on the high-dose segment of the treatment planning. In fact, each treatment room constrains was successfully used to carry on treatment planning for the different tumor sites, meeting the required prescribed dose. In this approach, all the sub-criteria of the conformal index [24], such as the homogeneity distribution, as indicated by IC & IH index values, and the value of locally deposited dose encompassing the GTV given by the FCV [25, 17], showed a rather similar protocol conformity providing few argument for equipment choice between the proton techniques assessed here.
ii) consequently, the main ground for optimization is the low-dose part, i.e. the dose distributed to organ at risk. As showed above, a fruitful approach of this point is the use of integrated NTCP parameters.

III – 1.4.5. Ballistic choice and anatomic particularities
Pelvis :
Pelvic organs as the rectum, already discussed above, and the bladder (which parameters are TD50 = 80 Gy; m = 0.11; n = 0.5 for symptomatic bladder contracture and volume loss end point, (Figure 2) display a high tolerance doses (TD50) with a relative spread out slopes (the parameter m) of the sigmoid tissue response and a very weak volume dependence (the parameter n). These clinical parameters indicate that the rectum and the bladder have a very low risk of clinical complications for the weak- and medium-doses and can be irradiated by multiple entry ports rather than a reduce number of beams that would produce an increase of the high-dose volume with a detrimental effect. For the hip, the Figure 2 shows a relative sensitivity for the medium doses. A choice of several irradiation ports allows reducing the dose to this structure. Thereby, in opposition of the conclusion drawn from the exclusive assessment of the cumulative DVH, multiple (anterior) beams are the best set-up for pelvic tumors.
Abdomen :
For abdominal treatment, the kidneys (TD50 = 28Gy; m = 0.10; n = 0.70 for clinical nephritis end point, (Figure 3) present a low tolerance dose (TD50), a steep slope of the sigmoid response (m) and a high volume dependence (n). These parameters indicate a threshold sensitivity for the low doses and suggest to avoid their irradiation as much as possible, for

instance by the suppression of any posterior irradiations. This choice is also supported by the presence of the spinal cord. The liver sensitivity is in the range of the mid-doses. The stomach and the small intestine have characteristics similar to the rectum and the bladder ones with no sensitivity for the low- and mid-doses and leading to multiple entry ports. Thereby a coplanar irradiation technique by multiple anterior entry ports with a more prominent stomach-spleen irradiated side (than liver side) is preferred for the abdominal tumor sites.
Thorax :
A different situation is produced by the lungs. The lung parameters, given above, indicate a high sensitivity to small- and medium-doses, and high volume dependence to radiation dose (Figure 4). Thereby a tissue response is expected for low doses and an irradiation choice by multiple entry ports is not recommended for thoracic location. So we propose as a ballistic choice for central thoracic tumor: a non-coplanar set-up which avoids any complication giving very low dose to the lungs. For a peripheral lung tumor we suggest a coplanar set-up with a reduce number of ports which avoid the heart regarding its sensitivity to mid-doses. Posterior ports are preferably excluded regarding the spinal cord and the brachial plexus location.

These tolerance parameters affected to the organs at risk provide therefore a powerful model for the choice-making of the best irradiation technique among IMRT, protons or light ions (Figure 9).

III – 1.4.6. Attempt of generalization
So far we obtained appropriate dose distributions without the need of rotating gantry providing we could have the choice between three different incidences. Beyond the above described examples, it could be advocate that other anatomic locations would need the use of sensitive angles only provided by a rotating gantry. Therefore, we complete the set of anatomic cases by two other examples of difficult locations simulated as a lateroverteb ral tumor located between the right kidney and the spine (Figure 7) and a large tumor very deeply located in the abdomen invading the spine (Figure 8).

The design of a "three-beam-room" allows the horizontal and vertical irradiation plus all the directions, elements of the surface traced by a moving straight line, the generatrix of a right circular cone that always passes through a fixed point, its vertex, located in the target isocenter. The generatrix is set at the angle $\theta \sim 50°$ to the circular cone axis, an optimal value that places the generatrix almost at equidistant position to the horizontal and vertical lines.
For a gantry, the other allowed directions are those supported by the circular cones of θ smaller or higher than 50°. Smaller angles involve the risk of overlapping oblique beam with the vertical line; and higher angles imply skimming beams, very tangential with the skin, of directions not appropriate for non-superficial tumor.
Thus the generatrix of $\theta \sim 50°$ is a natural compromise and appears as the most adequate and practical obliqueness of the ballistic plot. What is more, the high multiplicity of the directions supported by the cone of revolution, thanks to the isocentric rotating couch, does not justify additional incidences.

III – 1.5. Conclusion :

It is interesting to note that for the inter-comparison of different proton beam line equipments, the conformity indexes presented few interests whereas the cumulative DVH assessment and the NTCP calculations play a more important role for the choice-makings. Using this approach, this work has demonstrated that useful tools can be applied to make an objective

comparison of the quality of the different treatment set-up according to the dosimetric data and the tolerance assessment through NTCP concept. In this frame our results suggest that, providing to have a facility with at least three fixed incidences of beam (horizontal, vertical from above and oblique around 50°) and an isocentric rotating couch, it is possible to properly treat any location. Of course this makes certainly necessary to move the patient from one room to the other. Our discussion does not encompass non dosimetric parameters as: i) the comfort, the time necessary for operating fixed beams set-up, the availability of three fixed beams in the same facility; ii) the technical, quality insurance, maintenance and financial constrains of a rotating gantry. Therefore the strategic choice to provide or not a gantry does not rely on dosimetric criteria, but mainly on medico-economical parameters including session duration, cost, reliability of the equipment and maintenance cost, etc. Moreover, this study gives objective basis for the design of a compact set-up of a “three-beam-room” facility that could compete with now classical proton gantry equipment.

III – 1.ii. References :

[1] Internet site: http://ptcog.mgh.harvard.edu/

[2] Haberer, Th.; Debus, J.; Eickhoff, H.; Jäkel, O.; Schulz-Ertner, D.; Weber, U. The Heidelberg ion therapy center. Radiother. Oncol. 73: S186-S190; 2004.

[3] Bajard, M.; De Conto, J-M.; Remillieux, J. Status of the ETOILE project for a French hadrontherapy centre. Radiother. Oncol. 73: S211-S215; 2004.

[4] Lyman, J. T.; Complication probability as assessed from dose volume histograms. Rad. Res. 104:S-13/S-19; 1985.

[5] Kutcher, G. J.; Burman, C.; Brewster, M. S.; Goitein, M.; Mohan, R. Histogram reduction method for calculating complication probabilities for three-dimensional treatment planning evaluations. Int. J. Radiat. Oncol. Biol. Phys. 21:137-146; 1991.

[6] Gueulette, J.; Böhm, L.; Slabbert, J. P.; de Coster, B. M.; Rutherfoord, G. S.; Ruifrok, A.; Octave-Prignot, M.; Binns, P. J.; Schreuder, A. N.; Symons, J. E.; Scalliet, P.; Jones, D. T. L. Proton relative biological effectiveness (RBE) for survival in mice after irradiation with fractioned doses. Int. J. Oncol. Biol. Phys. 47, 1051-1058; 2000.

[7] Gueulette, J.; Slabbert, J. P.; Böhm, L.; de Coster, B. M.; Rosier, J.-F.; Octave-Prignot, M.; Ruifrok, A.; Schreuder, A. N.; Wambersie, A..; Scalliet, P.; Jones, D. T. L. Proton RBE for early intestinal tolerance in mice after fractioned irradiation. Radiotherapy and Oncology, 61, 177-184; 2001.

[8] Gueulette, J.; Blattmann, H.; Pedroni, E.; Coray, A.; de Coster, B. M.; Mahy, P.; Wambersie, A.; Goitein, G. Relative biologic effectiveness determination in mouse intestine for scanning proton beam at Paul Scherrer institute, Switzerland. Influence of motion. Int. J; Radiat. Oncol. Biol. Phys. 62, 838-845; 2005.

[9] International Commission on Radiation Units and Measurements. ICRU Report 50: Prescribing, recording, and reporting photon beam therapy. Bethesda, MD: International Commission on Radiation Units and Measurements, 1993.

[10] International Commission on Radiation Units and Measurements. ICRU Report 62: Prescribing, recording, and reporting photon beam therapy (supplement to ICRU Report 50). Bethesda, MD: International Commission on Radiation Units and Measurements, 1999.

[11]. Shaw, E.; Kline, R.; Gillin, M.; Souhami, L.; Hirschfeld, A.; Dinapoli, R. et al. Radiation Therapy Oncology Group: radiosurgery quality assurance guidelines. Int. J. Radiat. Oncol. Biol. Phys. 27:1231-9; 1993.

[12]. Shaw E, Scott C, Souhami L, Dinapoli R, Kline R, Loeffler J, et al. “Single dose radiosurgical treatment of recurrent previously irradiated primary brain tumors and brain metastases: final report of RTOG protocol 90-05”. *Int J Radiat Oncol Biol Phys* 47:291-8; 2000.

[13] Lefkopoulos, D.; Schlienger, M.; Touboul, E.; Hancilar, T.; Merienne, L.; Mitsoura, H.; et al. Quantitative evaluation of treatment planning for linac multi-isocentric radiosurgery. Proc of the Xith Intern Conf on: «Computers in Radiation Therapy», Xith ICCR, Manchester, UK. p.296-7; 1994.

[14] Lefkopoulos D, Dejean C, El-Balma H, Platoni K, Grandjean P, Foulquier JN et al. “Determination of dose-volumes parameters to characterise the conformity of stereotactic treatment

plans". *Proc of the XIIIth Intern conf on*: "Computers in Radiation Therapy", XIIIth ICCR, Heidelberg, Germany. p.356-8; 2000.

[15] Lomax NJ, Scheib SG. "Quantifying the degree of conformity in radiosurgery treatment planning". *Int J Radiat Oncol Biol Phys.* 55:1409-19; 2003.

[16] Martel, M. K.; Ten Haken, R. K.; Hazuka, M. B.; Turrisi, A. T.; Fraass B. A.; Lichter, A. S. Dose-volume histogram and 3D treatment planning evaluation of patients with pneumonitis. Int. J. Radiat. Oncol. Biol. Phys. 28:575-581; 1994.

[17] Burman, C.; Kutcher, G. J.; Emami, B.; Goitein, M. Fitting of normal tissue tolerance data to an analytic function. Int. J. Radiat. Oncol. Biol. Phys. 21:123-135; 1991.

[18] Miralbell, R.; Cella, L.; Weber, D.; Lomax, A. Optimizing radiotherapy of orbital and paraorbital tumors: intensity-modulated X-ray beams vs. intensity-modulated proton beams. Int. J. Radiat. Oncol. Biol. Phys. 47:1111-1119; 2000.

[19] Lomax, A. J.; Bortfeld, T.; Goitein, G.; Debus, J.; Dykstra, C.; Tercier, P.-A.; Coucke, P. A.; Mirimanoff, R. O. A treatment planning inter-comparison of proton and intensity modulated photon radiotherapy. Radiot. and Oncol. 51:257-271; 1999.

[20] Fuss, M.; Poljanc, K.; Miller, D. W.; Archambeau, J. O.; Slater, J. M.; Slater, J. D.; Hug, E. B. Normal tissue complication probability (NTCP) calculations as a means to compare proton and photon plans and evaluation of clinical appropriateness of calculated values. Int. J. Cancer (Radiat. Oncol. Invest): 90, 351-358; 2000.

[21] Smith, V.; Verhey, L.; Serago, C. F. Comparison of radiosurgery treatment modalities based on complication and control probabilites. Int. J. Radiat. Oncol. Biol. Phys. 40:507-513; 1998.

[22] Moiseenko, V.; Battista, J.; Van Dyk, J. Normal tissue complication probabilities: dependence on choice of biological model and dose-volume histogram reduction scheme. Int. J. Radiat. Oncol. Biol. Phys. 46:983-993; 2000.

[23] Schultheiss, T.; Orton, C.; Peck, R. Models in radiotherapy: volume effects. Med. Phys. 10:410-415; 1983.

[24] Feuvret L. et al. « Index de conformation et radiothérapie », *Cancer/Radiothérapie.* 8 : 108-119, 2004.

[25] Emami, B.; Lyman, J.; Brown, A.; Coia, L.; Goitein, M.; Munzenrider, J. E.; Shank, B.; Solin, L. J.; Wesson, M. Tolerance of normal tissue to therapeutic irradiation. Int. J. Radiat. Oncol. Biol. Phys. 21:109-122; 1991.

III – 2. Table :

Table 1 : Conformation index values

Tumor locations	Prescribed dose (CGE)	VT = GTV (mL)		Indexes	Room A	Room B	Room C	Room D	Room E
Tumor n°1	71	46.3		**Coverage RTOG**			0.80	0.70	
				HI			1.32	1.35	
				CI RTOG			1.64	3.90	
				TC			0.9	0.9	
				CI			0.55	0.24	
Tumor n°2	71	32.8		**Coverage RTOG**			0.94	0.92	
				HI			1.35	1.47	
				CI RTOG			7.51	7.37	
				TC			0.99	0.98	
				CI			0.13	0.13	
Tumor n°3	70	47.8		**Coverage RTOG**		0.95		0.95	
				HI		1.05		1.05	
				CI RTOG		2.00		1.90	
				TC		0.99		0.99	
				CI		0.49		0.52	
									Cop & Non-cop
Tumor n°4	70	75.1		**Coverage RTOG**		1.03			1.04 & 0.93
				HI		1.11			1.11 & 1.11
				CI RTOG		2.21			2.14 & 3.25
				TC		1			1 & 0.99
				CI		0.45			0.46 & 0.30
Tumor n°5	70	48.3		**Coverage RTOG**	1.02	1.03		1.04	
				HI	1.05	1.05		1.05	
				CI RTOG	3.5	3.46		3.70	
				TC	1	1		1	
				CI	0.28	0.28		0.27	
Tumor n°6	70	3.9		**Coverage RTOG**		1.02		1.02	
				HI		1.05		1.05	
				CI RTOG		5.70		5.22	
				TC		1		1	
				CI		0.17		0.18	
									Cop & Non-cop
Tumor n°7	60	560.7		**Coverage RTOG**		1.03			1.02 & 1.00

				HI		1.11			1 & 1
				CI RTOG		1.49			1.41 & 2.62
				TC		1			1 & 1
				CI		0.66			0.70 & 0.38
Tumor n°8	74	56.8 (CTV)		**Coverage RTOG**	0.97				0.97
				HI	1.12				1.12
				CI RTOG	2.56				2.61
				TC	0.99				0.99
				CI	0.38				0.38

Imax/IR	the homogeneity index (HI)
Imin/IR	the coverage index (Coverage-RTOG)
VIR/VT	the conformity index defined by the RTOG (CI RTOG)
VTIR/VT	the target coverage (TC)
VTIR/VIR	the conformity index (CI)

This table summarized the typical conformation indexes values of the treatment plans proposed in the different rooms for 8 different clinical cases. Indexes and rooms are defined in the Material and Method section. Tumors 1 & 2 are two head and neck tumors among seven studied, 3 & 4 are thoracic tumors among four studied, 5 & 6 are abdominal tumors, 7 is a pancreatic tumor and 8 a prostate tumor.

III – 3. Figures :

Figure 1:

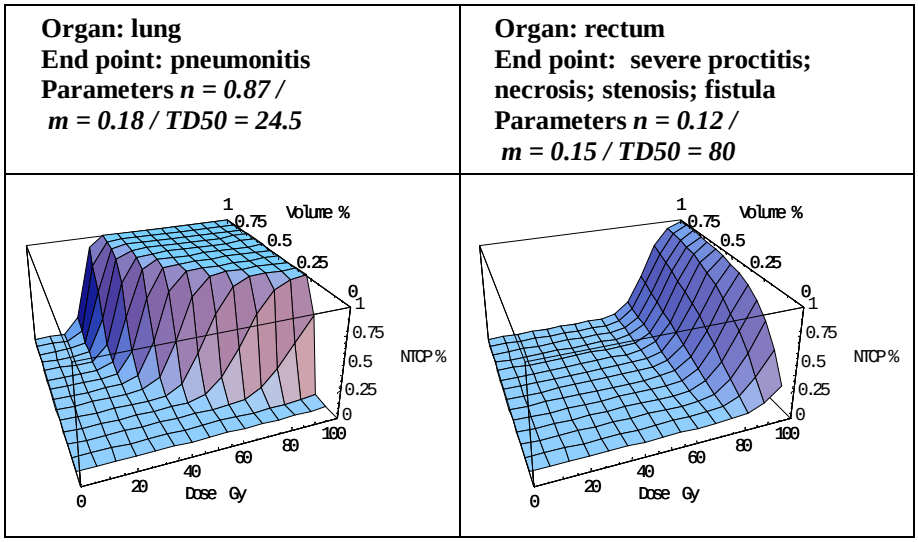

Complication probability (percentage) for lung & rectum displayed as a three-dimensional surface, function of dose (Gray) and partial volume (percentage). The shapes of the NTCP curves provide differences on the predictive part of the DVH for both organs. Original parameterization from Burman data [17].

Figure 2:

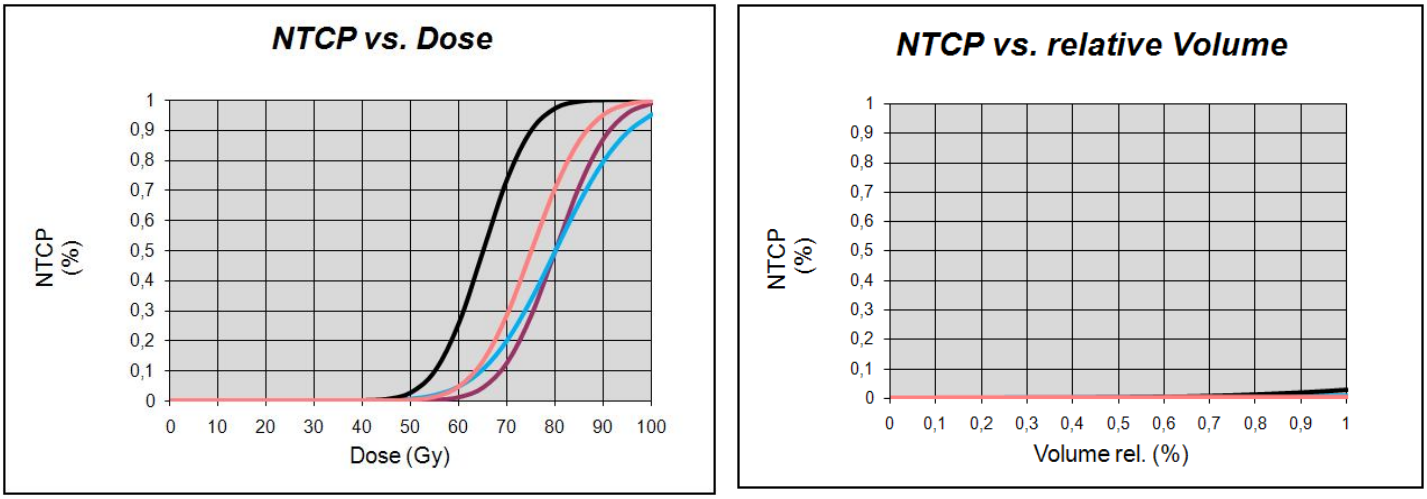

A **B**

Complication probability displayed as a function of dose and partial volume for uniform irradiation of whole organ. (**A**) Complication probability curves for the femoral head & neck (black / first along the top axis), cauda equina (orange / second along the top axis), bladder (brown / third along the top axis), rectum (blue / fourth along the top axis) as function of dose. (**B**) Complication probability curves for the cauda equina, femoral head & neck, bladder, rectum as function of uniform partial volume irradiation of 50 Gy. Original parameterization is from Burman data [17].

Figure 3:

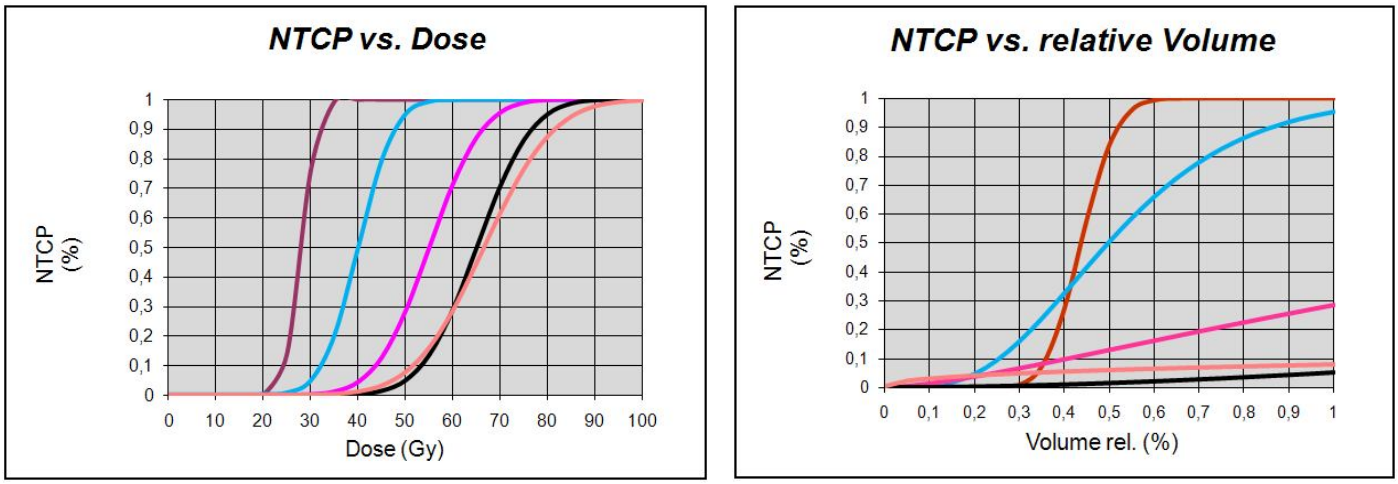

A **B**

Complication probability displayed as a function of dose and partial volume for uniform irradiation of whole organ. (**A**) Complication probability curves for the kidney (brown / first along the top axis), liver (blue / second along the top axis), small intestine (purple / third along the top axis), stomach (black / fourth along the top axis), spinal cord (orange / fifth along the top axis) as function of dose for uniform irradiation of whole organ. (**B**) Complication probability curves for the kidney (brown / first from the top), liver (blue / second from the top), small intestine (purple / third from the top), spinal cord (orange / fourth from the top) and stomach (black / fifth from the top) as function of uniform partial volume irradiation of 50 Gy. Original parameterization is from Burman data [17].

Figure 4:

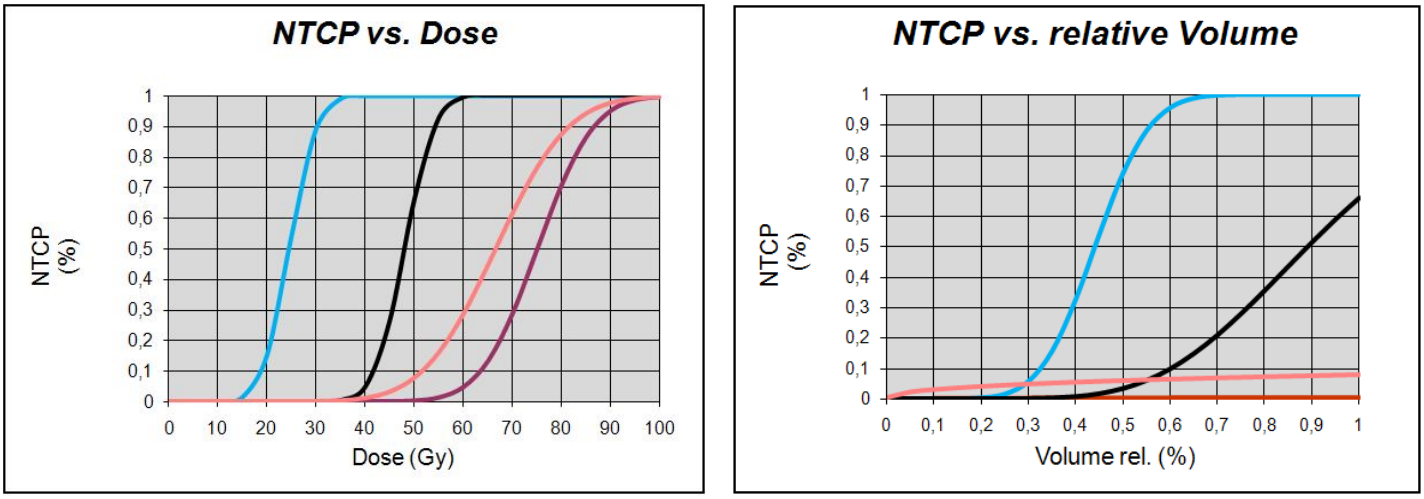

A **B**

Complication probability displayed as a function of dose and partial volume for uniform irradiation of whole organ. (**A**) Complication probability curves for the lung (blue / first along top axis), heart (black / second along top axis), spinal cord (orange / third along top axis), brachial plexus (brown / fourth along top axis), as function of dose for uniform irradiation of whole organ. (**B**) Complication probability curves for the lung, heart, spinal cord, brachial plexus as function of uniform partial volume irradiation of 50 Gy. Original parameterization is from Burman data [17].

Figure 5:

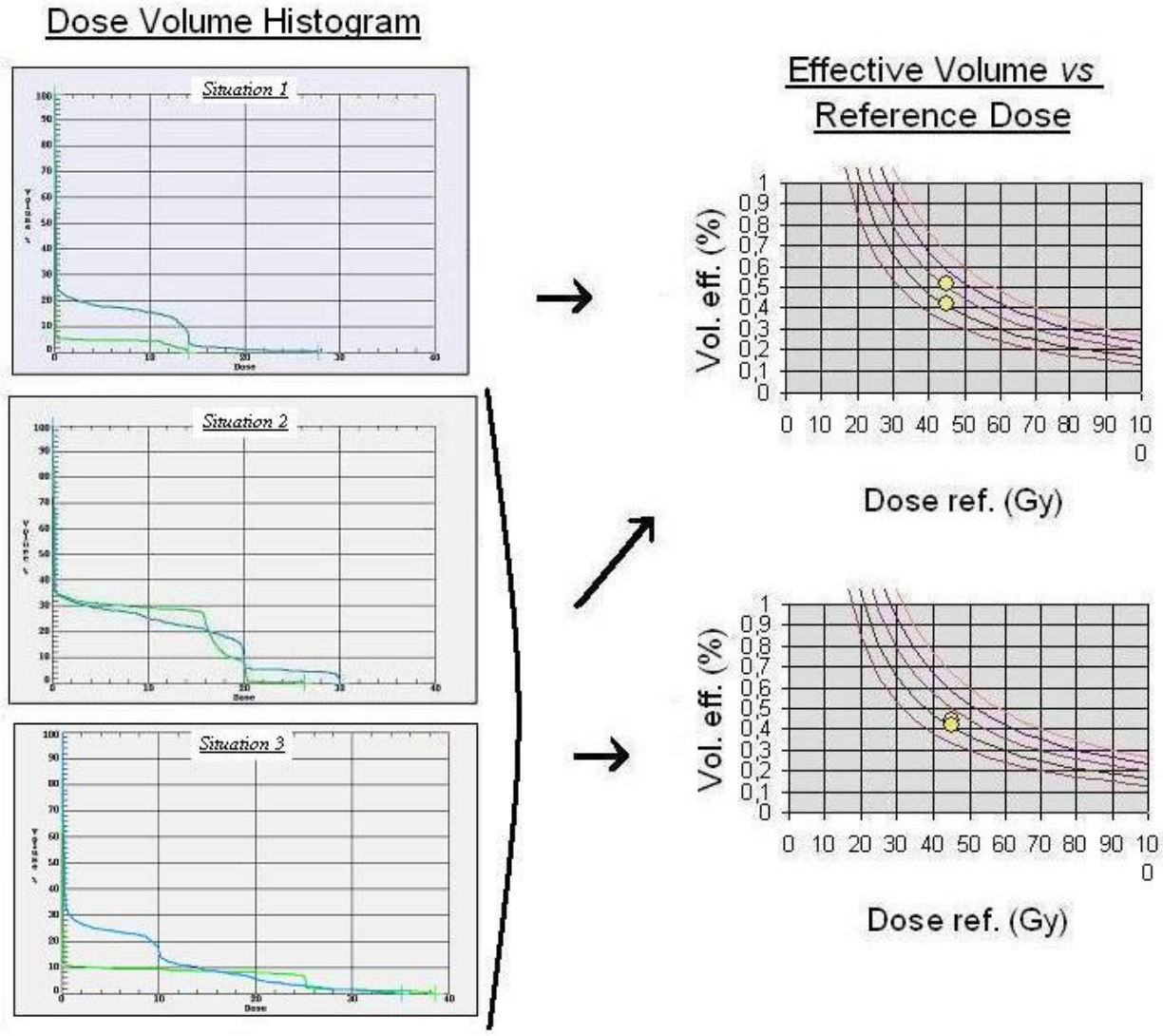

This didactic chart shows on *left column* the plots of cumulative dose-volume-histograms for 3 different techniques of irradiation showing different patterns of relative positions for the DVH curves of the same organ at risk. On the *right column* are presented corresponding plot's examples of Veff vs. reference dose (on an iso-NTCP graph (iso-NTCP lines are 5, 20, 50, 80, 95%).

- The first situation is characterized by thoroughly separated cumulative DVH curves providing obvious dosimetric distinction between the compared treatment plans (yet without certainty about the real clinical interest of this difference if no defined clinical endpoint is given).

- The second situation shows "a balanced" crossing of cumulative DVH curves for the organ at risk in a way that no straightforward decision could be made. Therefore more quantitative criteria based on clinical endpoint as given by the NTCP concept could be useful. NTCP could rank or not these techniques as showed by the example of iso-NTCP graph of the right column, providing the possibility of choice-making according to defined clinical endpoint.

– The third situation presents a high dose crossing of the DVH curves. The first curve, which seems apparently the best with less irradiation for a large part of dose-volume area, might provide in fact a higher complication probability according to its high dose position. Once again more quantitative criteria could discriminate these two situations.

<u>Figures 6</u> :

Entry ports of beam lines for abdominal and thoracic locations in different room configurations:

Figure 6D: ***Abdominal tumor, non-coplanar beams***	Figure 6C: ***Abdominal tumor, coplanar beams***
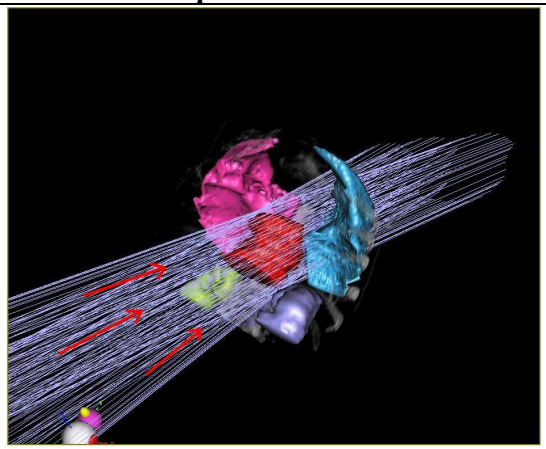	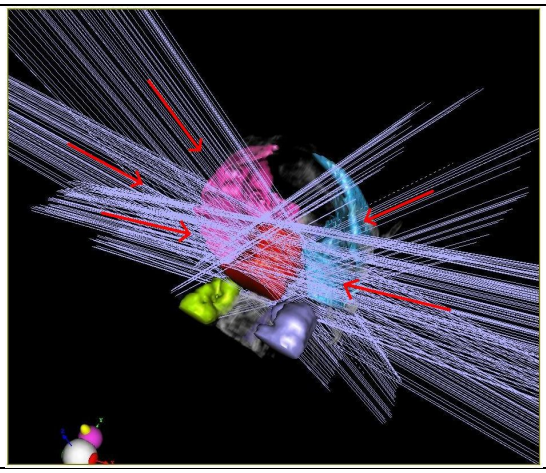
Figure 6B: ***Central lung tumor, non-coplanar beams***	Figure 6A: ***Peripheral lung tumor, coplanar beams***
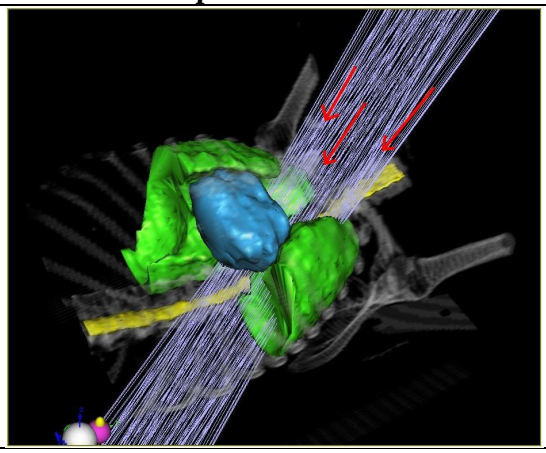	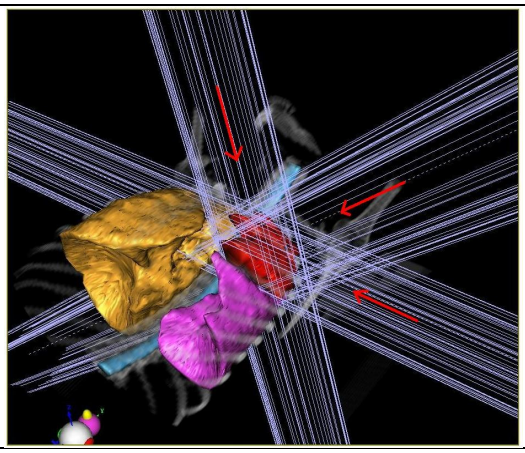

Entry ports of beam lines for abdominal and thoracic locations in different room configurations.

Figures 7 :

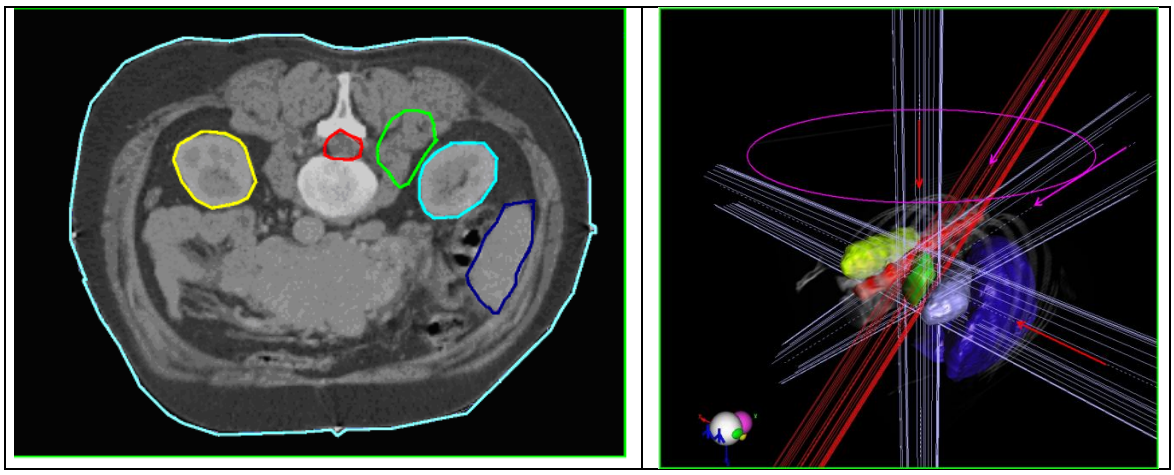

A retroperitoneal foreign body simulates a pararenal tumor. The tumor is delineated as the green mass in the screen captures. In both pictures the patient is in prone position. The red arrows indicate a right lateral beam and a posterior beam. The purple circle is the directrix (mathematical term) of a right circular cone with the purple arrow as generatrix (angle $\theta \sim 50°$ to the cone axis) and the isocenter tumor as the vertex of the cone. The surface of the circular cone simulates all the irradiation possibilities of an oblique fixed beam with a rotating isocentric couch. The two purple arrows indicate a right lateral oblique beam plus a postero-medial foot-oriented oblique beam. The ballistic for this simulated retroperitoneal pararenal tumor implies an ipsilateral irradiation.

Figures 8 :

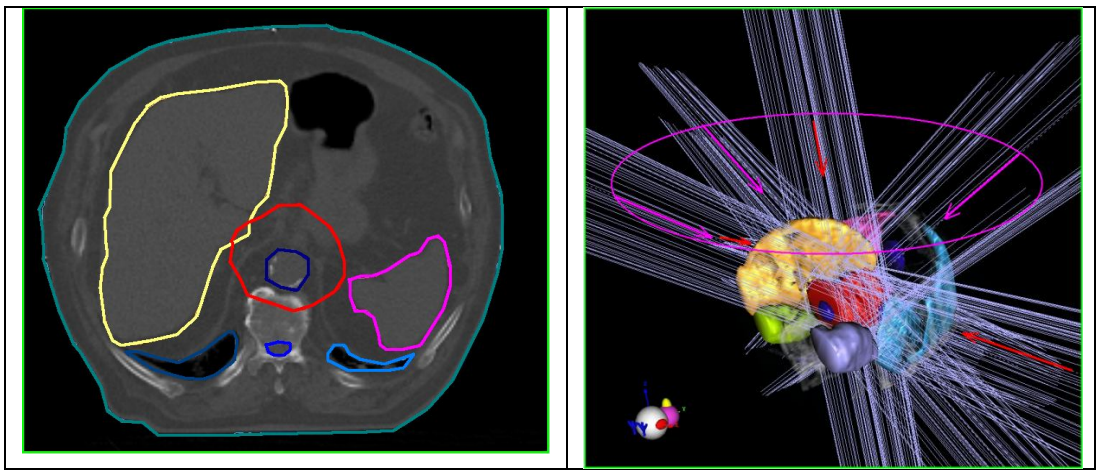

Paravertebral tumor. The tumor is delineated as the red mass in the screen captures. In the right picture, the patient is supine. The red arrows indicate a right and a left lateral beams plus an anterior beam. The purple circle is the directrix of a right circular cone with the purple arrow as generatrix (angle $\theta \sim 50°$ to the cone axis) and the isocenter tumor as the cone vertex. The surface of the circular cone simulates all the irradiation possibilities of an oblique fixed beam with a rotating isocentric couch. The three purple arrows indicate the right and left lateral oblique beams plus an antero-medial head-oriented oblique beam.

Figure 9 :

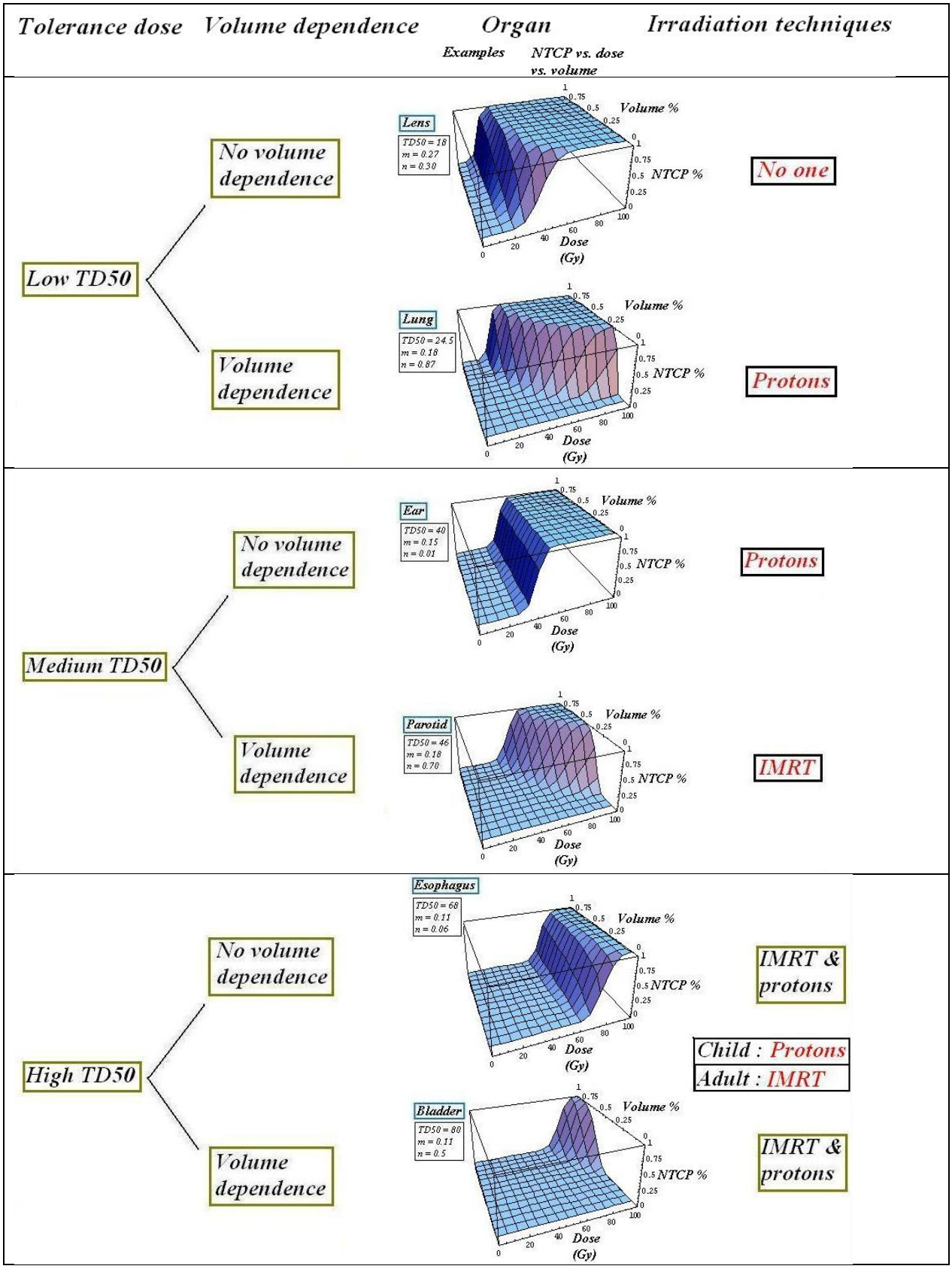

This didactic chart is an attempt of rational choice of the irradiation techniques according to the radiobiological characteristics of the principal organ at risk of a given treatment set-up as represented by TD50, volume dependence and NTCP behavior.

IV – Second Article :

IV – 1. A study of deterministic and stochastic effects for intracranial and head & neck tumors treated by protons for pediatric conditions: a quantitative comparative approach.

Yasid Boudam[1,2], Régis Ferrand[2], Anne Beaudré[3], Sylvie Helfre[2,3], Isabelle Flandin[4], Jean Louis Habrand[2,3], Jacques Balosso[1,4].

1 : Joseph Fourier University, Grenoble, France ; 2 : Protontherapy Center of Orsay - ICPO, BP65, F-91402 Orsay cedex, France; 3: Gustave Roussy Institut, Villejuif, France; 4: CHU de Grenoble.

Corresponding author: Pr Jacques BALOSSO
Department of Radiotherapy
Hôpital Michallon
BP 217
F-38043 GRENOBLE cedex 09
France
tel: +33 4 76 76 54 35
fax: + 33 4 76 76 56 29
JBalosso@chu-grenoble.fr

Key words: Radiotherapy, protons, hadrontherapy, onco-pediatry, deterministic risk, stochastic risk, treatment plan inter-comparison.

IV – 1.i. Abstract:

Purpose:
In the present work, representative pediatric intracranial and head & neck tumors have been studied. A solid and original approach is proposed for the estimation of the functional and anatomical development failures occurred by protontherapy (PT), for both deterministic and stochastic aspects. Clinical justifications and ballistic recommendations are released at last according to the different pathologies and clinical conditions.
Material and methods:
Seventeen medical records of young patients have been selected on the basis of their representativeness of four different pathologic types of intracranial and head & neck pediatric tumors: rhabdomyosarcoma, medulloblastoma, dysgerminoma and PNET. Different quantitative and qualitative criteria are combined to assess the tolerance of each treatment proposition. These criteria are the following: the treatment dosimetric quality indexes, the cumulative DVH, the cumulative irradiated volumes for different dose intervals and the carcinogenic risk estimation through different biological models.
Results:
The genetic condition (cancer prone diseases), the tumor location, the age of the patient (particular radiation sensitivity of very young patient), the differential sensitivity related to the age of treatment (early infancy, infancy, puberty) and the prescribed dose are the parameters interfering in the decision-making for the treatment planning in childhood radiotherapy. All these clinical parameters are combined to propose different standard techniques and treatment protocols with protons for these pediatric conditions.
Conclusion:
Although the PT is a highly performing technology, it can not entirely avoid some difficult compromises between efficacy and anatomical, functional or even neoplasic side effects inherent to the onco-pediatry. This investigation shows more clearly the limits inherent to the treatment of young patients, even by the use of PT. An appreciation which allows to pin point the strong and weak aspects of a technique which is called to develop strongly in a very near future.

IV – 1.1. Introduction :

Protontherapy applied for pediatric tumors is very attractive because of its ability to produce very accurate dose distributions with potentially much less irradiation to healthy tissues. However, radiation oncologists, experimented in pediatric photontherapy, have developed protocols with the concern of minimizing development failures for their young patients, often using as much as possible symmetrical and homogeneous treatment plan. The use of charge particles for such treatments is of interest since it allows very localized and conformal irradiations with intrinsically high dose gradients and strong dose heterogeneity. Therefore, the compromise between high dose-volume conformity, on the one hand, and potential consequences for healthy tissues especially at the point of view of the late effects, on the other hand, should be studied. In the present study we propose a ranking method for treatment plans, of intracranial and head & neck tumors in children, using a quantitative approach for the calculation of deterministic (development failures) and stochastic (secondary tumors incidence rate) effects. The objective of the present work is to provide to the clinicians arguments to discuss the choice of treatment plans for protontherapy on a relative risk (ratio of observed cases on the expected ones) of toxicity base.
Up to now very few propositions of analytical models for risk estimation of complications have been proposed in the frame of photon therapy [1] and even fewer for the comparison between photons and protons [2]. On the practical point of view also, very rare studies have compared treatment plans for real tumors as did Schneider et al. for Hodgkin's disease [3]. In the present work four different tumor types have been studied through 17 different real cases of patients aged from 1 to 20. The core methods of this study is i) the calculation of dose volume histogram for the assessment of the threshold-doses for organs at risk (OAR) and maturation areas; ii) the organ equivalent dose for radiation induced cancer incidence proposed by Schneider et al [4]. As a whole the decision making will rely on the compromise between expected toxicity to OAR, expected deficiency of maturation areas and the relative risk (between different treatment plans) of secondary cancers.

IV – 1.2. Material and method :

IV – 1.2.1. Patients' choice and treatment planning assessment

Seventeen medical records of young patients have been selected by two authors [AB and JLH] on the basis of their representativeness of four different pathologic types of intracranial and head & neck pediatric tumors often referred to their institution. Actually all these patients have been treated in the same institution by IMRT or 3D-CRT, photontherapy. Blindly toward the IMRT and 3D-CRT data two other authors belonging to another institution have computed the protontherapy treatment plans of the present study [YB and JB] starting only with anatomic data and tumor dose prescription. The patients' data are given in table 1.

IV – 1.2.2. Quantitative and qualitative criteria studied

Treatment dosimetric quality indexes have been taken from the RTOG [5, 6]. Two different indexes for dosimetric quality have been used: i) the homogeneity index (HI) defined as Imax/RI (Imax is the highest isodose, RI is the reference isodose chosen as the 95% of the prescribed dose); ii) the coverage index (Coverage-RTOG) defined as Imin/RI (Imin is the lowest isodose included in the tumor volume).
Treatment conformal quality indexes are three fold: i) the conformity index defined by the RTOG (CI RTOG) as VRI/VT [5,6] (VRI is the volume encompassed by the reference isodose, VT is the tumor volume equal to the GTV defined in the ICRU 50 report [7, 8]); ii) the target coverage (TC) defined as VTRI/VT [9, 10, 11] (VTIR is the volume of the tumor that is

encompassed by the reference isodose, $VT_{RI} = V_{RI} \cap VT$); iii) the conformity index (CI) defined as VT_{RI}/V_{RI} by Lomax et al. [11].

The cumulative DVH have been established for each dosimetric project to check the following data: the dosimetric constraints of healthy tissues (dose-volume relation and maximal doses), the assessment of the prescribed dose.

The calculations of the cumulative volumes irradiated for the dose intervals of [10 - 20 Gy] and [18 - 24 Gy] are used as criteria to determine respectively the risk of musculo-skeletal and skin hypo- & aplasia and somatotropic endocrine deficiency (first interval) and Intellectual Quotient maximum decrease of 10 points for whole brain irradiation (second interval).

Carcinogenic risk assessment
Assessment of the radiation-induced cancer incidence rates has been based on the estimates of the carcinogenic risks from ionizing radiation exposures as reported in UNSCEAR report 2000 [12]. These data have been computed by Schneider et al. for all types of solid tumors and for specific sites of solid tumors [4]. In the present study, the application of this method is limited to the relative comparison of the different treatment plans regarding the general risk for induction of solid tumors. Therefore we are allowed to use the carcinogenesis standard model for the solid tumors, adjusted to clinical parameters by Schneider et al. instead of the multiple specific sites models. This relative analysis is made in terms of dose-response assessment. Noteworthy, the reference volume – containing no specific organ, but healthy tissue of brain, head & neck region - chosen for the assessment of the carcinogenic risk, although arbitrary, should be kept constant throughout the study and should encompass at least the minimal isodose.
According to the different beam arrangements proposed by the different treatment plans, different dose-volume distributions are produced for each patient. The comparison of these different situations, for instance a large volume receiving low doses versus a small volume receiving large doses, cannot be done directly by the clinician. So that the comparison of calculated second cancer risk according to the standard model of carcinogenesis is useful. Briefly, the calculation of the organ equivalent dose (OED) makes possible to establish a correspondence between the inhomogeneous distribution of dose in the healthy tissue and the equivalent homogeneous one producing the same incidence of radio-induced cancer. Using the clinical parameters fitted by Schneider et al. we deduce the incidence rate for each treatment plan and can classify them according to these values. The radiobiology currently justifies this standard model as a competing process between the cell killing and the carcinogenic initiation where the radiation cell kill dominates over the carcinogenesis for high radiation doses. Wheldon and others [13, 14] relevantly introduce a more general analytical model including the normal & premalignant cell repopulation / proliferation phenomena along with the cell mutational radiosensitivity. Noteworthy, this phenomenon of active proliferation precisely characterizes the maturation areas of the pediatric tissues related to the maturation age. Based on the standard model, the generalization at these analytical concepts, including the repopulation kinetics, allow in this work a better understanding of the stochastic risk for the pediatric tissues and some more accurate comments, as proposed in the discussion section (see Figure 1).

IV – 1.2.3. Equipment used for the study
The dosimetries and DVH have been computed with either an ISIS or an ISOGRAY treatment planning software produced by the DOSIsoft Corp. (DOSIsoft SA, 45/47 av. Carnot – F-

94230 Cachan, France) routinely used for the protontherapy planning at the ICPO[4].

IV – 1.3. Results :

IV – 1.3.1. Ballistic study[5]

The respect of the threshold dose constrains of the OAR, and their optimizations when possible, generated the following ballistic choices:

Medulloblastoma
The CTV includes the posterior fossa and the brainstem. The considered OAR are the cochlea. The prescribed dose ranges from 50 to 54 Gy. The dosimetric constraints to the normal tissues and the volume minimization of isodoses in the normal cerebral parenchyma lead to an optimal irradiation with 5 coplanar beams (2 laterals, one posterior and 2 posterior oblique right and left) or another coplanar irradiation set-up with higher inter-beams angles. In case of mandatory lying position (with a unique horizontal fixed beam) an irradiation with 6 non-coplanar beams (lateral oblique) is proposed.

PNET [6]
The CTV is included in temporal and parietal areas, and very closed to the brainstem or even encompassing part of it. OAR included in the CTV, according to each patient case, are either the chiasm or the pituitary gland; for cochlea and optic nerve(s) only close proximity was observed. The prescribed dose is 54 Gy. The typical peripheral position of these tumors is consistent with coplanar or non-coplanar ipsilateral irradiations. The proposed solutions are threshold: i) 4 ipsilateral coplanar beams; ii) the same set-up plus 2 non-coplanar beams, namely supero- and infero- lateral oblique; iii) to compare with the other treatment plans, in particular for skin dose, we studied also a fully circular coplanar set-up (of course avoiding eyes).

Germinal tumors
The CTV includes the total volume of cerebral ventricles. The OAR are the chiasm, the brainstem and the spinal cord. The prescribed dose ranges from 40 to 54 Gy. A ballistic of 4 to 6 beams is proposed with lateral and lateral oblique beams in the same frontal plan.

Head & Neck rhabdomyosarcoma
The CTV includes the frontal sinus, the ethmoidal sinus and one maxillary sinus or is located in the rhino-pharyngeal region and the base of the skull. The OAR are multiple: eyes, lens, optic nerves, chiasm, cochlea's, thyroid, parotids and the other salivary glands. The prescribed dose ranges from 40 to 55 Gy. As a general rule, proton ballistic solutions should avoid to end a beam in closed contact to an OAR. Thus, optic tract needs oblique incidences to respect this rule. More specifically for cranio-facial tumors, the presence of air cavities, the sinus, which could be filled by secretion, could dramatically alter the beam range. Therefore the sinus presence prevents the use of patches, otherwise commonly used in protontherapy when sensitive OAR are located beside the CTV. Actually patch set-up would produce important

[4] Institut Curie – Centre de Protonthérapie d'Orsay.
[5] Usual terms for beam arrangement are used in this paper : so called "coplanar beams" are geometrically coplanar beams designed in the anatomical transversal plan; any other situations are named "non-coplanar beams".
[6] Primitive NeuroEctodermal Tumor.

overdose in the present case. For contralateral lens and parotid the goal was to completely avoid these OAR. In regards to these constraints a 4 beams ballistic is proposed for the facial tumors with a cranio-caudal beam, a coplanar ipsi lateral beam, a latero-oblique postero-anteriror and caudo-cranial beam and an oblique antero-posterior cranio-caudal beam (allowing avoiding one of the two lenses). For the rhino-pharyngeal tumor, a four-beam ballistic with coplanar ipsilateral beams is proposed.

IV – 1.3.2. Conformity indexes

In all the cases treated by protontherapy the conformation of the 95% isodose to 95% of the tumor volume is perfectly obtained:
- the dose homogeneity assess by both the coverage index (Coverage-RTOG =Imin/RI) and the homogeneity index (HI=Imax/RI) is excellent in any cases (CIRTOG range from 0.91 to 1.01 ; HI range from 1.04 to 1.06 , see the table 3 for all the index values).
- the target coverage (TC=VTRI/VT) is excellent and of same value (~0.99) for all the treatment plans. The tumor is circumscribed perfectly by the isodose 95%.

Considering these indexes (Coverage-RTOG, HI, TC) all treatment plans are equally fulfilling both the dosimetric constraints and the prescribed dose. Therefore these indexes do not permit further discrimination among these treatment plans.

About the other indexes:
Mild differences can appear for the conformity index defined by the RTOG (CI RTOG =VRI/VT) and the conformity index (CI=VTRI/VRI). Both are related to the volume of the reference isodose and to its - more or less important - spreading out into peripheral healthy tissues. A treatment is theoretically ideal when these indexes, CI RTOG & CI, are both equal to 1:
- CI RTOG ranges from 1 to 2 according to the treatment plan, with the exception of the germinal tumor having CI RTOG = 2.09. Thus the constraints of the treatment plans are respected for each of them and a minor deviation is only observed for the treatment of the germinal tumor.
- For CI, an irradiation is considered as conformal by Lomax et al., if and only if this index is equal to or higher than 0.6. According to this criterion, the irradiations of the medulloblastoma, PNET, parapharyngeal rhabdomyosarcoma are conformal. Some minor differences for CI RTOG & CI values are observed between plans of the medulloblastoma and the PNET ones. The details will be commented for each of them in the next section.

For the germinal tumor and the sinusian rhabdomyosarcoma, it appears that the RI for peripheral healthy tissues is not conformal according to the criterion mentioned above. These tumors seem to offer only one choice of treatment plan and prevent intrinsically all irradiation of better index. Indeed, the presence of sinus in the CTV of the sinusian rhabdomyosarcoma produces greater density heterogeneity and therefore a worse conformation of the 95% isodose (RI) to the CTV. For the germinal tumor, the CTV includes the whole cerebral ventricles, that are spread out and complex structures. Encompassing the totality of the ventricles by the reference isodose implies mandatory an important irradiation volume of non cortical healthy cerebral parenchyma, which is translated by suboptimal CI RTOG & CI values (respect. >2 & <0.6).

IV – 1.3.3. Comparison of CI RTOG & CI and secondary cancer risk (in relative terms) for the PNET and medulloblastoma treatment plans

Medulloblastoma

Three treatment plans are proposed: 2 coplanar and 1 non-coplanar.

For coplanar treatments a set of 5 beams is given for each of them:

- one plan concentrates the delivered dose exclusively by posterior irradiation as described above (treatment plan [a]).
- the other distributes the dose with higher inter-beam spacing with oblique interiors' (treatment plan [b]).

The non-coplanar one is delivered in a frontal plan with 6 beams. Overlapping beams should be avoided as much as possible (treatment plan [c]).

The conformity indexes indicate for [a], [b] and [c] treatment plans the respect of protocol and conformity constrains. The ranking, according to CI RTOG & CI values, establishes the following order: [c] better than [b] better than [a]. It can be observed that the larger is the number of beams and their inter-beam angles, the better is the conformation of the RI.

The study of the mid and low doses distributions is the following (see the table 5) :

- the cumulative volumes for [10-20 Gy] isodose interval of each treatment plan give a classification such as [a] better than [b] better than [c].
- the [18-24 Gy] interval gives an order such as [a] equivalent to [c] better than [b].

So [a] offers the best distribution for the low- and mid- doses whereas [b] and [c] are less distinguishable with [b] better for low-doses and [c] better for mid-doses.

It can be observed that the isodose volume distribution in the healthy tissues is altered according to the treatment plan.

To decide between these treatment plans, [b] and [c], the low- and mid- doses relative impact on stochastic risks has been evaluated (see the table 4). The classification yields [a] better than [b] better than [c]. Thus from a stochastic point of view, the treatment plan [b] is better than [c] in spite of more important mid-dose volumes according to the standard model that shows a decrease in risk beyond 12 Gy for solid tumors and thus the risk is greater with the low-doses (see Figure 2).

PNET

The tumor is lateral and located in left parietal.

Three treatment plans are proposed, two plans by ipsilateral irradiation with coplanar beams [d] and non-coplanar beams [e] and one plan with bilateral irradiation with coplanar beams [f].

According to the conformal indexes values, the treatments [d], [e], [f] respect protocol and conformity constraints. The ranking according to CI RTOG & CI values gives by conformal order of the reference isodose, [d] better than [e] better than [f] (see table 3). The same ranking is obtained for the isodose intervals of interest ([10-20 Gy] and [18-24 Gy]) (see table 5) and the risk of second malignancies (see table 4) .

So an ipsilateral irradiation is preferred for a lateral tumor of peripheral localization. A bi-lateral irradiation for such a location should be avoided because of the larger volume of low and mid-doses. Among the ipsilateral treatment plans, for all the dose levels, the coplanar set-up is the best one; moreover the non-coplanar treatment irradiates also a greater scalp surface.

IV – 1.3.4. Other tumors treatment plans

The germinal tumor, the sinusian rhabdomyosarcoma and the parapharyngeal tumor involve the choice of a unique treatment plan for each of them in respect of (i) the dose-volume constraints to the OAR, (ii) the dose threshold to the musculoskeletal system and skin, (iii) the minimization of volumes of irradiation in the healthy tissue.

Germinal tumor
The irradiation on a same frontal plan allows avoiding the irradiation of the healthy cerebral parenchyma in frontal, occipital and parietal areas.
The volume encompassed by the isodose interval [18-24 Gy] is large relatively to the tumor volume but not enough to reach the cortex region.
The volume of the isodose interval [10-20 Gy] is large also with a symmetrical distribution of the 10 Gy isodose on the lateral musculoskeletal tissues.

Parapharyngeal Rhabdomyosarcoma
The parotid and salivary glands adjacent to the tumor are injured. Dosimetric choices can safeguard the salivary glands opposite to the tumor by an ipsilateral irradiation, avoiding this way the xerostomia. The treatment of these superficial tumors implies high isodoses in surface regions which lead to muscular aplasia. Thus the irradiation will arrest tissue development in the mandibular region adjacent to the tumor and leave a print.
An ipsilateral irradiation with 4 beams allows minimizing the isodose volumes as much as possible and permitting to reduce in the same time the second malignancy risk.

Sinusian tumor
These tumors include the maxillary sinus, the ethmoidal and frontal ones and are surrounding one eye. The treatment will injure this eye but the other one can be completely spared. Doses superior to 20 Gy are reaching the surface close to the tumors and could produce a severe development arrest of the musculoskeletal tissues. The effects of the threshold doses have to be considered carefully; in fact the dose fractionation alters, from a deterministic point of view, the possible consequences of the radiation. The beams ports in more lateral areas will nevertheless reach doses between 10 and 20 Gy able to produce less severe hypo- and aplasia of these regions. A part of the frontal area of the brain is irradiated in the range of 18 to 25 Gy, values reached in the overlapping area of superior and antero-oblique beams. And finally, low doses are delivered in the frontal part of the brain by the anterior and superior beams.

IV – 1.4. Discussion:

The late effects on maturing tissues are an additional and critical constraint for childhood radiotherapy and have high impacts on the ballistic choices. The tolerance doses commonly used for adults in dosimetry (for complication probability of 5% and 50%), such as those tabulated by Emami et al. [15], take into account only the adult healthy tissues with no clinical endpoint regarding development failure for pediatric treatments. Actually on of the important concerns in onco-pediatry are the late effects that will compromise the young patient development with apparently no clinical damages at the very end of the treatment itself. These late effects are multiple with i) anatomical alterations as physical growth failure, musculoskeletal hypo- or aplasia with cosmetic changes occurred by asymmetric fat distribution according to the particular radiation sensitivity of adipose tissue; ii) functional alterations as neuro-psycho-cognitive ones due in particular to myelinisation changes in an irradiated normal brain. Thus, an additional difficulty for choice-making of treatment plan of

pediatric malignancies is to include the likelihood of immature organs injuries and the possible damages in the development of the child into a healthy adult.

What is more, the effect of dose- , tissue- , volume- and age-dependency of the maturing areas for the cerebral tissue or skeleton (for example vertebra and skull) vary during the childhood development (number, localization and sensitivity variation). Unfortunately a systematic and precise description of the anatomic structure and the localization of maturing areas according to the patient age and their corresponding dose tolerances is not available yet although general patterns of development are known [16]. Due to this lack of knowledge, the treatment delivery with specific sparing of sensitive sites could be difficult to plan and a conservative attitude could be proposed as a surrogate constraint: a homogeneous dose distribution with multiple beams. At first sight, the millimeter precision of proton beam could lose a part of its interest since more fields are necessary to obtain homogenous dose distribution in surrounding tissues such as for the photon IMRT technique. Indeed an antagonism appears between the proton precision and the uncertainty about the number and localization of maturation areas.
However, the consequence of this multiplication of beams is the increase of the tissue volume irradiated at low-doses that raises questions about the risk of stochastic effects (secondary cancers). In fact, this increase of low-dose volumes worsens the carcinogenic risk because of the premalignant cells initiation and repopulation / proliferation [14] in zones of maturation. On the other hand such dose distributions could avoid any deterministic toxicity related to high doses in OAR, but precluding the effectiveness of classical ranking of the treatment plans using DVH and even NTCP approach. Therefore, the possibility to evaluate the stochastic risks become necessary, and even required, for the choice-making among different treatment plans including propositions with numerous beams. This approach is possible thanks to analytical models of carcinogenic incidence rate, and has been applied in this work.

IV – 1.4.1. Dose constraints and dysfunctional growth of irradiated child, review and comments

The maturing tissues sensitivity and the development of the child in healthy adult is taken into account in the clinical requests for treatment planning. The tables of tolerance doses detail the thresholds of dose imposed to the OAR and the related clinical failures [table 2].
For brain irradiations, it has been reported: i) mild changes following 18 Gy to the whole brain in children with leukemia [17]; ii) some impairment in young children for doses of 18 to 24 Gy, whereas doses > 24 Gy involve risks of IQ decline [2] and iii) an IQ decrease of 10-25 points for whole brain irradiation of 24 Gy [18].
A growth defect occurs proportionally to the dose of cranial irradiation by its impact on hypothalamic-pituitary axis. Growth velocity during puberty is very sensitive to brain irradiation at this age [19]. Doses > 24 Gy to the whole brain induce severe growth hormone deficiency whereas doses ≤ 24 Gy may cause dysfunctional response to stimulation of growth hormone with normal levels of basal GH secretion [20].
For the musculo-skeletal system, hypoplasia occurs after doses of 10 Gy and aplasia after irradiations of 20 Gy [21, 22].

The pragmatic clinical approach needs a hierarchy among these different types of constraints. We have followed the following order: i) the respect of the threshold doses to the OAR (lens, eyes, optic nerve, chiasm, pituitary gland, hypothalamus, cerebral parenchyma, brainstem, spinal cord, thyroid, salivary glands); ii) the sparing of the musculo-skeletal tissues (hypo- or

aplasia concern); iii) the minimization of the isodose volumes and their associated stochastic risks.

The impact of these three constraints on the ballistic choices differs according to the clinical request: i) for the dose constraint to the healthy tissues, some beam orientations are mandatory to avoid these organs; ii) for the sparing of musculo-skeletal system and skin, the number of beams is increased to homogeneously distribute the dose; and iii) for the isodose volumes and their respective stochastic risks, in the frame of the standard model, the number of beams has to be reduced since the irradiation volume to lower doses is clearly related to the radiation-induced carcinomas according to different reports [1, 23]. Therefore regarding these clinical constraints, the ballistic implications can be antagonistic so that an order of priority fixed by advance is necessary and a compromise has to be made.

IV – 1.4.2. Stochastic effects, solid tumors and bone tissue cancer incidences

The studies show that the occurrence of secondary carcinoma is within the volume of irradiation [24, 25, 26]. The standard model of the dose-response relationship of second cancer incidence (restricted to solid tumors) has a shape of an asymmetrical peak with a maximum value around 12 - 13 Gy, followed by an exponential decay according to the clinical data fitted by Schneider et al [Figure 2]. This decay is explained by either the crude cell death beyond a certain dose or by the rising burden of mutations which leads to the cell death [27]. All this is detailed thereafter.

Le Vu et al. [28] observed that among childhood's solid cancers, ***the osteosarcoma*** was the most frequent second primary tumor type occurring during the 20 years following the treatment of an initial tumor. Tucker reports a SMN distribution for bone tissue neoplasia of 34% in the skull or mandible (in contrast to 4% primary neoplasia usually reached for children), 38% in the axial skeleton (in contrast to 21%), 28% in the long bones (in contrast to 2%). A great amplitude is observed for the skull and mandible, which are sensitive areas precisely for the rhabdomyosarcoma, the PNET and the medulloblastoma particularly investigated in this work. Le Vu et al. observed that the relative risk appeared linear (at least for low doses) according to the local dose of radiation, and the excess of relative risk per gray was estimated to 1.8. Moreover, two very different populations should be considered: i) one population has genetic predisposition. The relation between risk of bone SMN and genetic factors is clearly demonstrated for some conditions [29, 30]), as the bilateral retinoblastoma (RR of 999), Ewing sarcoma (RR of 649), rhabdomyosarcoma (RR of 297) and nephroblastoma (RR of 106) [31]. Consistently, in LeVu report these RR of secondary osteosarcoma (cohort compared to the general population) for 20 years of cumulative incidence is in the order of one thousand. ii) the population with no identified genetic alterations has a relative risk of secondary osteosarcoma for 20 years of cumulative incidence in the order of twenty [28]. Therefore, the structure of the observed population is very sensitive toward the level of the observed risk; in particular the proportion of retinoblastoma is to be carefully considered. However Tucker et al. [31] observed that although a very different risk level, the general shape of the dose-response curve is similar for retinoblastoma patient and other patients. Consistently with these caveats, Schneider et al. have proposed a dose-response relationship for secondary bone sarcomas for an Hodgkin's disease population, with a much lower risk, but with a very smooth shape with a maximum around 30 Gy and thereafter a very low decrease until more than 80 Gy. This shape along with its maximum position (centered on 30 Gy) is consistent with Le Vu and Tucker reports [28, 31] and more generally with the radiobiological comments as following.

Clearly the standard model is in agreement with the previous clinical data found in the literature in the frame of the "initiation – killing" competing phenomena. This current model is changed to the linear model when cell proliferation is additionally incorporated due to homeostatic control of the tissue after cell loss and/or cell repopulation in the maturation areas, after irradiation. The fractionation implies additional changes by its inherent inverse dose-rate effect, known as the "dose-protraction effect". For patients without genetic predisposition, the fractionation of the dose can therefore leads to a considerable reduction of the SMN rate, likely in connection with the effectiveness of the DNA repair mechanisms [27]. The curve appears flattened until giving an apparent linear relation in agreement with different clinical data. Additionally, the genetic sensitivity of the hereditary malignancies, which can be taken into account by the biological model, induces changes in magnitude of the carcinogenic response with higher amplitude of the asymmetrical peak in the standard model and a steeper slope in the linear model [see Figure 1].

All together, these convergent data and biological rational showed that secondary bone sarcoma is a specific condition. In the standard model it appears in a particular range of dose, but it can display multiple dose-response behaviors (magnitude variation, linear behavior…) which are to be specifically considered for the childhood treatment strategy as proposed in the present work.

For ***tissues other than bones***, identified risks of SMN are also to be considered. Actually, the conditioning preparation for bone marrow transplantation with total body irradiation yields a cumulative incidence of SMN of 8.3% at 13 years after treatment [32]. This value is important and shows that the irradiation of large volumes, even at low doses, could imply high secondary malignancies rates. Along the same line, an important relative risk of 21.7 of secondary central nervous system tumors for children < 6 years is observed after treatment by prophylactic cranial irradiation for acute lymphoblastic leukemia [33, 34, 35]. This particular sensitivity of young patient brain is precisely observed during the period of rapid proliferation and maturation of the cerebral tissue, period of high risk of deterministic and/or stochastic debilitating development after irradiation. This is true until the late infancy.

Thus the genetic condition (cancer prone diseases), the tumor location (central or near the surface), the age of the patient (particular radiation sensitivity of very young children), the differential sensitivity and response of the bones versus the parenchyma, along with the prescribed dose are all the parameters that should be taken into account in the decision-making for treatment planning in childhood radiotherapy.

IV – 1.4.3. Peripheral tumors near the surface

In the frame of protontherapy, for a prescribed dose of 55 Gy to the target volume, a dose of 20 Gy [7] at least is imposed to a part of the surrounding bone tissue whatever the technique proposed (ipsi- or bi-lateral irradiation). This is due to the inherent limit of the physic of the beam and the peripheral position of the tumor. These hot spots of dose to the surface could represent a significant factor of neoplasic osteosarcoma occurrence, particularly in the case of cancer prone genetic conditions. This genetic aspect represents an important point in regard to the difference of magnitude between the radio-responses (genetic versus non-genetic) and distinguishes the different propositions given below.

[7] 20 Gy is the threshold dose of aplasia in the osteo-muscular tissue; moreover this value is almost the lower limit of dose of the plateau in the plot of second malignant neoplasm (SMN) for bone tissue in the standard model (cf fig.2).

The clinical data for the ***regular situations*** (non cancer prone conditions) report a relative risk of bone SMN in the order of 20 [28, 31]. In this part three periods will be distinguished: early infancy, infancy and pre-adolescence considered together and lastly adolescence or puberty.
1) For infancy and the pre-adolescence stage the hypothesis of a flat analytical model and a plateau from 20 – 25 Gy, with then a very slow exponential decay for the higher doses (standard model hypothesis of carcinogenesis, Figure n° 2) is considered since low repopulation / proliferation process for bone tissue is observed during this period [16]. According to this smooth shape, the modelized response for the bones, outside of cancer prone condition, for doses higher than 20 Gy delivered to the bone tissue by an ipsilateral irradiation will induce a malignancy rate nearly equal to the one induced by dose limited to 20 Gy since both are in the plateau[8]. Moreover, few important parenchymas are irradiated, minimizing the occurrence of secondary solid tumors. This latter aspect is important since all this area is characterized by a rapid postnatal growth which slows in late infancy and ceases in adolescence, with a stochastic and deterministic debilitating risk particularly sensitive at this period as specified in previous section. Thus the neuroendocrine deficiencies are avoided thanks to the ipsilateral irradiation and the sparing of the healthy cerebral parenchyma. However, in regard to the deterministic effect, the threshold dose of 20 Gy is reached and the aplasia of the area closed to the tumor might consequently be induced whatever the proposed technique of irradiation. The deterministic and stochastic aspects imply only one possibility of compromise: 4 or even 5 *ipsilateral* beams.

The same ballistic scheme is applied in other periods of age but the predictions for the stochastic adverse effects are more pessimistic. Developmental skeletal pattern has a peak growth rate in the early infancy and another during the puberty.

2) The early infancy appears for both the bone and the cerebral tissues particularly sensitive. The maturation areas in these tissues induce a linear model of carcinogenesis since the repopulation kinetic is included in the model [14, 16]. The sensitivity of these proliferation areas should avoid any dose hot spot and mandates a homogeneous dose distribution with consequently numerous beams and an important volume of irradiation to the skull and the scalp. Noteworthy, thanks to the gradient of dose allows by PT the irradiation of the brain is much reduced, comparatively to the X-rays, thus reducing the risk of SMN in the cerebral tissue. This aspect of healthy parenchyma sparing is very important at this age where the brain is in its most sensitive period [16]. But the skull irradiation, even with a technique as accurate as the PT, induces for so young patients a clearly higher risk of neoplasic osteosarcoma.

3) For the adolescence period, the bone tissue sensitivity is principally to be considered, as specified above, and the risk of SMN in the skull is therefore the main concern. However, in regard to the lesser sensitivity of the brain at this period the general prognostic might appear at this age less pejorative than for early infancy.

The clinical data for ***cancer prone conditions*** report a very large relative risk of bone SMN in the order of 1000 [28, 31] and support: i) for children in period of infancy and the pre-adolescence the hypothesis of the standard model of induced carcinogenesis (an asymmetrical peak of great amplitude and an exponential decay for the high doses); ii) for children in early infancy or in the period of puberty, the linear model with a very steep slope. According to these carcinogenic hypothesis, the modelized response for the bone tissue in cancer prone condition, for doses above 20 Gy delivered by an ipsilateral irradiation could produce a

[8] This effect is enhanced by the fractionation schedule and its inverse dose rate effect, in that the curve peak is erased and the differences of response above 20 Gy are subsequently minimized.

steeply rising rate of neoplasic osteosarcoma compared to the one induced by only 20 Gy (which is already relatively high). If bilateral irradiation ports are used, about 20 Gy are still delivered to the bones closed to the tumor but the inherent occurrence of bone SMN in this area will be diminished compared to the former proposition of ipsilateral irradiation. However, additional doses of low values are delivered by these controlateral ports to larger volume of tissues with additional SMN risk in bone and healthy parenchyma. Thus the question is raised, for the cases of cancer prone conditions, if it is better to irradiate the bone tissue to higher dose with no radiation to the parenchyma, or to distribute lower doses to the bone and a larger volume of healthy parenchyma? In such a situation, the decision making would need information of exact absolute risk of each proposition. Unfortunately, such solid information is not available yet and this problem could be a suggestion for a clinical trial.

IV – 1.4.4. Non-peripheral tumors

For a non-peripheral tumor location, no unique ipsilateral irradiations are proposed. The *bilateral set-up* with a homogeneous dose distribution to the skin / muscolo-skeletal system appears the most preferred. This distribution minimizes as much as possible deterministic effects such as the psycho-neuro-cognitive effect and the hypo- or aplasia effect. However, this set-up induces a greater risk of carcinogenesis due to the large volume of irradiated tissues. To minimize the burden of this stochastic effect one should minimize the importance of the irradiated *volume* in the brain (small number of beams), and moderate the *dose* level delivered to the skull, which has a linear response in the ranges of low doses (multiplication of the entry ports) whatever the patient age. Although antagonistic, a compromise can be brought in the frame of a bilateral irradiation with 4 to 6 beams according to the value of prescribed dose. But in spite of this solution, it should be kept in mind, once again, that this technique is not 'the panacea'. Thus for the children in early infancy this ballistic induces a non negligible SMN risk for both the brain and the bone because of the particular developmental sensitivity of these tissues at this period. One can clearly consider that this age is of the most pejorative prognostic for SMN, especially for this type of ballistic (i.e. bilateral and symmetrical). For children in infancy and pre-puberty, an intermediate sensitivity is observed for the brain and a lower for bone, therefore a special attention should be brought to the brain. In adolescence period, the attention should better be brought to the bone tissue according to the growth rate of the skeletal at this period.

IV – 1.5. Conclusion :

So many parameters are involved in the radiobiological response of the tissues, particularly for childhood patients, that there is not a unique solution to propose as irradiation scheme. Although this real complexity, some general propositions could be drawn from this study. The protons allow, thanks to their precision, to respect the deterministic constrains of the treatment better what would conventional X-ray treatments do. Beyond this, the choice-making rely also on the optimization of the stochastic risk to develop a SMN after treatment, and therefore the finding of the best compromise between deterministic and stochastic constraints. As a general manner, the risk of neoplasia imply to avoid the great irradiation volumes and the hot spots in bone tissue for children, especially for those treated for retinoblastoma, Ewing or soft tissue sarcoma. The most straightforward tool to obtain this optimization is the DVH, however the effective comparison of different treatment plan would need an NTCP and OED approaches. A relative NTCP comparison remains unfortunately impossible for childhood treatments due to the lack of consistent radiobiological data. Nevertheless, the comparison of the SMN risk between different treatment plans is possible, even for childhood, and could be an interesting

approach of this question. Actually, this is of utmost importance for the particular population of cancer prone conditions as retinoblastoma, Ewing and soft tissue sarcoma primitive tumor. However, although PT is clearly of better value in ballistic term compared to the X-ray, this technique cannot completely avoid the debilitating risks related to the sensitivity of the childhood maturation tissues. The further optimization of the radiotherapy in childhood neoplasia needs substantial progress in the knowledge of the radiobiological models that apply to this particular population of patients. In the frame of this progress the right place of presently developing ion beam radiotherapy will have to be assessed. The complexity of the dose-effect relationship could make possible the existence of particularly advantageous applications of particle therapy in childhood, to investigate in the future.

IV – 1.ii. References :

[1] Hall EJ, Wuu CS. Radiation-induced second cancers: The impact of 3D-CRT and IMRT. *Int J Radiat Oncol Biol Phys* 2003;56(1):83-88.

[2] Fuss M, Poljanc K, Hug EB. Full Scale IQ (FSIQ) changes in children treated with whole brain and partial brain irradiation. A review and analysis. *Strahlenther Onkol* 2000;176:573-581.

[3] Schneider U, Lomax A, Lombriser N. Comparative risk assessment of secondary cancer incidence after treatment of Hodgkin's disease with photon and proton radiation. *Radiat Res* 2000;154:382-388.

[4] Uwe Schneider et al. Estimation of radiation-induced cancer from three-dimensional dose distributions: Concept of organ equivalent dose. *Int. J. Radiation Oncology Biol Phys* 2005;61(5):1510-1515.

[5] Shaw, E.; Kline, R.; Gillin, M.; Souhami, L.; Hirschfeld, A.; Dinapoli, R. et al. Radiation Therapy Oncology Group: radiosurgery quality assurance guidelines. *Int J Radiat Oncol Biol Phys* 1993;27:1231-1239.

[6] Shaw E, Scott C, Souhami L, Dinapoli R, Kline R, Loeffler J, et al. "Single dose radiosurgical treatment of recurrent previously irradiated primary brain tumors and brain metastases: final report of RTOG protocol 90-05". *Int J Radiat Oncol Biol Phys* 2000;47:291-298.

[7] International Commission on Radiation Units and Measurements. ICRU Report 50: Prescribing, recording, and reporting photon beam therapy. *Bethesda, MD: International Commission on Radiation Units and Measurements* 1993.

[8] International Commission on Radiation Units and Measurements. ICRU Report 62: Prescribing, recording, and reporting photon beam therapy (supplement to ICRU Report 50). Bethesda, MD: International Commission on Radiation Units and Measurements, 1999

[9] Lefkopoulos, D.; Schlienger, M.; Touboul, E.; Hancilar, T.; Merienne, L.; Mitsoura, H.; et al. Quantitative evaluation of treatment planning for linac multi-isocentric radiosurgery. Proc of the Xith Intern Conf on: «Computers in Radiation Therapy», Xith ICCR, Manchester, UK; 1994. p. 296-297.

[10] Lefkopoulos D, Dejean C, El-Balma H, Platoni K, Grandjean P, Foulquier JN et al. "Determination of dose-volumes parameters to characterise the conformity of stereotactic treatment plans". *Proc of the XIIIth Intern conf on*: "Computers in Radiation Therapy", XIIIth ICCR, Heidelberg, Germany; 2000. p. 356-358.

[11] Lomax NJ, Scheib SG. "Quantifying the degree of conformity in radiosurgery treatment planning". *Int J Radiat Oncol Biol Phys* 2003;55:1409-1419.

[12] UNSCEAR. Report to the General Assembly: Sources and effects of ionizing radiation. Volume II; Annex I: Epidemiological evaluation of radiation-induced cancer.

[13] Lindsay KA, Wheldon EG, Deehan C, Wheldon TE. Radiation carcinogenesis modelling for risk treatment-related second cancer tumors following radiotherapy. *The British Journal of Radiology* 2001;71:529-536.

[14] Sachs RK, Brenner DJ. Solid tumor risks after high doses of ionizing radiation. *Proc Natl Acad Sci U S A* 2005;102:13040-13045.

[15] Emami, B.; Lyman, J.; Brown, A.; Coia, L.; Goitein, M.; Munzenrider, J. E.; Shank, B.; Solin, L. J.; Wesson, M. Tolerance of normal tissue to therapeutic irradiation. *Int J Radiat Oncol Biol Phys* 1991;21:109-122.

[16] Halperin EC, Constine LS, Tarbell NJ, Kun LE. Pediatric radiation oncology, 1994 (2nd edn). New York: Raven Press.

[17] Muchi H, Yamamoto K, et al. Studies on the assessment of neurotoxicity in children with acute lymphoblastic leukaemia. *Cancer* 1987;59:891-895.

[18] Meadows AT, Gordon J, Massari DJ, et al. Declines in IQ scores and cognitive dysfunctions in children with acute lymphocytic leukaemia treated with cranial irradiation. *Lancet* 1981;7:1015-1018.

[19] Silver JH, Littman PS, Meadows AT. Stature loss following skeletal irradiation for childhood cancer. *J Clin Oncol* 1990;8:304-312.

[20] Kirk JA, Raghupathy P, Stevens MM et al. Growth failure and growth-hormone deficiently after treatment for acute lymphoblastic leukemia. *Lancet* 1987;1:190-193.

[21] Furst CJ, Lundell M, Ahlback SO et al. Breast hypoplasia following irradiation of the female breat in infancy and early childhood. *Acta Oncol* 1989;519-523.

[22] Rosenfield NS, Haller JQ, Berdon WE. Failure of development of the growing breasts after radiation therapy. *Pediatr Radiol* 1989;19:124-127.

[23] Followill D, Geis P, Boyer A. Estimates of whole-body dose equivalent produced by beam intensity modulated conformal therapy. *Int J Radiat Oncol Biol Phys* 1997;38:667-672.

[24] Hancock SL, Tucker MA, Hoppe RT. Breast cancer after treatment of Hodgkin's disease. *J Natl Cancer Inst* 1993;85(1):25–31.

[25] Sankila R, Garwicz S, Olsen JH, et al. Risk of subsequent malignant neoplasms among 1,641 Hodgkin's disease patients diagnosed in childhood and adolescence: a population based cohort study in the five Nordic countries. *J Clin Oncol* 1996;14:1442–1446.

[26] Li FP. Colon cancer after Wilms' tumor [letter]. *J Pediatr* 1980;96:954–955.

[27] Hall EJ. Radiobiology for the radiologist, 1994 (4th edn). Philadelphia: J. P. Lippincott.

[28] Le Vu B, de Vathaire F, Shamsaldin et al. Radiation dose, chemotherapy and risk of osteosarcoma after solid tumors during childhood. *Int J Cancer* 1998;77(3):370-377.

[29] Eng C, Li FP, Abramson DH, et al. Mortality from second tumors among long-term survivors of retinoblastoma. *J Natl Cancer Inst* 1993;85:1121–1128.

[30] Kitchin FD, Ellsworth RM. Pleiotropic effects of the gene for retinoblastoma. *J Med Genet* 1974;11:244–246.

[31] Tucker MA, D'Angio GJ, Boice JD et al. Bone sarcomas linked to radiotherapy and chemotherapy in children. *N Engl J Med* 1987;317:588-593.

[32] Bhatia S, Ramsay NKC, Steinbuch M, et al. Malignant neoplasms following bone marrow transplantation. *Blood* 1996;87:3633–3639.

[33] Takaue Y, Sullivan MP, Ramirez I, et al. Second malignant neoplasm in treated Hodgkin's disease. *JAMA* 1986;140:49–51.

[34] Nygaard R, Garwicz S, Haldorsen T, et al. Second malignant neoplasms in patients treated for childhood leukemia. *Acta Paediatr Scand* 1991;80:1220–1228.

[35] Neglia JP, Meadows AT, Robison LL, et al. Second neoplasms after acute lymphoblastic leukemia in childhood. *N Engl J Med* 1991;325:1330–1336.

IV. 2. Tables :

Table 1: Patient characteristics

File number	*Age (years)*	*Gender*	*Pathology*	*Tumor location*	*Total dose (Gy)*
1	20	M	Embryonic rhabdomyosarcoma	Ethmoid + int orbital + max sinus + intracranial (supra orbital)	50.0
2	9	M	Alveolar rhabdomyosarcoma	Sphenoid, ethmoid and posterior orbital	50.40
3	17	M	Embryonic rhabdomyosarcoma	L parapharyngeal region	65.0
4	16	F	Alveolar rhabdomyosarcoma	Extension ext wall piriform sinus, R post region cavum	52.0
5	15	F	Embryonic rhabdomyosarcoma	Cavum + oropharyngeal (L amygdala) + base of the skull	41.40
6	11	M	Medulloblastoma (C71.6)	Posterior fossa with dorso-lumbar-medullary metastasis	53.60
7	3	F	Medulloblastoma (C71.6)	V4	50.4
8	3	F	Medulloblastoma (C71.6)	Metastatic medulloblastoma (CRL)	50.0
9	6	M	Medulloblastoma (C71.6)	M+ hypophysary, CRL+	54.0
10	10	M	Dysgerminoma	Pineal gland	40.0
11	7	M	Dysgerminoma	Pituitary axis	39.60
12	18	M	Dysgerminoma	Pineal gland	54.0
13	13	M	Anaplastic astrocytoma	Thalamo-peduncularis	54.0
14	12	M	Anaplastic oligodendroglioma (C71.-)	Thalamus and left cerebral peduncles	54.0
15	17	F	Pilocytic astrocytoma (C71.-)	Low grade oligoastrocytoma subtotal resection	54.0
16	10	M	Anaplastic oligodendroglioma (C71.-)	Thalamus	54.0
17	1	M	Carcinoma	Right parietal	50.40
18	1	F	Neuroblastoma	Surrenalian	21.60

Table 2: Tolerance doses

Endocrinal glands and other OAR:

	Dose	***Failures***
Hypothalamus	18 Gy	Hyposecretion of growth hormone
Hypophysis	40 Gy	Hyposecretion of all the hormones
Brain	18 Gy	Difficulty of training still IQ decline
Optic nerve, chiasma	50 Gy	Blindness
Lens	10 Gy	Cataract

Osteo-muscular system and skin:

	Dose	***Failures***
Temporary cartilage	10 Gy	Growth arrest
Vertebra (asymmetrical irradiation)	10 Gy	Scoliosis-kyphosis
Muscles and subcutaneous tissue	10 Gy	Hypotrophy
Dental follicles	20 Gy	Hypotrophy
Muscles	20 Gy	Hypoplasia

These tables give the tolerance doses for different systems and organ or tissue according to clinical endpoints in pediatric condition. These threshold doses are at the present time the dosimetric constraints commonly recommended in the treatment centers and considered in the present work.

Table 3 : Conformation index values

Patient files	**1**	**5**	**6-[a]**	**6-[b]**	**6-[c]**	**10**	**13-[d]**	**13-[e]**	**13-[f]**
Prescribed dose (CGE)	50.0	41.4	53.6	-	-	54.0	54.0	-	-
VT = CTV (ml)	69.4	202.5	142	-	-	42	280	-	-
Indexes									
Coverage RTOG	0.91	0.97	1.01	1.01	0.97	0.96	0.95	0.99	1.01
HI	1.05	1.04	1.06	1.06	1.06	1.05	1.05	1.05	1.05
CI RTOG	1.79	1.48	1.61	1.45	1.08	2.09	1.25	1.39	1.55
TC	0.99	0.99	0.99	0.99	0.99	0.99	0.99	0.99	1
CI	0.55	0.67	0.61	0.68	0.92	0.47	0.79	0.71	0.64

Imax/IR	the homogeneity index (HI)
Imin/IR	the coverage index (Coverage-RTOG)
VIR/VT	the conformity index defined by the RTOG (CI RTOG)
VTIR/VT	the target coverage (TC)
VTIR/VIR	the conformity index (CI)

This table summarizes the values obtained for the conformation indexes of the treatment plans proposed for 4 different clinical cases (i.e. rhabdomyosarcoma, PNET, dysgerminoma, medulloblastoma). The indexes are defined in the second table. The files 1 & 5 are the sinusian and the parameningeal rhabdomyosarcoma treatment plans. The treatment plans 6 -[a], -[b] & -[c] are for the medulloblastoma, the ballistic schemes being defined in the Results/Medulloblastoma section. The file 10 is the dysgerminoma. The histology of the 13 -[d] -[e] & -[f] is the PNET, the ballistic schemes being defined in the Results/PNET section.

Table 4: Estimated cancer incidence for solid tumors

Patient files	***OED (Gy)***	***Estimated cancer incidence [/10,000/year]***
1	0.79	22.02
5	0.98	26.96
6-[a]	1.05	28.68
6-[b]	1.47	38.84
6-[c]	1.71	44.3
10	1.56	40.97
13-[d]	0.76	21.17
13-[e]	1.13	30.77
13-[f]	1.33	35.57

This table summarizes the organ equivalent dose (OED) values and their respective estimated cancer incidence according to the standard model of carcinogenesis and the Schneider et al. parameterization [4] for the SMN of solid t. The clinical cases linked to the patient files number are detailed in table 1 and in caption of table 3.

	Medulloblastoma		PNET	
	Ratio [c]/[b]	**Ratio [c]/[a]**	**Ratio [f]/[e]**	**Ratio [f]/[d]**
Relative Risk	**1.14**	**1.54**	**1.15**	**1.68**

The values of the relative risk of second cancer (of solid type) are summarized for the medulloblastoma and the PNET treatment plans for an estimated cancer incidence evaluated according to the Schneider et al. parameterization [4]. The relative risks are calculated as the ratio of the estimated cancer incidence of a treatment plan using a large number of beams versus a treatment plan with a reduce number of beams. These results are obtained considering that the peak value for SMN incidence is 12 Gy.

Table 5: Volume versus dose intervals

Patient files	**Volume cm3** ***10Gy - 20Gy***	**Volume cm3** ***18Gy - 24Gy***
1	340	100
5	257	111
6-[a]	149	101
6-[b]	177	117
6-[c]	287	98
10	417	170
13-[d]	336	39
13-[e]	376	89
13-[f]	592	289

This table summarizes the values of the cumulative volumes irradiated (cm3) for the dose intervals of [10 - 20 Gy] and [18 - 24 Gy] for 4 different clinical cases. The clinical cases linked to the patient files number are detailed in table 1 and in caption of table 3.

IV – 3. Figures :

Figure 1 :

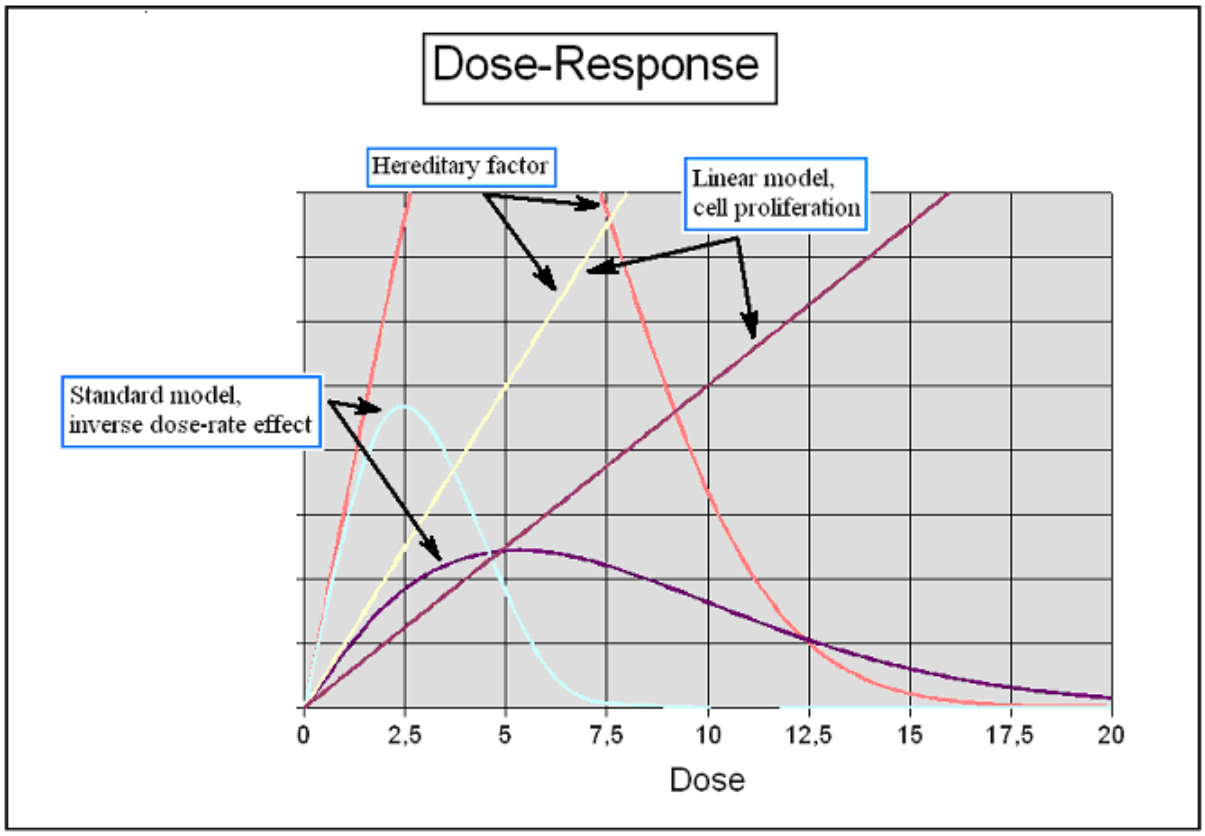

This chart shows the two oncogenic models: the standard model (cell sterilization phenomena) that describes the behavior of non proliferating tissues and the linear one (cell proliferation or tissue repopulation) that describes the risk for proliferating tissues. Each model could undergo transformations also shown on the figure. The standard model is modified by the inverse dose-rate effect due to fractionation and its magnitude is enhanced by hereditary factors; similarly the slope of the linear model is increased by hereditary factors. These representations have been computed according to the analytical model developed by Sachs et al [14] with arbitrary parameters.

Figure 2 :

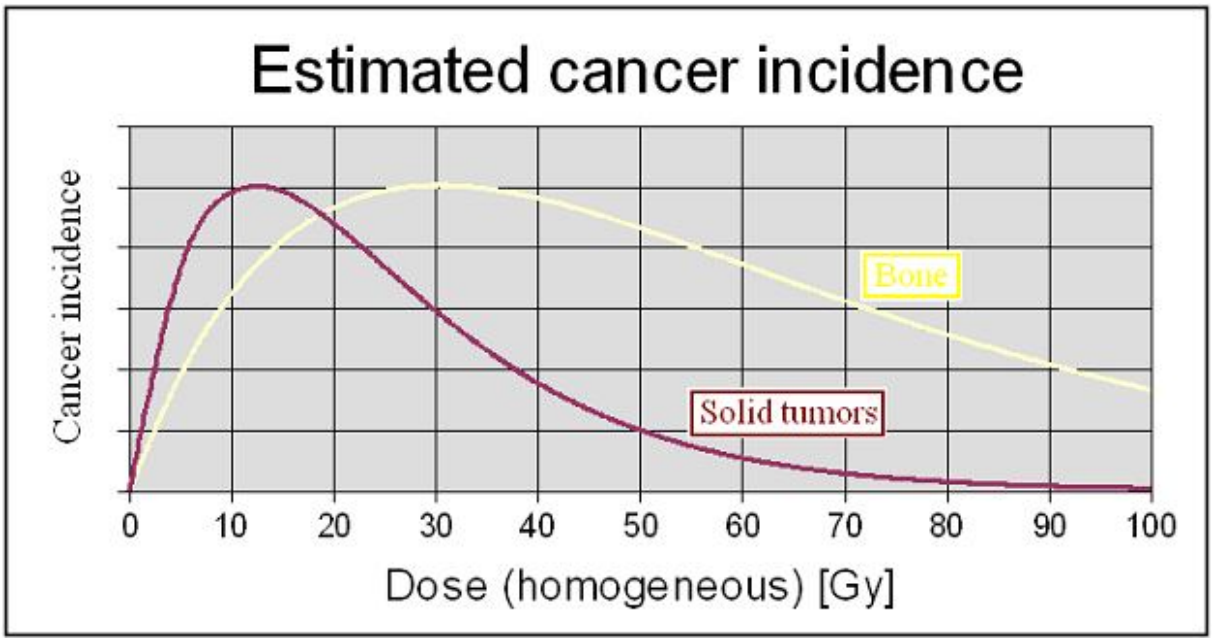

This chart represents with the same arbitrary carcinogenic amplitude bone and solid tumors curves to emphasise the relative positions of their maxima and their general shape. This representation is made according to the standard model with the parameterization used by Schneider et al [4]. This is a simplified visualization of the risks of solid secondary tumors (brown / first along the top axis) and bone tumors (yellow / second along the top axis).

V - Pages liminaires du troisième article :

V – 1. Les modèles de calcul suggèrent avec les ions carbone un risque néoplasique radio-induit moindre que pour les photons

Ce troisième chapitre tente de définir certains problèmes relatifs aux atteintes du tissu sain par les ions carbone. L'article 3 propose ainsi toute une discussion sur les ions carbone et le risque de carcinogénèse radio-induit. Clairement, le traitement par ce type d'irradiation ne voit-il pas ses bénéfices potentiels être dégradés par le risque d'induction néoplasique après traitement chez l'adulte et plus spécifiquement chez l'enfant, notamment par rapport aux photons ?

Une discussion est menée dans l'*article 3* sur la base de simulation de données par l'utilisation de modèles de calcul i.e. le modèle *standard* et le modèle de *repopulation* (détaillés dans l'article). Les données épidémiologiques et l'utilisation de la littérature permettent de mieux cerner les phénomènes (parfois antagonistes) mis en jeu dans la carcinogenèse radio-induite. Les ions carbone en entrée de faisceau, dans le plateau et dans le pic de Bragg sont alors comparés à une irradiation photon (15 MeV d'énergie maximale). La simulation de données semble indiquer que les ions carbone induiraient un phénomène de stérilisation cellulaire (phénomène de mort cellulaire des cellules dysplasiques *in vivo*) à doses *intermédiaires* & *hautes* dans les tissus & organes chez l'adulte et l'enfant. En conséquence les ions carbone permettraient de diminuer le risque carcinogène par rapport aux photons dans les tissus à cinétique de repopulation importante (les tissus en développement et en maturation chez l'enfant). Le maintien de cet effet de stérilisation des cellules dysplasique par les ions carbone dans les tissus en développement et maturation est particulièrement remarquable car il prédit une diminution du risque néoplasique des ions légers *a contrario* de la simulation des données en photon et des données épidémiologiques des photons trouvées dans la littérature. En effet, à même dose physique les photons induisent une augmentation constante du risque pour les tissus en développement (le faible âge du patient au moment du traitement étant un critère péjoratif). Enfin l'hypofractionnement de la dose accentue cette action bénéfique des ions carbone. La stérilisation cellulaire par les ions carbone fait chuter drastiquement les niveaux de risque carcinogène chez l'adulte et l'enfant.

V – 2. La question posée de la radioprotection des tissus sains chez l'enfant

Cette simulation est un premier signe encourageant pour l'utilisation des ions carbone en onco-pédiatrie mais qu'en est-il de la radioprotection des tissus sains irradiés (i.e. risques déterministes) et plus particulièrement dans les tissus et organes en développement et en maturation ? Les caractéristiques radiobiologiques des ions carbone (paramètres de radiosensibilité intrinsèque) sont-ils un avantage *ou* un désavantage au traitement des plus jeunes patients ? Sur quel critère fonder sa prise de décision lorsque sont présentés divers choix de balistique, notablement chez l'enfant ? La discussion suivante essaie de poser les premiers jalons de l'étude qui devra être menée sur la radioprotection des tissus sains après traitement par ions carbone, en particulier chez l'enfant.

V – 3. Description succincte du développement cérébral postnatal – croissance & maturation

La neurogenèse avec organisation corticale (gyrification[9]) a lieu lors des différentes phases de maturation cérébrale ***prénatale***. A la naissance, la multiplication des neurones aura pris fin à quelques exceptions près (e.g. présence de cellules souches neurales dans le gyrus dentelé de l'hippocampe), le nombre de neurone est alors considéré comme fixe et la genèse de nouveaux sillons terminée. Le processus de développement cérébral ***postnatal*** implique spécifiquement une multiplication des connections neurales (croissance des dendrites & axones, appelée synaptogenèse), une myélinisation des axones (appelée myélogenèse, elle induit une accélération de la transmission des influx) et un développement de la glie. Ce développement cérébral ne se fait pas de manière homogène. Le développement de l'arborisation dendritique[10] et de la myélinisation est en effet séquentiel, se réalisant suivant une chronologie d'événements bien précise.

Une période importante de genèse (i.e. synaptogenèse & myélogenèse) a lieu dans les 2 premières années de vie de l'enfant. Le périmètre crânien prend alors 14 centimètres pour ne gagner dans les 16 années de vie suivantes que 6 centimètres. Après cette intense période de genèse de 2 ans, un remodelage séquentiel des constructions synaptiques initiales prend place par un jeu complexe de croissance *vs* stabilisation *vs* élimination sélective des connections neuronales, il s'agit alors d'une régression ciblée du nombre de synapse initialement en excès (après l'intense genèse des 2 premières années). Ce remodelage suit une chronologie spatiale (i.e. les structures du cerveau) et temporelle (âge de l'enfant) dont l'architecture peut s'avérer assez complexe [5]. L'IRM fonctionnel (IRMf) permet de visualiser ces zones en activité. Le métabolisme inhérent au développement différentiel des aires cérébrales s'accompagne en effet d'une modification locale du débit sanguin cérébral. Le développement cérébral peut sommairement se résumer tel que suit.

Au départ le métabolisme cérébral est intense au niveau des noyaux gris centraux et des régions sensitivo-motrices. Le développement gagne à 3 mois les régions occipitales, puis temporales et à 8 mois les régions frontales. La croissance est ainsi inhomogène avec un pic de la synaptogenèse dans le cortex moteur (région fronto-pariétale à l'avant du sillon central) entre 6 mois et 2 ans. La synaptogenèse prend part dans le cortex visuel (occipital) puis le cortex auditif (temporal) jusqu'à 2-3 ans alors que dans le cortex frontal elle va de 1 an jusqu'à la puberté.

Quand à la myélogenèse, elle commence dans le cortex moteur pour s'étendre à l'avant et à l'arrière. Elle se fait à partir de 1 an et se prolonge jusqu'à la puberté et permet le développement des fibres d'associations cortico-corticales (radiations optiques, acoustiques…), cortico-cérébello-corticales, etc. Ces faisceaux seront importants dans la mise en réseau des différentes zones cérébrales, associations appelées *réseaux neuronaux* à l'origine des capacités évoluées (psycho-cognitives, sensitives…) du cerveau humain. Un paragraphe leur sera consacré plus bas car leur implication dans le choix de traitement par ions carbone pour l'enfant gagnerait à être étudiée. En effet, les ions carbone permettent-ils de créer un différentiel thérapeutique avantageux en évitant ces structures fragiles par rapport aux traitements photons et protons ?

[9] Création des circonvolutions cérébrales

[10] Chez l'adulte chaque neurone établit 1000 à 10000 connections avec d'autres neurones.

V – 4. De la nécessité de ne pas léser les structures cérébrales – Protocoles pédiatriques

Tel que l'*article 3* tendrait à le montrer, le risque carcinogène après irradiation par ions carbone semblerait moindre par rapport aux photons, particulièrement en cas d'hypofractionnement de la dose. Qu'en est-il des possibles lésions occasionnées par les ions carbone (d'EBR ~ 3 en fin de parcours) sur les aires cérébrales ? Chez l'enfant où se réalisent le développement et la maturation des circuits neuronaux, serait-il plus judicieux d'utiliser les ions carbone de diffusion latérale et distale moindre plutôt que les protons ? Cependant l'impact des ions carbone du point de vue de la radioprotection des tissus sains est encore à étudier.

L'avantage du profile de dose inversé (pic de Bragg), de la diffusion latérale et de l'EBR des ions carbone appliqué à un plan de traitement *vs* les protons et l'IMRT a largement été exposé par Oliver Jäkel et ses collègues du DKFZ de Heidelberg et Darmstadt. La caractéristique du design dosimétrique par ions carbone est une balistique à 2 ou 3 faisceaux d'irradiation, mais ce faible nombre de faisceaux oblige à certaines précautions sur le choix de leurs incidences. La précision millimétrique des ions carbone trouverait en définitif leur pleine justification si cette précision permettait d'éviter les structures cérébrales les plus sensibles, mais quelles sont-elles ?

Il est reconnu dans la littérature que la radiosensibilité intrinsèque des tissus et organes est particulièrement grande en période de croissance et de maturation [6]. Le cerveau croît très vite jusqu'à l'âge de 5 ans (où il a atteint 90% de sa taille adulte), sa croissance ralentit pour se stabiliser à la puberté ; les modèles généraux de développement des différents organes, cerveau inclus, seront exposés plus en détail dans l'*article 3*. Or comme l'a montré Jannoun et al. [7] il y a corrélation entre l'âge du traitement et les séquelles produites par irradiation (les enfants de moins de 5 ans sont en effet la population la plus sensible aux lésions post-radiatives). En effet les tests de QI pratiqués chez les patients après radiothérapie montrent : *(i)* pour une irradiation cérébrale avant l'âge de 5 ans une mesure du QI moyen de 72 ; *(ii)* pour un traitement entre 6-10 ans, un QI moyen de 93 ; *(iii)* pour un traitement entre 11-15 ans, un QI moyen de 107. L'expérience clinique révèle ainsi que l'âge au traitement est bien un critère prépondérant.

Pourrait-on établir un design optimisé de la dosimétrie permettant malgré le jeune âge du patient d'éviter une telle atteinte de ses capacités psycho-cognitives ? Pour cela une liste claire des zones les plus importantes et les plus sensibles devrait être établie en fonction de l'âge.

V – 5. Métabolisme très actif du cortex préfrontal pendant l'enfance – siège des capacités d'abstraction

Une étude de Shaw P. et al. [8] publiée dans la revue *Nature* (30 mars 2006) révèle une relation surprenante entre le développement du cortex cérébral *vs* le QI chez l'enfant. L'étude porte sur 307 enfants âgés de 6 à 20 ans, soumis pour chacun d'eux à un minimum de deux examens IRMf espacés de deux ans, parallèlement à un test QI de Wechsler, évaluant leur capacité de raisonnement ainsi que leurs connaissances verbales et non-verbales.

Il apparaît que les changements les plus importants interviennent dans le cortex préfrontal, les capacités psycho-cognitives des enfants y seraient corrélées. La vitesse d'épaississement vs amincissement de cette zone préfrontale de même que l'importance des différentes phases de ce processus seraient en relation avec les résultats du test QI scindant les enfants en 3 groupes distincts d'intelligence à savoir de catégorie moyenne (QI compris entre 83 et 108), élevée (109 - 120) ou supérieure (121 - 145).

Les enfants de 7 ans du groupe « supérieur » ont de manière étonnante un cortex plus mince que la moyenne (cf figure 9) qui s'épaissit jusqu'à l'âge de 11 – 12 ans (pic plus tardif que les enfants de catégorie « moyenne » et « élevée ») avant de s'amincir à nouveau. Les enfants du groupe « moyen » ont un cortex plus épais qui s'amincit lentement à partir de 8 ans. Ainsi la dynamique des phases d'épaississement *vs* amincissement du cortex préfrontal joue un rôle prépondérant dans les résultats de QI. Les enfants de QI supérieur montrent un épaississement du cortex préfrontal plus rapide et pendant une plus longue période que les autres alors que l'épaisseur corticale au final devient identique à celle des enfants de QI moyen (et inférieur à celle des enfants de QI élevé).

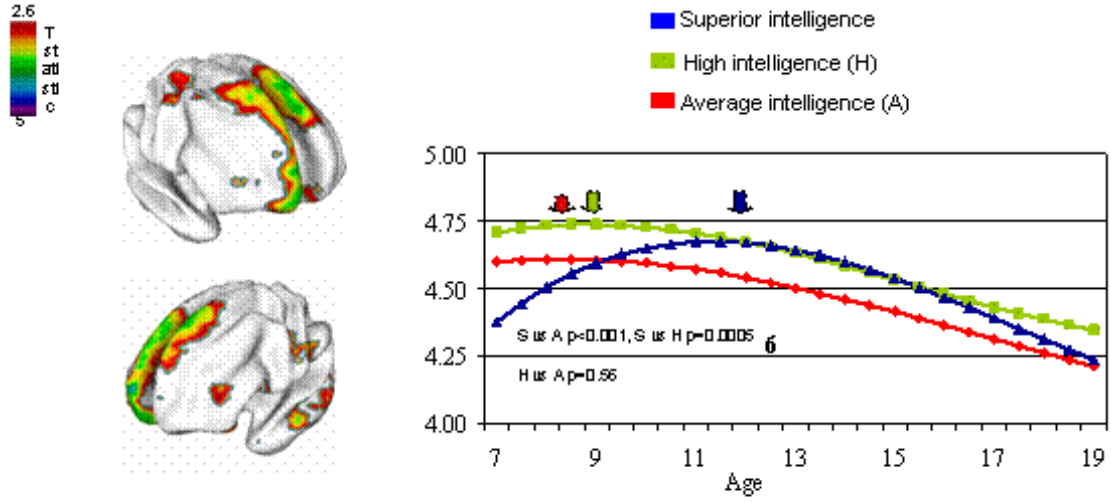

Figure 9 : Evolution de l'épaisseur du cortex préfrontal *vs* l'âge de l'enfant pour 3 groupes distincts d'intelligence i.e. catégorie moyenne (en rouge), élevée (en vert) et supérieure (en bleu). L'étude s'est faite sur une population de 307 enfants âgés de 6 à 20 ans. Source: NIMH Child Psychiatry Branch, study of Drs. Philip Shaw, Judith Rapoport, Jay Giedd and colleagues at NIMH and McGill University report on their findings in the March 30, 2006 issue of *Nature*

V – 6. Architecture complexe des circuits neuronaux

La solution à la conservation des capacités psycho-cognitives des patients serait-elle alors simplement d'éviter le cortex préfrontal à cet âge en interdisant toute irradiation non-coplanaire supérieure (i.e. irradiation oblique cranio-caudale antéro-postérieure) ? Cela peut en effet être un début de solution, mais la zone corticale préfrontale est de plus impliquée dans divers circuits neuronaux plus vastes encore dont la lésion impliquerait l'atteinte de l'édifice dans son ensemble. Il en existe en outre d'autres totalement indépendant et dont l'intégrité apparaît, suivant leur nature, de certaine importante pour toute intégration sociale future.
La littérature rapporte que le défaut de maturation des réseaux préfronto-striataux (aires dorsolatérales + cingulaires antérieures + striatum) entraîne un défaut d'activation des fonctions attentionnelles et exécutives (c'est le cas des enfants hyperactifs) [9, 10] Ils sont mis en évidence par une baisse du débit sanguin cérébral et du métabolisme cellulaire dans ces régions.

De même une diminution du volume du vermis cérébelleux chez l'enfant engendrerait un défaut de fonctionnement du circuit cérébello-thalamo-préfrontal et un ralentissement dans la capacité de réaction tant motrice que cognitive [10]. Un contingent de fibres d'association (projections cérébelleuses) émanant du cervelet et se projetant sur le cortex frontal, le thalamus, le corps calleux expliqueraient les perturbations des fonctions sensorielles,

attentionnelles, motrices et cognitives consécutives aux tumeurs de la fosse postérieure [11]. L'atteinte du cervelet chez l'enfant entraînerait le ralentissement psychomoteur et cognitif [12] du fait de son rôle de coprocesseur pour les fonctions cognitives et de sa richesse en connexions avec le thalamus, les aires préfrontales entre *autres*.

L'atteinte du complexe diencéphalo-limbique-réticulaire et du cortex préfronto-temporal gauche (pour les droitiers) est reconnue dans le déclenchement de certaines neuropathologies comme la dépression ou certains symptômes schizotypiques [13].

La multiplicité de ces circuits et leur importance à toute intégration sociale future oblige à un effort considérable de réflexion pour le design de la dosimétrie puisque n'est permis pour les ions carbone qu'un faible nombre de faisceaux d'irradiation.

V – 7. Dosimétrie et balistique originale des ions carbone – Diverses questions soulevées

La réponse de la plasticité du cerveau comme parade à l'atteinte et au dysfonctionnement de certains circuits neuronaux n'apparaît pas toujours optimale. Durston et al. [14] montrent pour exemple qu'un défaut de maturation chez certains enfants des régions fronto-striatales ventrales (responsables des fonctions attentionnelles et exécutives) est en effet compensé par un réseau plus diffus impliquant les régions postérieures du lobe pariétal inférieur, la cingulaire postérieure aussi bien que les régions préfrontales dorsolatérales. Ce modèle singulier représente un mécanisme compensatoire au dysfonctionnement du circuit original mais ne permet pas en définitif d'atteindre le niveau de performance du circuit initial, ce second circuit d'activation étant en effet rencontré chez les enfants hyperactifs (à faibles capacités attentionnelles). La plasticité du cerveau est utile et permet alors un moindre mal mais la compensation ne peut reproduire la qualité du circuit neuronal initial. En effet quel serait l'impact sur certaines maladies neuropathogiques telles la *dépression chronique* si le développement du cortex préfronto-temporal gauche devait être remis en cause chez l'enfant ? La simple attente après irradiation par ions carbone d'une compensation par plasticité cérébrale serait-elle une justification acceptable pour les traitements pédiatriques ?

Il serait aussi intéressant de déterminer la place d'une rééducation orientée en fonction des troubles attendus concernant l'irradiation de certaines zones fonctionnelles. Ne serait-il pas plus prudent par exemple de prévenir tout trouble schizotypique, si l'atteinte des circuits neuronaux référents est considérée possible, en orientant le patient après traitement vers les médecins psychiatres pour un suivi étalé dans le temps ? De même pour toute autre atteinte d'un circuit neuronal spécifique et des fonctions neurocognitives correspondantes par un suivi après traitement par les spécialistes adéquats.

En pratique chirurgicale, l'intervention sur certaines tumeurs intracrâniennes oblige le chirurgien à ne pas intervenir sur l'hypothalamus ventromédian de peur de léser cette zone, centre du sentiment de satiété et de faim. Sa lésion par chirurgie se traduit en effet par une hyperphagie chez le patient s'accompagnant de tous les risques sanitaires connus pour cette pathologie. A l'image de cette pratique, il faudrait éviter en radiothérapie certaines zones cérébrales primordiales lors du développement de l'enfant par décision collégiale des cliniciens, radiobiologistes et épidémiologistes auxquels il faudrait ajouter des neuro-pédiatres. Pour cela, un certain nombre de questions devraient être soulevées et étudiées. Quel est l'impact réel des ions carbone sur la dynamique d'évolution des processus de synaptogenèse-myélogenèse *vs* régression synaptique lors des processus de croissance et de maturation chez l'enfant ? Une gradation des circuits neuronaux par ordre d'importance (en fonction de l'âge) est-elle possible pour un meilleur design dosimétrique ? Pourrait-il s'en dégage t-il un choix balistique cohérent et reproductible pour les indications qui seront à traiter à l'avenir ? etc…

Pour exploiter les caractéristiques de très faible diffusion latérale et distale et l'EBR des ions carbone *vs* les protons et créer alors un véritable différentiel thérapeutique avec les autres techniques, il faudrait connaître en détail ces structures fragiles. Le choix judicieux de 2 ou 3 faisceaux d'irradiation de la tumeur impliquerait en outre de faibles niveaux de volumes d'isodoses aux tissus sains. Les ions carbone laisseraient ainsi les capacités cognitives intactes tout en permettant de réduire les risques carcinogènes radio-induits grâce à leurs caractéristiques propres (*cf* article 3).

VI - Troisième Article :

VI – 1. Second malignant neoplasia: discussion of the modelization of carcinogenic risks for the carbon-ions versus the photon-treatments

Yasid Boudam[1], Jacques Balosso[1,2].

1 : Joseph Fourier University, Grenoble, France ; 2 : CHU de Grenoble.

Corresponding author: Pr Jacques BALOSSO
Department of Radiotherapy
Hôpital Michallon
BP 217
F-38043 GRENOBLE cedex 09
France
tel: +33 4 76 76 54 35
fax: + 33 4 76 76 56 29
JBalosso@chu-grenoble.fr

Key words: Radiotherapy, hadrontherapy, carbon-ions, stochastic risk, carcinogenic effect, second malignant neoplasia.

Acknowledgments: YB receives his doctoral fellowships from University Claude Bernard-Lyon1 (ETOILE project) and Siemens-Medical System; le Comité départemental of Savoie of the Ligue National contre le Cancer has supported all expenses for the realisation of this work in France and in Germany; we also are very grateful to Claudia Fournier and Wilma Weyrather from GSI (Darmstadt) for valuable discussions and basic data for modelization.

VI – 1.i Abstract :

Purpose: to assess the effect of carbon-ions versus photons as effective inducers of second neoplasm's after anti-cancer treatments for adults and children. The comparison is based on epidemiological data & their conclusions and present predictive models of radiation induced cancer. The goal is to estimate, for carbon-ions, the susceptibility to cancer induction within irradiated tissues and organs, in particular in pediatric conditions, and then to contribute to assess the benefit / risk balance of carbon-ion radiotherapy.

Material and methods: The calculation uses present models of carcinogenesis namely the *standard* model and the *repopulation* model. The *standard* model takes into account the *initiation* of the malignancy and the *cell killing* (loss of the cell reproducibility), whereas the *repopulation* model introduces a third parameter, the *proliferative kinetics* of the cells in growing tissues. The input data are drawn from radiobiological experimentations made by others and the prediction is computed as a relative comparison of carbon-ions (in entrance, plateau and Bragg peak) versus photons (15 MeV of maximal energy).

Results: The developmental stage in pediatric conditions is recognized of a particular concern for the risks of secondary neoplasia. The predictive assessment allows concluding to a potential advantage of the carbon-ions in the *intermediate* and *high* doses range of irradiation in entrance, plateau and Bragg peak. This differential effect favoring the carbon-ions is maintained even for the "pediatric" tissues yet recognized as highly sensitive. Lastly, hypofractionation schedules allow increasing even more the beneficial effect of carbon-ions toward the risk of carcinogenesis.

Conclusion: The set of complex radiobiological effects acting within tissues to induce different dose-responses of neoplasic risk can have contradictory actions. The *standard* and the *repopulation* models provide a comprehensive insight in spite of their purely theoretical aspect. They reveal some encouraging possibilities for the treatment of children by carbon-ions, especially when the choice of hypofractionation will be possible.

VI – 1.1. Introduction :

The introduction of high LET beams in anticancer treatments is considered as a valuable progress to obtain better cure rates for radioresistant tumors. However, the clinical use of such radiations having at the point of view of the radioprotection high quality factors for stochastic effects (Wr of the ICRP) raise concerns about their impact on the risk of secondary malignant neoplasia (SMN) in normal tissues of cured patients.
The case of carbon ions is considered in priority thanks to the quick development of new treatment facilities operating carbon-ions beams in the present time. Numerous articles report detailed dose effect curves for cell survival related to specific energy and particle-beams. Other scientific reports collect numbers of specific biological effects induced by ion irradiations i.e. double strand breaks induction or chromosomal aberrations (translocation, deletion…). These events are considered as representative of the risk of premalignant cells production, themselves potential sources of secondary malignant neoplasia in irradiated normal tissues [1].
The large biological and clinical experience gathered in photon-beam radiotherapy considered from the point of view of the radiocarcinogenesis could lead to the idea that similar basic knowledge on carbon ions would allow simple extrapolation and provide clinical conclusions on carbon-ions SMN risk. However very controversial results are obtained even in the well known photon-beam applications: it can be observed after photon irradiations opposite results of dose-effect relationship on SMN risk [See literature gave as references in Ron (2006) [2]].
In fact, the fundamental models of biological action of radiations do not impact directly the risk of SMN and more sophisticated relationships should be taken into account. Therefore, it is unreasonable to simply rely conclusions on the respective risk of two types of radiations simply to their basic yield of molecular or chromosomal damage efficiencies.
A valuable contribution for an improved description is to take into account the growth kinetic factor, organs- or tissues-specific. A very good consistency, for photon-beam clinical results, is obtained by Sachs & Brenner by combining classical biological modelization of cell transformation induced by molecular damages in surviving cell and the gompertzian model of growth kinetic of the considered tissues [3]. The goal of the present paper is to provide a similar approach for the carbon-ions-beams using dose effect curves for survival and transformation of cells by photons and carbon-ions [4], and to make a critical comparison of the SMN risks of photons and carbon-ions treatments in particular for pediatric treatments. The concept of higher susceptibility of the growing and maturing tissues and its consequences for carbon-ions treatments is discussed in detailed.

VI – 1.2. Material and method :

VI – 1.2.1. Extraction of experimental data and fit with parameterized models:

The relation between basic radiobiological phenomena as premalignant transformation rate, cell killing and/or proliferation/repopulation effects (tissue- age- specific) is convincingly modelized as dose-dependent cancer risks by Wheldon and coworkers [5, 6]. Their model is characterized by the intrinsic *cellular radiosensitivity* parameters $\{\alpha,\beta\}$ (see Figure 1) and *mutational radiosensitivity* parameters $\{\gamma,\delta\}$ (see Figure 2). On the other hand, the radiation-induced accelerated repopulation/proliferation of the normal and premalignant stem cells is based on equations developed by Sachs and Brenner [3]. Then we adjusted the four parameters transformation equations of Wheldon et al. to the biological data published by Bettega and coworkers [4]. It allows us to obtain the $\{\alpha,\beta\}$ & $\{\gamma,\delta\}$ experimental parameters from *in vitro* data of survival and transformation by *carbon ions* including photon data

provided as control in the same experiments [4]. These parameters are extracted for three specific beam energies and LET on target i.e. i) 266.4 MeV/u (LET 13.7 keV/μm), ii) 86.5 MeV/u (29.5 keV/μm), iii) 9.65 MeV/u (172 keV/μm). These energies respectively representing the beam quality in entrance, plateau and Bragg peak areas. This first step provides the values of transformation frequency for photons and carbon-ions for cell at risk. These basic data show only the premalignant cells induced after irradiation but do not predict at this stage the real SMN risk in vivo.

In summary, as shown in Figure 3 of the present paper as well as in the one of Bettega et al. paper [4] *transformation frequencies in entrance channel, plateau and Bragg peak* are consistently different. When the LET increases (from entrance to Bragg peak) the transformation effect increases also, with maxima for decreasing dose levels due to competitive cell killing. This latter point is already known for the photons & heavy particles and previously reported by others [6, 7] who interpreted the incidence of cancer as an increasing function of mutational sensitivity (γ, δ) but a decreasing function of intrinsic radiosensitivity (α, β).
However this basic model of cellular risk, quoted above as *transformation frequency*, does not prejudge directly the present risk of SMN to dread in clinical situation. To do so it is necessary to go through successive steps of complexity: the first one is the introduction of dose and fractionation to obtain the so called “standard model” (initiation + killing) [5, 3], then the concept of repopulation in the so called “repopulation model” which exhaustively includes growth kinetic equations of the radioinduced premalignant cells and the growth kinetics of the normal stem cells. The last step could be the introduction of a proportionality factor (B) linking the yield of premalignant cells to the excess of clinically observed relative risk of SMN [3]. As the introduction of the B value does not alter the shape of the curves, in the present paper we propose to limit the comparison of different therapeutic approaches to the use of the standard and the repopulation model only and calculating the simple precarcinogenic action of each beam.

VI – 1.2.2. Predictions of cancer incidence through different biological models: The standard "initiation + killing" model:

As first estimation of dose-response relationship in radiation-related cancer risks, the standard *initiation-killing* model [3, 8, 9] is taking into account the competitive production of radio-induction premalignant cells versus the cell loss by cell killing, with no consideration to the cellular repopulation of the irradiated tissue. The radiosensitivity parameters used in the standard model are naturally those obtained thanks to the survival data and transformation data (figure 1&2) tabulated in table 1.

VI – 1.2.3. Repopulation model with carcinogenic effects, cell killing, and additionally cell proliferation/repopulation effects:

Pluripotent cells are continuously regenerating normal tissues[11] [10, 11]. This tissue growth kinetic increases the multiplication of premalignant radiation-induced cells, thus promoting the development of transformed cell population ultimately producing SMN. It is necessary to include in our modelization this cell kinetics criterion because of the homeostatic control of the tissue counteracting the radiation cell-killing by the repopulation [10, 11] or because of the cell multiplication occurring in the tissues of growing up children [13].

[11] Concept of the stem cells and their role in the maintenance of tissue structure and function in reaction to ionising radiation of normal tissue.

VI – 1.2.4. Principle of the present study:

The predicted number of induced premalignant cells versus the dose is modelized here as previously done using the radiosensitivity parameters tabulated in table 1. This repopulation model includes two additional free parameters :

(i) the repopulation rate parameter λ, established from studies of second cancer after radiotherapy of Hodgkin's disease for both lung [14] and breast cancer [15, 16] by Rainer K. Sachs et al. [3] with $\lambda = 0.4$ (chosen and fixed value along all the present study).

(ii) the growth rates ratio per type of cells ***r***, reflects, in the frame of the same growth pattern, the relative differences of growth rate between normal stem cells and premalignant cells, the latter being at the most as proliferative than the former but never more. It is precisely defined as the ratio *r* of the per-cell proliferation rate of pre-malignant cells to the per-cell proliferation rate of normal cells. Rainer K. Sachs et al [3] reported for lung cancer a value of $r_{lung} = 0.96$ and for the breast cancer a value of $r_{breast} = 0.76$. As a conservative approach we choose for the present study to consider the variation of *r* in the range of [0.5 to 0.9] values which can be met in the scientist literature [3, 17].

Instead of considering these parameters as deep cellular characteristics, in this work, we consider them as tissue dynamic parameters accessible by the fit of clinical data as practically obtained by Rainer K. Sachs. This will allow us thereafter to introduce and link these parameters to the radio-susceptibility for cancer of the periods of high physiological changes of childhood.

VI – 1.3. Results:

VI – 1.3.1. Standard "initiation + killing" model of carcinogenesis risks

The *standard model* in figure 4 modelises the precarcinogenic action of the carbon-ions for a 3 Gy *dose/fraction* such as used for the treatments in GSI; the precarcinogenic action of the photon radiation (same figure) is modelized for a 2 Gy dose/fraction such as communly used in X-rays treatments. Each level of energy of the carbon-beams, namely 266.4 MeV/u, 86.5 MeV/u and 9.65 MeV/u, are respective to the energies in intrance, plateau and bragg peak regions of the beam.

In normal fractionation schedule (figure 4) the carbon-ions induce a risk lower than the photon irradiation. The risk of carbon-ions beam in decreasing order is the following: the intrance, the plateau and lastly the Bragg peak. Noteworthly the Bragg peak region (9.65 MeV/u) induces the lower risk amplitude in reverse aspect to its broader amplitude *in vitro* (see figure 3) in the assessment of the *cellular transformation frequency per cell at risk* at low dose range (calculated by Bettega et al.).

The more hypofractionated schedule of the figure 5 (*5 Gy/fraction*) highlights the difference of the precarcinogenic action between carbon-ions and photons. This premalignancy rate falls down dramatically with carbon-ions to almost disappear in Bragg peak.

VI – 1.3.2. Initiation/inactivation/proliferation model including a pattern of cellular growth kinetics

Two different fractionation schedules for the C-beam are applied: *i) 3 Gy/fraction* schedule routinely used in GSI; *ii)* a more *hypofractionated* schedule.

i. Induction of the premalignancy with 3 Gy/fraction for the C-beams and 2 Gy/fraction for the photon-beam

The *r repopulation ratio* is fixed, first at the value r = 0.5 (figure 6), second it is increased to r = 0.7 (figure 7) then up to r = 0.9 (figure 8). The latter are closer to those ued by Sachs et al [3, 17] for Hodgkin's diseases.

When the *repopulation model* is introduced (figure 6, 7 & 8), the Bragg peak region (*9.65 MeV/u*) produces at *low dose range* more premalignancy than the photon beam. This unfavorable relative result extends along the cumulated dose axis (abscises) with the increase of *r* parameter, i.e. for *r* = 0.5 the critical dose-range is [0-4] Gy, for *r* = 0.8 it is [0-10] Gy and for *r* = 0.9 it is [0-20] Gy. However, in any case beyond the intercept of the C-beam and the photon-beam curves, the premalignancy rate of the Bragg-peak of the C-beam is always decreasing to zero at deferent values of dose according to r, i.e. for *r* = 0.5 the zero is reached for 8 Gy, for *r* = 0.7 it is reached for 15 Gy, and 45 Gy for *r* = 0.9. To summarize, the Bragg peak region induces a risk of premalignancy higher than the photons one only at *low* doses ranges, and becomes less toxic than photons for intermediate and high dose ranges.

In an obvious different way, the entrance energy (*266.4 MeV/u*) and plateau energy (*86.5 MeV/u*) C-beam curves are very close to the photon-beam curve at low doses and then cross it to go below the photon-beam curve at higher doses. However, once again, the crossing is shifted to higher doses when *r* is increasing, i.e. at 5 Gy for *r* = 0.5; at 8 Gy for *r* = 0.7 and at 25 Gy for *r* = 0.9 (see figure 9). The amplitude of this phenomenon is progressively reduced with the increase of *r* and becomes smaller for *r* = 0.9. To summarize, the increase of the proliferative kinetic seems to slow down the predicted beneficial effect of the carbon ions over photons at high dose, although the difference seems to remain advantageous.

At first glance, compared to photons, the repopulation model predicts for the C-beam Bragg peak a risk of premalignancy higher in the low doses range for thereafter in the intermediate and higher doses decreasing far below photons to reach zero. For the entrance and plateau parts of the C-beam the premalignancy risk appears in the same order than the photons one and decrease below it at higher doses. In both situations, the increase of the repopulation parameter *r* is shifting these figures to higher doses.

ii. Induction of malignancies in C-beam hypofractionation schedule compared to 2 Gy/fraction photon-beam for a constant repopulation ratio (r = 0.8)

The figure 9 shows the curves of C-beam premalignancy risk for standard fractionation (*3 Gy/fraction)*, as reference for the study of the effect of *dose/fraction* escalation.

The premalignancy risk of the Bragg peak region (9.65 MeV/u) is situated far above photons in the control-figure (*3 Gy/fraction* – figure 9) at low doses [0-10] Gy. When the dose per fraction is increased [*6* & *10 Gy/fraction*], as in increasingly hypofractionated schedules, the model predicts a rapid decrease of the premalignancy risk in Bragg peak until becoming identical to the photons when *10 Gy/fraction* is reached (see figures 10 & 11). For the intermediate doses the Bragg peak induces a premalignancy risk lower than the photons whatever the fractionation schedules (i.e. *3, 6* & *10 Gy/fraction*) – the higher the *dose/fraction* the lower the premalignant risk level – until reaching the nullity.

For the entrance and plateau parts of the C-beam, for standard fractionation (figure 9), the premalignancy risk is similar to the photon's risk in low doses up about 12 Gy for then decreasing continuously under the photon curve. The increase of the *dose/fraction* showed in figures 10 & 11 produces a decrease of the premalignancy risk at low total doses and an abrupt diminution in the intermediate total doses with a clear advantage of C-beam over photon beam.

Considering the repopulation model studied in the paragraphs *(i)* & *(ii)*, the effects onto the premalignancy risk of the repopulation kinetic (factor *r*) and the *dose/fraction* value can be schematically summarized as: i) for a constant repopulation ratio *r*, the higher the *dose/fraction* the lower the premalignancy risk; ii) for a constant *dose/fraction value*, the higher the repopulation ratio *r* the higher the premalignancy risk. This antagonistic effect was suggested by the authors of this model when they related the competing effect between the repopulation and the cell killing processes in the pathway of the carcinogenesis in X-rays treatment.

VI –1. 4. Discussion :

VI – 1.4.1. Cell-killing & organ repopulation are antagonizing each other in carcinogenic effect

Not withstanding any bystander effect, it is axiomatic that no cancer can arise from irradiated cells that have received lethal doses [8]. This phenomenon is called the cell sterilization effect where premalignant mutated cells disappear from the pathway of malignant transformation by cell death beyond a certain threshold dose of irradiation [13, 18]. This cell sterilization phenomenon can easily be modelized by the *transformation frequency per cell at risk* expression[12] combining the linear-quadratic expression of cell *survival probability* and the *premalignant cell induction* expression. However, this simple model may not predict on its own the complexity of the dose-response relationship for the SMN occurrence. Actually it does not take into account the cellular repopulation involved in organ and tissue growth and repair. This repopulation can expand the tiny population of mutated surviving cells to promote the development of the risk of SMN.

This fundamental impact of the tissue growth is emphasized by Sachs & Brenner [3]. They highlight, following others, the antagonistic effect between the cell killing sterilization after a radiation treatment and the rapid proliferation of the premalignant stem cells, following the normal stem cells active proliferative response – as notably in homeostatic tissues – between fractions and after treatment completion. The intensity of this cellular activity within the irradiated tissue is an important weighting factor of the final risk of the SMN.

Thus this biological model integrates the parameters of mutational sensitivity (γ and δ) and intrinsic cellular radiosensitivity (α and β). These parameters allow to compute the malignancy induction and the killing effect of the standard expression (initiation + inactivation). By introducing the growth velocity of the tissues and organs, the model involves two more growth kinetic parameters: the repopulation rate λ and the repopulation ratio *r*, these *proliferative kinetic factors* will be commented thereafter in detail. So the global process is modelized by four equations integrating all these parameters that allow to weight independently each phenomenon, namely the post-inactivation after irradiation, the malignancy occurrence and the repopulation velocity in the irradiated organ. This achieves a consistent framing of the epidemiological data by relating the radiobiological and clinical aspects in the etiology of the carcinogenesis occurrence among patients and more specifically childhood as seen hereafter.

---

[12] ***Transformation frequency per cell at risk*** $(10^{-4}) = 10^4.e^{-\alpha D -\beta D\wedge 2}.(1 - e^{-\gamma D -\delta D\wedge 2})$

➔ With $(e^{-\alpha D -\beta D\wedge 2})$ the surviving fraction expression, $[10^4.e^{-\alpha D -\beta D\wedge 2}]$ the frequency of surviving cells and $[1 - e^{-\gamma D -\delta D\wedge 2}]$ the fraction of cells that are made premalignants.

VI – 1.4.2. Carcinogenic risk increase and decrease in childhood treatment – a varying vulnerability

Rubin and Casarett [19] classified the living tissues according to their reproductive kinetics in an attempt to correlate their reproductive and functional characteristics with their radiosensitivity. Even earlier, underlying investigations observed that the higher the level of undifferentiating and proliferative activity of the cells, the higher the radiosensitivity (law of Bergonie and Tribondeau). With this in mind, an image of the radiosensitivity for each organ might be shaped. Moreover, the identification of the different cell populations within each tissue and organ provides a description of different compartment and different stages of differentiation and reproductive kinetics along the live and the responses of these tissues. As a consequence, their susceptibility to the irradiation damages could be quite complex. One can take into account: i) the parenchyma compartment with more or less specialized cell lines from an undifferentiated stage regularly and rapidly dividing to a highly differentiated stage non-dividing; ii) the stoma compartment with the connective tissue and the vasculature of intermediate differentiation stage irregularly dividing. The stem cells, present in some specific compartments, maintain the tissues in a functional steady state [10, 11], counteracting any post-irradiation alterations by compensatory proliferation, achieving the homeostasis [20, 12] however contributing in the same time to the radiosusceptibility of the tissues. Therefore, the radiosusceptibility will follow the contain and the activity of stem cells. But, whereas the adult stem cells are rare[13], the adult tissues being in a mature steady state with a slow renewal velocity, the immature tissues of children perform a very active evolution until reaching their final sizes, being for that of first concern. The sequences of the rapid proliferation are recognized as particularly vulnerable particularly for the fetus, the infant & young-child [21], involving a complex mosaic of dose-response relationships for the carcinogenic risk sometime even conflicting. Actually, numerous studies collected clinical data about SMN risk and gave for children antagonistic conclusions as pointed out by E Ron et al. [2]. This inconsistency reflects in fact the varying tissue susceptibility in young patients in parallel with the varying growth velocity (age- and tissue-dependant). In useful way these contradictory epidemiological results of pediatric secondary tumors are convincingly linked by E.Ron et al. to the proliferative model of Sachs & Brenner which integrates this set of competing effects (i.e. as mentioned in § (VI. 1.4.1.) the “initiation+inactivation & repopulation/proliferation” model).

Thus the growth pattern of the childhood tissues & organs is of particular concern especially because it appears that the proliferative areas bear an inherent susceptibility to malignant transformation. How locate these areas when the complexity may be such as a slow renewal velocity in some development stage may become suddenly activated by irradiation stimulation? Moreover a thorough and detailed description of active proliferation periods for each organ doesn’t actually exist. Useful general growth patterns are provided in the literature (thereafter exposed) and may help predict the sensitivity to potential SMN for the young patients.

VI – 1.4.3. Partial review of the patterns of the organ growth – a necessity to estimate the potential risk of malignancies in childhood

The vulnerability of the tissues to carcinogenic effects is correlated to the cellular activity and maturation process within them. Thanks to useful general patterns of development for different organs (growth rate *vs* age-years of patients), fruitful observations may be obtained,

[13] e.g. an estimated of 1 in 10,000 to 15,000 cells in the bone marrow is a hematopoietic (bloodforming) stem cell [22].

namely a straightforward relationship between the epidemiological outcomes of cancer risk for these organs and their stage of growth according to the patient age at the time of the irradiation. Thus the risk of thyroid, breast and brain cancer, acknowledged as high among the children [2, 21], are compared to the correspondent growth patterns for each of these organs. The goal is here to illustrate the consistency of such a correlation between the risk and the organ growth (parameterized by the ratio *r* in ***§ (VI – 1.4.4.)***).

VI – 1.4.3.i. Thyroid growth pattern versus risk of thyroid cancer

The investigations show a significant susceptibility of the thyroid gland to post-radiation cancer risks among young patients [23, 24, 25] but no significant dose-response relationship for young adults, older than 20 years [26, 27]. E. Ron suggested that this commonly observed disparate response between children and adult tissues is due to differences of cell repopulation. Growth and maturation processes, which are more active in children tissues than in adult's ones, amplify the cancer risk during childhood. This could apply to the thyroid cancer which is correlated during all the growing process to the physiological development of the gland. Indeed the literature reports a steady evolution of the thyroid volume up to 15 – 18 years of age [13, 28, 29]; beyond this age there is not any more growth that explains the absence of significant dose-response relation for thyroid cancer after 20 years. Precisely, the growth pattern is characterized by 2 periods of rapid proliferation activity, the first one taking place all during infancy[14] & early childhood, the second one during adolescence after the middle childhood stage of slow-down growth. Sadetzki S. et al. [23] report for different age groups the following thyroid carcinogenic excess of relative risks per gray (ERR/Gy): 33.9 during infancy & early childhood (first rapid development stage of thyroid physiological growth), 12.9 during to middle childhood (relative slow-down stage) and 21.1 during adolescence (second and last rapid development stage). Investigations among A-bomb or Chernobyl survivors [26, 30] confirmed this distribution of risks by age ranges, where adolescence are lesser at risk than childhood with large prevalence of risk for children under 5 years old and no significant risk among adults above 16 y. Furthermore, the sex-ratio of the incidence of thyroid cancer is unbalanced with a higher rate in females than in males [23, 25, 30], this higher rates follows the higher increase of the thyroid volume (and its inherent cells proliferation) for girls after the menarche [28].

VI – 1.4.3.ii. Risk of breast cancer

The breast tissue as for the testes and ovaries follows the genital growth pattern [13] with little change in early life – i.e. infancy, early & middle childhood – and rapid development at puberty up to 20 years of age and even after for breast. This developmental stage corresponds with the period of sensitivity of breast tissue to the SMN occurrence after an ionizing irradiation, where the carcinogenic risk is the highest between 10 and 20 years of age, all during the main breast growth time [24]. A lower risk is observed from 20 to 30 years of age and declines significantly thereafter (> 30y). This decrease of risk after 20 years is explained by the size evolution of the breast tissue which is nearly completed at 20 years, declining thereafter and completely stopping at 30 years.

VI – 1.4.3.iii. Risk of brain cancer

The neural pattern (brain & head) is characterized, once again, by a rapid growth in infancy & early childhood – at 5 years of age the brain reach's approximately 90 percent of its adult weight – it slows in middle childhood and ceases in adolescence [13]. Furthermore the carcinogenic risk in the central nervous system (CNS) *vs* the age of occurrence reveals an

[14] Age ranges : infancy (birth to 2 years old), early childhood (3 to 8 years old), middle childhood (9 to 11 years old), adolescence (12 to 18 years old).

striking parallel with this neural development pattern. Neglia et al. [31] find a strong linear dose-response relationship for the CNS tumor occurrence among children, the highest risk occurring for children exposed before 5 years of age. During this period occurs the most drastic changes in brain tissues with the spreading connections of the dendrites, the myelinization processes and the increase in connections between the neurons.
Interestingly enough, a thorough investigation of the relationship between the CNS vulnerability and the changes of the brain structures would be valuable. A comparison of the epidemiological data *vs* the spatial mapping of brain growth could give a kind of 4D map of all vulnerabilities according to the CNS location[15] and time scale[16] for the young patients. This would allow timely avoiding some specific parts of the CNS for the planning of childhood radiationtherapy. For example, the maturation areas in the frontal lobe from 3 to 6 years of age or the maturation of temporal and parietal lobes from age 6 to the puberty etc. This could decrease the risk of carcinogenesis after treatment or avoid some cognitive and affective development failures that could produce chronicle disturbance.

VI – 1.4.4. The ratio of the per cell growth rates *"r" as organ-susceptibility-factor*

Sachs et al. formalized the difference of growth kinetic (*per-cell growth rate*) between the premalignant and the normal stem cells by a repopulation ratio, namely *r* (*r* = per-cell proliferation rate of pre-malignant cells / per-cell proliferation rate of normal cells). The difference of kinetic is assumed to come from the disruptive pathway induced by clastogenic[17] activities in post-irradiation surviving cells as *apoptosis*, *reproductive death* or *loss of clonogenicity* [3, 32, 33, 34].
In the context of irradiated tissues the induction of premalignant cells, as represented by $\{\gamma, \delta\}$, is never equal to zero thus the ratio *r* cannot be equal to zero by the fact of an extremely unbalanced ratio between normal and premalignant cell growth. Therefore, the existent of any significant value of *r* can also indicate that some proliferation processes are taking place in the irradiated tissue and thus indicating that the growth process of the organ, parameterized by λ, is due to repopulation instead of hypertrophy.
Thus, in a more clinically oriented reasoning, the *r* factor recognizes the *mechanism of organ growth* i.e. hypertrophy *vs* proliferation. The mechanism of hypertrophy - an increase in size of the cells - renders the organ less susceptible to SMN than the process of proliferation. When in *§ **(VI – 1.4.3.)*** the vulnerability of the tissues to the debilitating effects follows some patterns of organ growth, it is the factor λ that characterizes the extend of organ *growth rate*. Since some growth takes place, $\lambda > 0$, the *mechanism of organ growth* and the relative proportion between pre-malignant cells and normal cells is expressed by the factor *r*. Therefore, whatever the value of r, a very low value of λ will preclude any SMN, on the other hand for a high value of λ , the risk of SMN will follow the value of *r*. The combinations of intermediate range of growth rate λ and proliferative fraction *r* reflect all the kinetic range of the growing tissues and the inherent panel of susceptibilities to post-radiation damages.
In the present work, we fixed the λ value of organ growth arbitrary – according to the value found in the literature 0.4 – for a set of *r* values. By varying this *r* values, a large variety of pediatric situations may be characterized at different developmental stages and for different degrees of vulnerability.

VI – 1.4.5. The carbon-ions could induce a lower risk of precarcinogenesis due to the cellular sterilization effect

[15] i.e. frontal, parietal, temporal… lobe areas.
[16] i.e. infancy, early or middle or late childhood, etc…
[17] Defining a process causing disruption or breakages of chromosomes.

When the tissue proliferative activity of an irradiated tissue rises – simulated by the rise of *r* ratio – the clonogenicity is increasing, thus promoting the development of neoplasms. The repopulation model shows nicely this variation of the clonogenicity in correlation with the variation of *r,* as shown in the results section. *A contrario* the malignant transformation in the normal tissues is challenged by the "cell-killing" effect, which extend is related to the nature of the beam *i.e.* the particles *vs* the photons. Similar distributions of physical dose brought by carbon-ions *vs* photons in tissues produce different radiobiological damages in term of cell inactivation and by consequence in term of neoplasic risk. This "cell sterilization" opposes the mutational action inherent to the radiation dose, and the balance of these antagonistic phenomena results in different precarcinogenic induction rates. In which extend does this cell sterilization prevail in the tissue *vs* the premalignant induction for the carbon-ions *vs* the photons? The following paragraphs show that the prevalence of the cell sterilization due to carbon-ions could result in less neoplasic risk than for photons.

VI – 1.4.5.i. The precarcinogenic risk in Bragg peak

For the tissues of low renewal kinetic – e.g. the adult condition in mature steady state – the Bragg peak region of the carbon-ions induces in usual fractionation schedule a precarcinogenic risk lower than with photons. This tissue slow renewal condition is simulated by the standard model and by a low repopulation ratio *r* in the repopulation model: the standard model (figure 4) shows in the Bragg peak region a very clear advantage against the photons with a lower risk of precarcinogenesis; the repopulation model with low *r* factor (figure 6&7) shows a slight disadvantage at *very-low* doses, but a declining risk down to an insignificant levels of risk at *low*, *middle* and *high* doses.

For the tissues of rapid renewal kinetic – e.g. the pediatric condition – the risk of precarcinogenesis in Bragg peak is consistently higher (figure 8) at *low* doses; but for *middle* & *high* dose range the risk becomes far lower than for photons.

Usually the treatment protocols deliver a high dose to the tumor by the mean of multiple Bragg peak shot subsequently resulting in a low level of precarcinogenesis risk. Interestingly enough the fast growing tissues, highly sensitive to the risk of neoplasia in photon treatments (X-rays) – such as the thyroid, breast or brain in childhood *(see § **VI – 1.4.3.**)* – do not appear particularly sensitive to precarcinogenesis in the Bragg peak region for *intermediate* and *high* doses.

Lastly at the ballistic point of view the accurate conformation of the Bragg peak to the tumor shape allows naturally to reduce negative effects due to this part of beam within normal tissues.

VI – 1.4.5.ii. The precarcinogenic risk in beam entrance and plateau

For the *very-low* dose range of particles the slow growing tissues undergo a precarcinogenic action at the entrance and along the plateau region similar to the one of photons. Once again, the case of the low renewal kinetics is modelized by the standard model and for low *r* ratio by the repopulation model figures 4,6&7. Consistently, the particles' risk of precarcinogenesis induced in entrance & plateau decreases advantageously *vs* photons for the *low*, *middle* and *high* dose range. Noteworthy, the same scheme with two successive domains exists for the tissues of fast renewal kinetics. Namely, the fast growing tissues (figure 8) undergo a precarcinogenic risk at the entrance and plateau similar to the photon radiation at *low* & *low-middle* doses for progressively falling at *high-middle* & *high* doses to lower levels than those of photons.

As previously seen for the Bragg peak region, the entrance and plateau of a particle beam seem to have a therapeutic advantage *vs* photons with a lower risk when applied to conditions of proliferation acceleration. This latter condition is of particular concern with the X-rays.

VI – 1.4.6. Phenomena of cellular sterilization enhanced by hypofractionation

Both the standard model and the repopulation model show for an increase of the *dose per fraction* a dramatic decrease of the premalignancy risk for light ions as carbon-ions. This low risk induced by the carbon-ions appears clearly very advantageous compared to photons (see figure 11). This may be explained by the enhancement of the cell-killing for high dose per fraction of carbon-ions, even the repopulation activity in a fast growing tissue may not be able to counteract this effect of sterilization. Thus, with hypofractionation, the premalignant transformation frequency collapses.

Interestingly enough, clinical trials of hypofractionation scheme in carbon ions therapy are initiated at the NIRS in Japan. The studies tend to demonstrate that changes in the organ function (determinist adverse effects) after hypofractionation are minor and all toxicities judged tolerable [35, 36, 37]. Whereas the usefulness of such hypofractionated scheme is questioned in term of tumor control and determinist effects, it appears in the present work that the benefice of such hypofractionated treatment could significantly decrease the risk of *second malignant neoplasic* induction.

VI – 1.4.7. The RBE emphasized the differences between particles beams and photons

In the present work, the comparison of the carcinogenic risks between the particles and photon beams is made taking into account the physical dose. If the comparison would have been done for *cobalt gray equivalent* doses (CGE = Dose * RBE), the effects produced by a given dose of particles would be compared to the photons ones produced by a higher physical doses with a magnitude equal to the RBE, and thus in a dose range even more unfavorable to the photons. In clinical situations (i.e. Carbon treatment dose = 20-30 Gy ⇔ X-treatment dose > 50 Gy), the previous conclusions should therefore be confirmed and strengthened.

VI – 1.5. Conclusion:

It often appears incomprehension of the pattern of carcinogenesis among the health professionals informed by the literature of apparent contradictory epidemiological data: referring sometimes radiation treatments as carcinogenic inducers of more or less relevance and sometimes radiations are considered as non-significant neoplasic inducers. The complex set of competing effects within the tissues and organs induces a mosaic of dose-response patterns according to the weight of each effect. According to the *malignant induction* within the tissue *vs* the *cell sterilization* capacity of the beam *vs* the *proliferative activity* of the tissue, the final risk of carcinogenesis for the same physical dose can vary noticeably. It is noteworthy that the proliferative kinetics linked to organ growth appears as a particular concern when the data refer to growing “pediatric” tissues. As remarkable achievement, the models of prediction present the intrinsic characteristics of carbon-ions as able, at some degree, to limit and even reduce the risk of second malignancy and that more notably for children. However, these characteristics are based on predictive models and are to be taken carefully. They provide however some encouraging signs, carbon-ions being called without doubts to treat in a near future an increasing number of young patients. To do so, the optimal modalities of treatment have to be determinate in terms of dose and fractionation schedule and the present prediction about hypofractionation shows it clearly as a potentially positive factor. The Japanese way of hypofractionation applied at NIRS might be at first sight the best way to counteract the carcinogenic risk when treating by carbon-ions. Carefully designed clinical trials must be undertaken to clarify these hypothesis before large scale clinical application.

VI – 1.ii. References:

[1] Sachs, R. K., Chan, M., Hlatky, L. and Hahnfeldt, P. Modeling Intercellular Interactions during Carcinogenesis. *Radiat. Res.* 2005;164: 324–331.

[2] Ron E et al. Childhood Cancer – Treatment at a Cost. Journal of the National Cancer Institute. 2006; 98(21): 1510-1511.

[3] Sachs, R.K. and Brenner, D.J. Solid tumor risks after high doses of ionizing radiation. *PNAS*. 2005;102(37):13040-45.

[4] Bettega D, Calzolari P. et al. Neoplastic transformation induced by carbon ions. GSI Report 2006-1.

[5] Wheldon, E.G., Lindsay, K.A., Wheldon, T.E. The dose-response relationship for cancer incidence in a tow-stage radiation carcinogenesis model incorporating cellular repopulation. *Int J Radiat Biol.* 2000;76:699-710.

[6] Lindsay KA, Wheldon EG, Deehan C and Wheldon TE. Radiation carcinogenesis modelling for risk of treatment-related second tumors following radiotherapy. *The British Journal of Radiology*. 2001; 74:529–536.

[7] Masao Suzuki, M., Piao, C.Q., Hall, E.J., Hei, T.K.. Cell killing and chromatid damage in primary human bronchial epithelial cells irradiated with accelerated 56Fe ions. *Radiat. Res*. 2001; 155 : 432–439.

[8] Mole, R. H. Ionizing radiation as a carcinogen: practical questions and academic pursuits The Silvanus Thompson Memorial Lecture delivered at The British Institute of Radiology on April 18, 1974. *Br. J. Radiol.* 1975; 48(567):157–169.

[9] Gray, L. H. in *Cellular Radiation Biology; A Symposium Considering Radiation Effects in the Cell and Possible Implications for Cancer Therapy, a Collection of Papers* (Williams & Wilkins, Baltimore). 1965; pp. 8–25.

[10] Dorr, W. Radiobiological models of normal tissue reactions. *Strahlenther. Onkol.* 1998; 174(3):4–7.

[11] Clarke, R. B., Anderson, E., Howell, A. & Potten, C. S. Regulation of human breast epithelial stem cells. *Cell Prolif*. 2003; 36(1): 45–58.

[12] Sacher, G. A. & Trucco, E. Theory of radiation injury and recovery in self-renewing cell populations. *Radiat. Res.* 1966; 29(2): 236–256.

[13] Halperin EC, Constine LS, Tarbell NJ, Kun LE. Pediatric radiation oncology, 1994 (2nd edn). New York: Raven Press. Chapter 19 – Section: Influence of the developmental stage of the target organ on its sensitivity to therapy.

[14] Gilbert, E. S., Stovall, M., Gospodarowicz, M., Van Leeuwen, F. E., Andersson, M., Glimelius, B., Joensuu, T., Lynch, C. F., Curtis, R. E., Holowaty, E., et al. Lung cancer after treatment for Hodgkin's disease: focus on radiation effects. *Radiat. Res.* 2003;159;161–173.

[15] Travis, L. B., Hill, D. A., Dores, G. M., Gospodarowicz, M., van Leeuwen, F. E., Holowaty, E., Glimelius, B., Andersson, M., Wiklund, T., Lynch, C. F., et al. Breast cancer following radiotherapy and chemotherapy among young women with Hodgkin disease. *JAMA.* 2003; 290(4):465–475.

[16] van Leeuwen, F. E., Klokman, W. J., Stovall, M., Dahler, E. C., van't Veer, M. B., Noordijk, E. M., Crommelin, M. A., Aleman, B. M., Broeks, A., Gospodarowicz, M., et al. Roles of radiation dose, chemotherapy, and prophylactic surgery for BRCA1 and BRCA2 mutation. *J. Natl Cancer Inst*. 2003; 95(13): 971–980.

[17] Koh, E.S., Huan Tran, T., Heydarian, M., Rainer K Sachs, R.K., Tsang, R.W., David J Brenner, D.J., Pintilie, M., Xu, T., Chung, J., Paul, N. and David C Hodgson, D.C. A comparison of mantle versus involved-field radiotherapy for Hodgkin's lymphoma: reduction in normal tissue dose and second cancer risk. *Radiation Oncology*. 2007;2:13 (15 March 2007).

[18] Brenner, D. J. & Hall, E. J. Conditions for the equivalence of continuous to pulsed low dose rate brachytherapy. *Int. J. Radiat. Oncol. Biol. Phys.* 1991; 20:181–190.

[19] Rubin P., Casarett G.W.. Clinical Radiation Pathology. Vols 1 & 2. Philadelphia: W.B. Saunders, 1968.

[20] Dorr, W. & Kummermehr, J. Accelerated repopulation of mouse tongue epithelium during fractionated irradiations or following single doses. *Radiother. Oncol.* 1990; 17(3):249–259.

[21] Haller, J.O., Slovis, T.L., Joshi, A. Pediatric Radiology, 2005 (3rd edn). Springer. Chapter 2: Understanding radiation and its effects on children.

[22] Weissman, I. Stem cells: units of development, units of regeneration, and units in evolution. Cell. 2000; 100(1):157-168.

[23] Sadetzki S., Chetrit A., Alexandra L., Stovall M., Novikov I. Risk of thyroid cancer after childhood exposure to ionizing radiation for tinea capitis. *J Clin Endocrinol Metab*. 2006;91(12):4798-4804.

[24] Dickerman J.D. The late effects of childhood cancer therapy. *Pediatrics.* 2007;119(3).

[25] Ron E., Lubin J.H., Shore R.E., Mabuchi K. et al. Thyroid cancer after exposure to external radiation: a pooled analysis of seven studies. *Radiation Research.* 1995;141(3):259-277.

[26] Imaizumi M., Usa T., Neriishi K. et al. Radiation dose-response relationships for thyroid nodules and autoimmune thyroid diseases in Hiroshima and Nagasaki atomic bomb survivors 55 – 58 years after radiation exposure. *JAMA.* 2006; 295:1011-1022.

[27] Shore R.E. Issues and epidemiological evidence regarding radiation induced thyroid cancer. *Radiat Res.* 1992;131:98-111.

[28] Fleury Y., van Melle G., Woringer V., Gaillard R.C., Portmann L. Sex-dependent variations and timing of thyroid growth during puberty. *J Clin Endocrinol Metab.* 2001;86:750-754.

[29] Ueada D. Sonographic measurement of the volume of the thyroid gland in healthy children. *Acta Paedriatr Jpn*. 1989;31(3):352-354.

[30] Cailleux A.F., Schlumberger M. Les conséquences thyroïdiennes de l'accident de Tchernobyl. *ACOMEN*. 1998 ;4(4).

[31] Neglia J.P., Robison L.L., Stovall M., Liu Y., Packer R.J., Hammond S., et al. New primary neoplasms of the central nervous system in survivors of childhood cancer: a report from the Childhood Cancer Survivor Study. *J Natl Cancer Inst*. 2006; 98:1528–1537.

[32] Chang, W. P. & Little, J. B. Delayed reproductive death as a dominant phenotype in cell clones surviving X-irradiation. *Carcinogenesis*. 1992; 13(6):923–928.

[33] Held, K.D. Radiation-induced apoptosis and its relationship to loss of clonogenic survival. *Apoptosis*. 1997; 2: 265-282.

[34] Trott, K. R., Jamali, M., Manti, L. & Teibe, A. Manifestations and mechanisms of radiation-induced genomic instability in V-79 Chinese hamster cells. *Int. J. Radiat. Biol.* 1998;74(6):787–791.

[35] Kato H, Tsujii H, Miyamoto T, et al. Results of the first prospective study of carbon ion radiotherapy for hepatocellular carcinoma with liver cirrhosis. *Int J Radiat Oncol Biol Phys*. 2004 ; 59:1468-76.

[36] Kato H, Yamada S, Yasuda S, et al. Two-fraction carbon ion radiotherapy for hepatocellular carcinoma: preliminary results of a phaseI/II clinical trial. *J Clin Oncol.* 2005;23(16S):4124.

[37] Tsujii H, Kamada T, Baba M, et al. Clinical advantages of carbon-ion radiotherapy. *New J Phys*. 2008; 10:075009(16pp).

VI – 2. Table :

Table 1:

	Cellular intrinsic radiosensitivity parameters		**Mutational radiosensitivity parameters**	
	α (per Gy)	β (per Gy)	γ (per Gy, per $10^{\wedge 6}$)	δ (per Gy, per $10^{\wedge 6}$)
15 MeV photons	0.22	0.027	25	0
C-beam 266.4 MeV/u, 13.7 keV/µm	0.25	0.040	25	0
C-beam 86.5 MeV/u, 29.5 keV/µm	0.40	0.040	48	0
C-beam 9.65 MeV/u, 72 keV/µm	1.50	0.000	290	0

Values of the cellular intrinsic and mutational radiosensitivity parameters according to experimental data (figure 1 & 2) and their standard linear-quadratic responses.
Set point N = 10^6. The set point number N refers in our model of calculation to the organ's stem cells number in its original steady-state.

I – 3. Figures :

Figure 1:

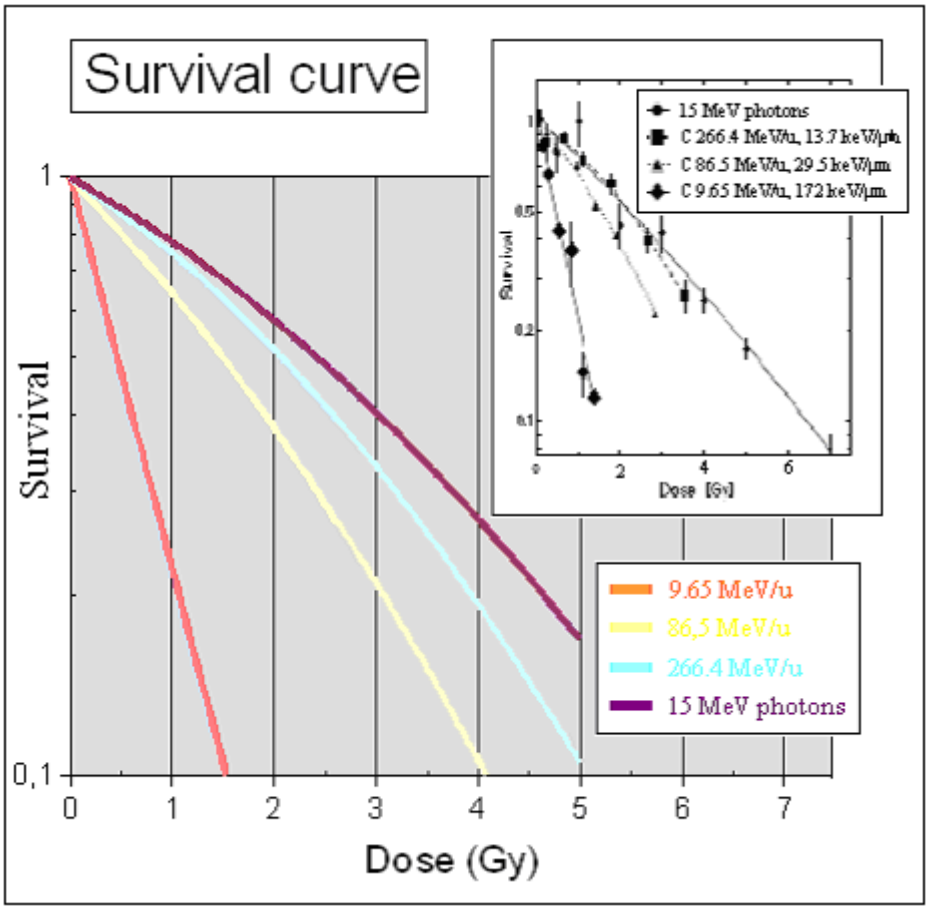

Modelization for photons and carbon ions of the survival curves as function of dose according to the linear-quadratic model with cellular intrinsic radiosensitivity parameters (α, β) tabulated in table 1.

Figure 2:

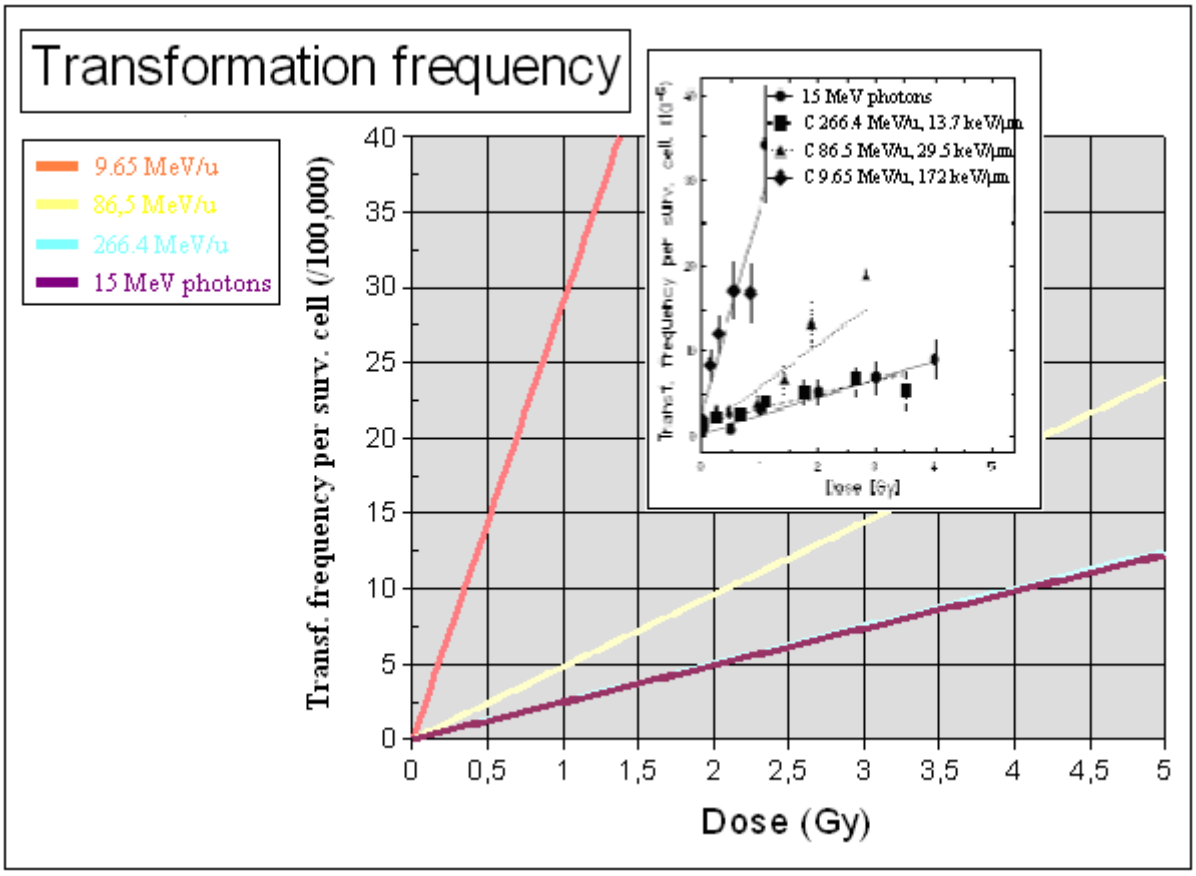

Modelization for photons and carbon ions of the transformation curves as function of dose according to the linear-quadratic model with mutational radiosensitivity parameters (γ, δ) tabulated in table 1.

Figure 3:

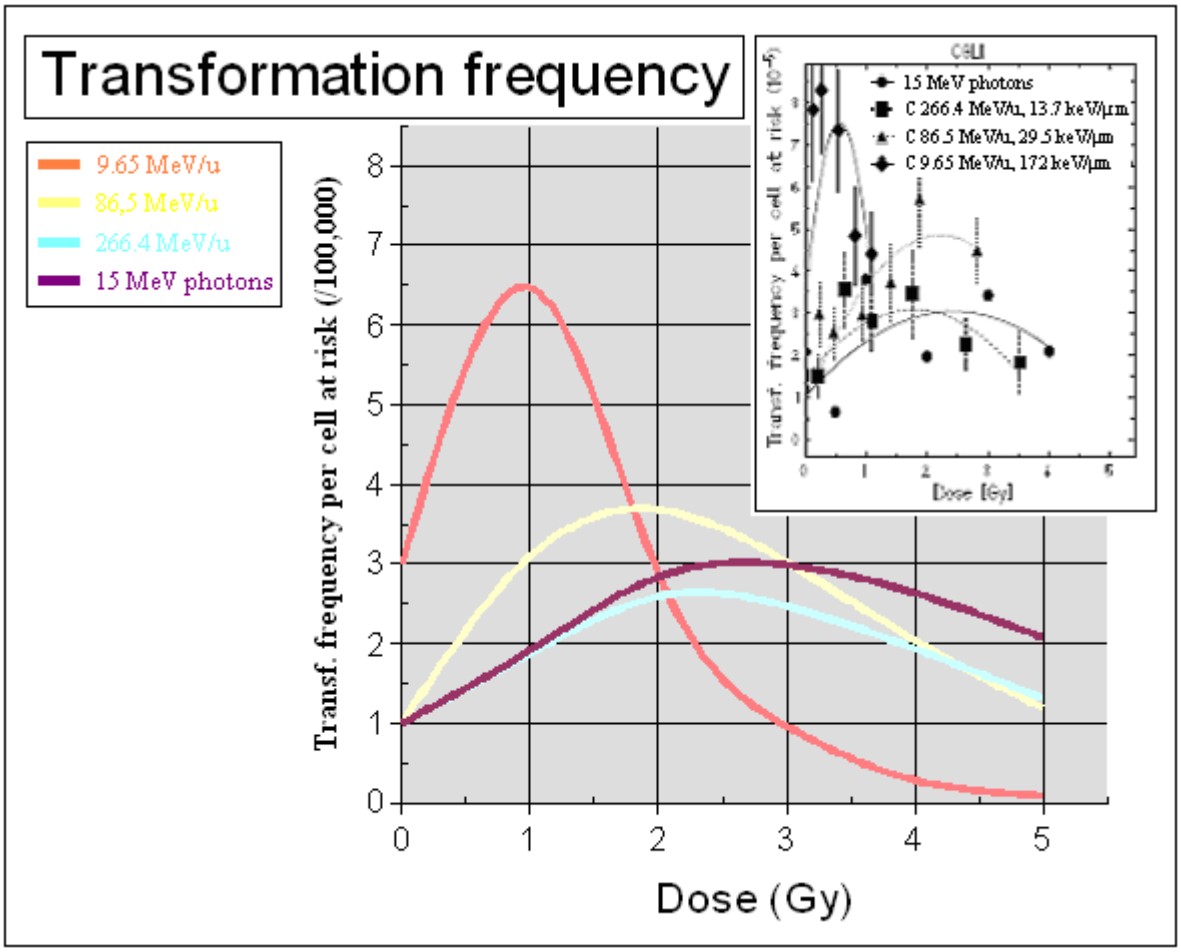

Transformation frequency for photons and carbon ions calculated according to the linear-quadratic models with cellular intrinsic and mutational radiosensitivity parameters (α, β, γ and δ) tabulated in table 1.

Figure 4:

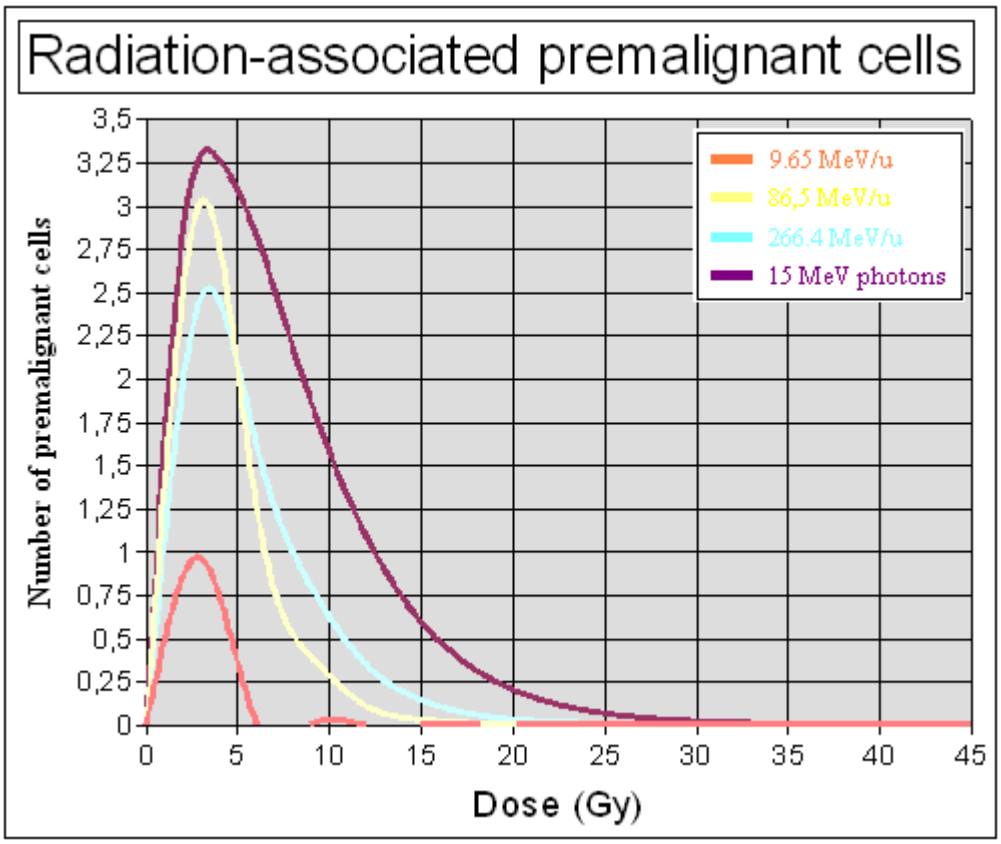

Modelization of the radiation-associated premalignant cells induced by photons and carbon ions according to the *standard model*. The radiosensitivity parameters are tabulated in table 1. The fractionation schedule applied for the C-beam is *3 Gy/fraction* (routinely used in treatment in GSI) and *2 Gy/fraction* for the photon-beam.

Figure 5:

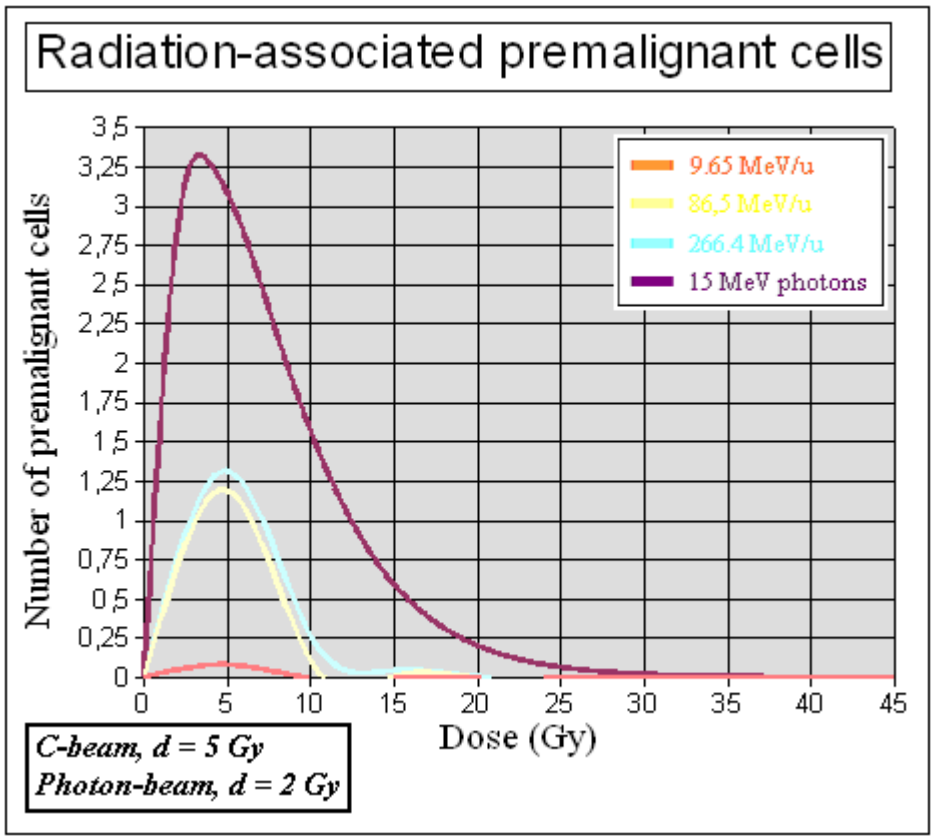

Modelization of the radiation-associated premalignant cells induced by photons and carbon ions according to the *standard model*. The radiosensitivity parameters are tabulated in table 1. The fractionation schedule applied for the C-beam is *5 Gy/fraction* and *2 Gy/fraction* for the photon-beam.

Figure 6:

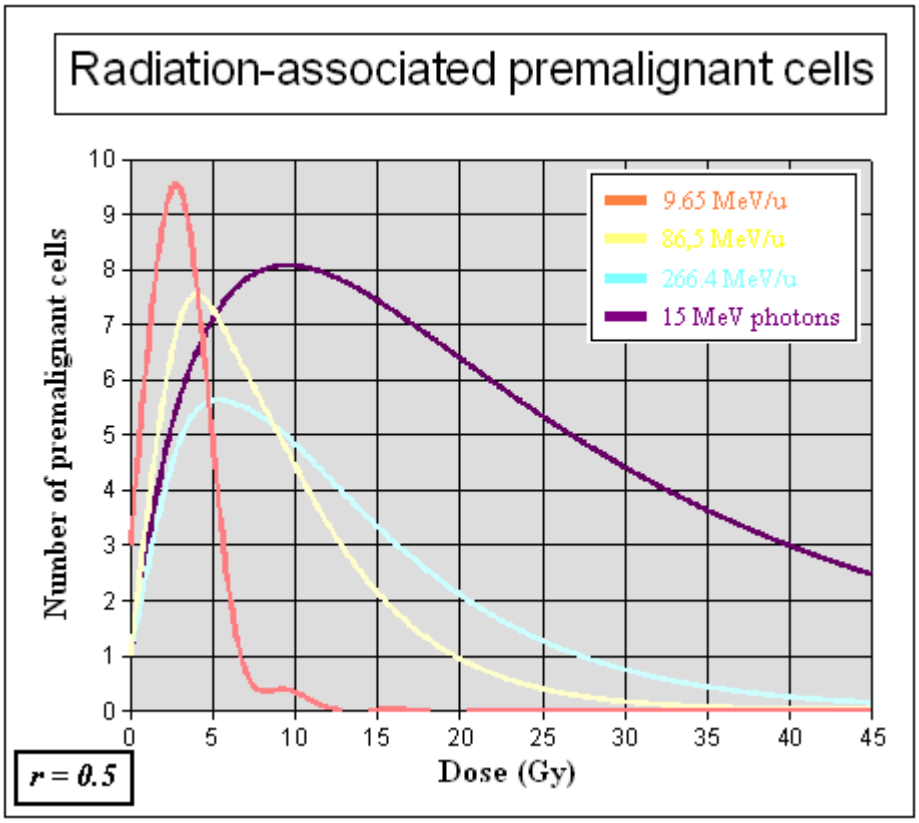

Modelization of the radiation-associated premalignant cells induced by photons and carbon ions according to the *repopulation model*. The radiosensitivity parameters are tabulated in table 1. The fractionation schedule applied for the C-beam is *3 Gy/fraction* and *2 Gy/fraction* for the photon-beam. The *repopulation rate parameter* is $\lambda \mathbf{T} = 0.4$. The *repopulation ratio* is $\boldsymbol{r} = 0.5$.

Figure 7:

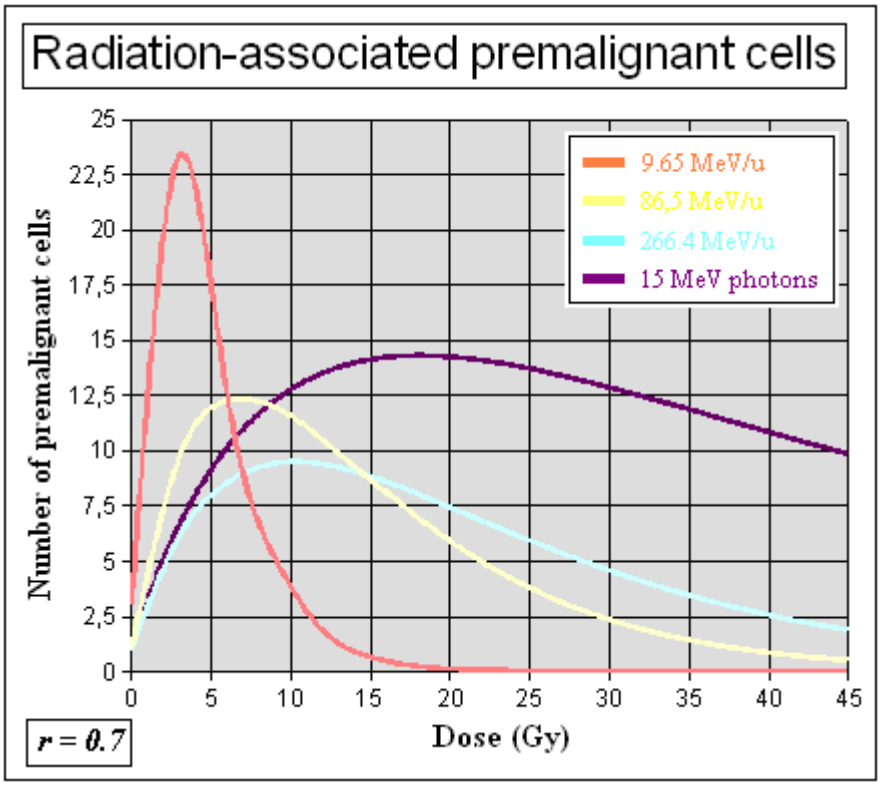

Modelization of the radiation-associated premalignant cells induced by photons and carbon ions according to the *repopulation model*. The radiosensitivity parameters are tabulated in table 1. The fractionation schedule applied for the C-beam is *3 Gy/fraction* and *2 Gy/fraction* for the photon-beam. The *repopulation rate parameter* is $\lambda \mathbf{T} = 0.4$. The *repopulation ratio* is $\boldsymbol{r} = 0.7$.

Figure 8:

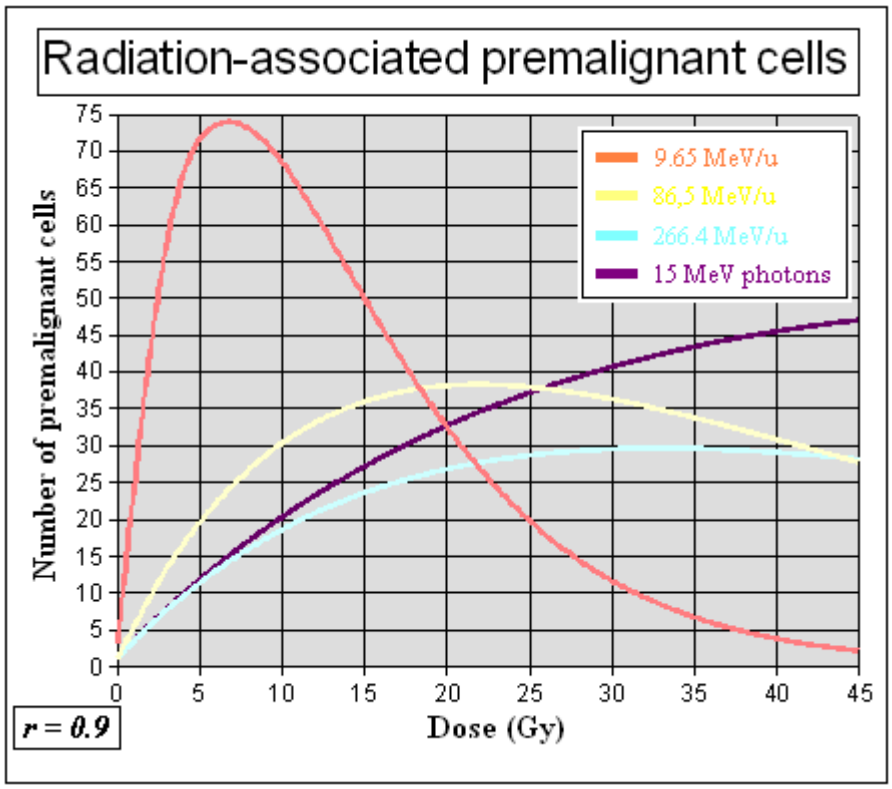

Modelization of the radiation-associated premalignant cells induced by photons and carbon ions according to the *repopulation model*. The radiosensitivity parameters are tabulated in table 1. The fractionation schedule applied for the C-beam is *3 Gy/fraction* and *2 Gy/fraction* for the photon-beam. The *repopulation rate parameter* is $\lambda T = 0.4$. The *repopulation ratio* is $r = 0.9$.

Figure 9:

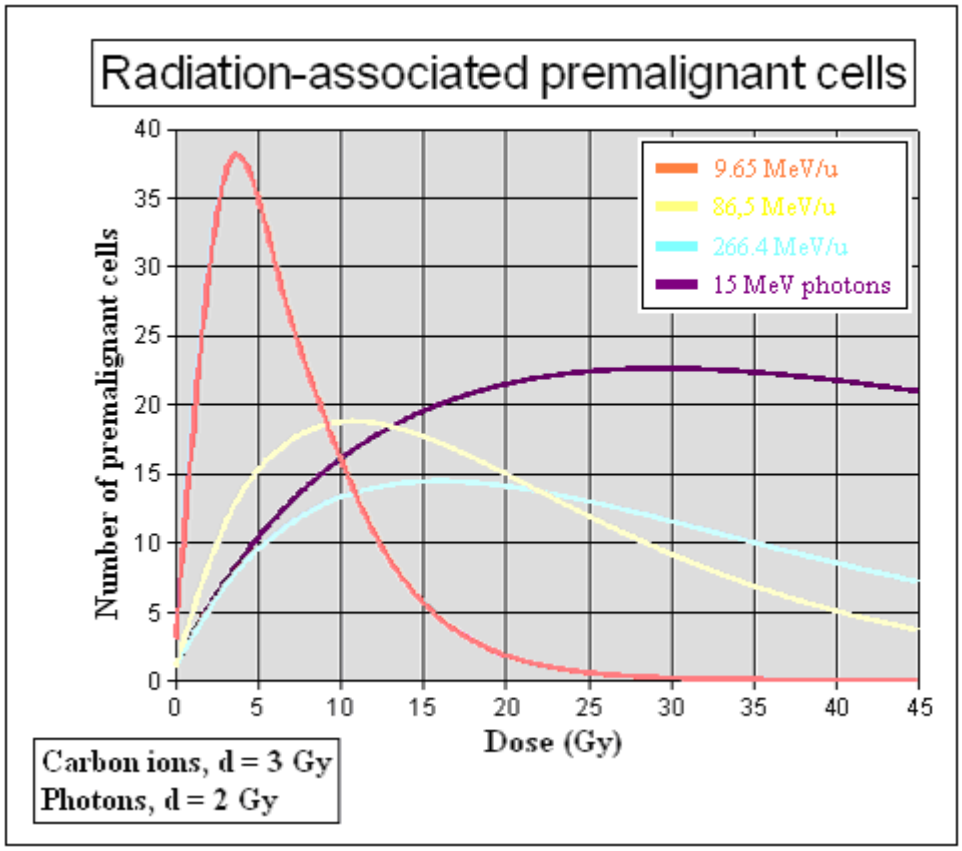

Modelization of the radiation-associated premalignant cells induced by photons and carbon ions according to the *repopulation model*. The radiosensitivity parameters are tabulated in table 1. The fractionation schedule applied for the C-beam is *3 Gy/fraction* and *2 Gy/fraction* for the photon-beam. The *repopulation rate parameter* is $\lambda \mathbf{T} = 0.4$. The *repopulation ratio* is $\boldsymbol{r} = 0.8$.

Figure 10:

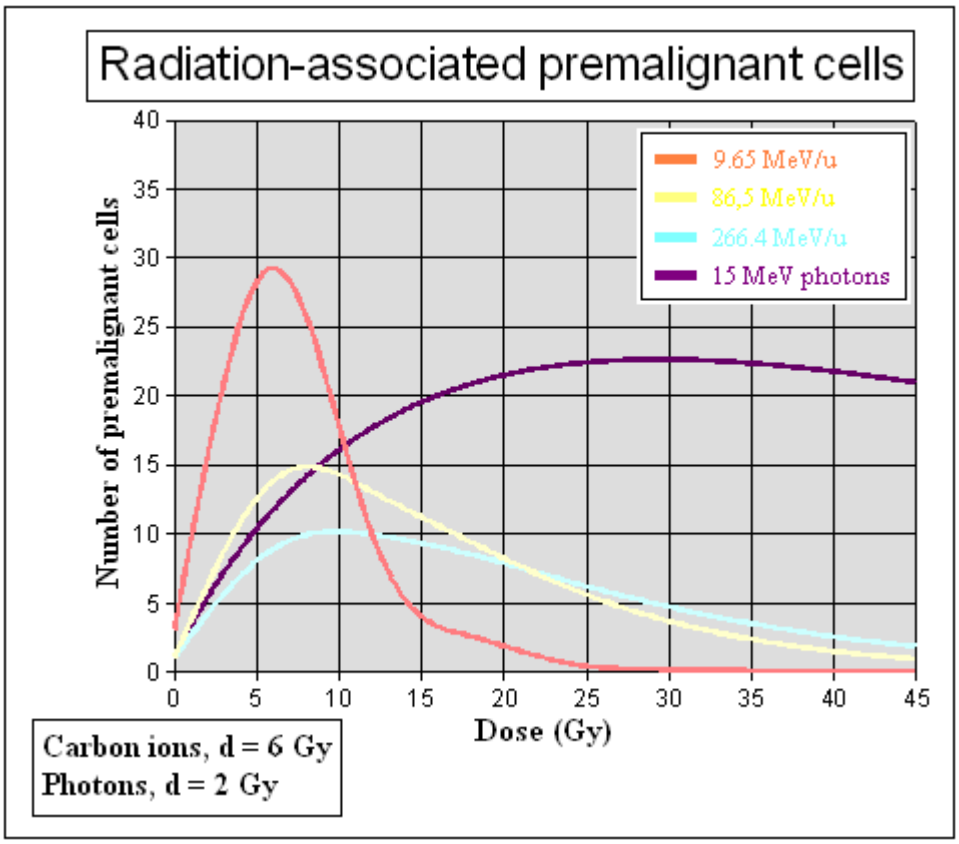

Modelization of the radiation-associated premalignant cells induced by photons and carbon ions according to the *repopulation model*. The radiosensitivity parameters are tabulated in table 1. The fractionation schedule applied for the C-beam is *6 Gy/fraction* and *2 Gy/fraction* for the photon-beam. The *repopulation rate parameter* is $\lambda \mathbf{T} = 0.4$. The *repopulation ratio* is $\boldsymbol{r} = 0.8$.

Figure 11:

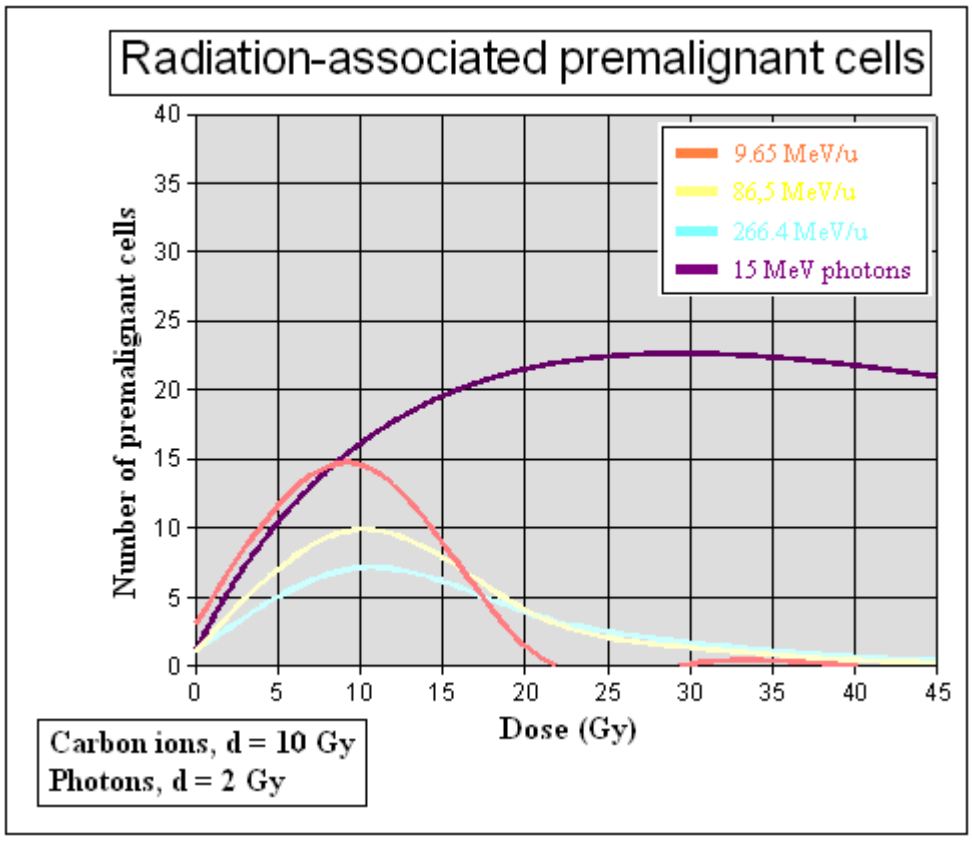

Modelization of the radiation-associated premalignant cells induced by photons and carbon ions according to the *repopulation model*. The radiosensitivity parameters are tabulated in table 1. The fractionation schedule applied for the C-beam is *10 Gy/fraction* and *2 Gy/fraction* for the photon-beam. The *repopulation rate parameter* is $\lambda \mathbf{T} = 0.4$. The *repopulation ratio* is $\boldsymbol{r} = 0.8$.

VII - Conclusion

L'étude de multiples situations anatomo-pathologiques en thérapie protons ne dégage pas d'incidences balistiques originales et particulières à la gantry. D'un strict point de vue dosimétrique, rien ne différentie l'usage d'une gantry de celui du design d'une salle à trois faisceaux horizontal-vertical-oblique. La typologie balistique des plans de traitement révèle uniquement le recours abondant aux faisceaux obliques (obliquité d'environ 50° d'inclinaison par rapport à l'axe vertical). La gantry ne crée pas de meilleure dosimétrie mais permet l'avantage (entre *autres*) du gain de temps dans le traitement, des modalités pratiques d'un positionnement unique du patient. De plus le traitement sous anesthésie générale de l'enfant oblige à son utilisation.

Concernant les caractéristiques intrinsèques du faisceau de protons, nombre de publications font état de leur faible diffusion latérale et distale et de l'avantage balistique décisif qui en découle. La réduction des volumes d'isodoses inhérente à l'irradiation proton induit une diminution des risques de complications post-radiques aiguës, chroniques et de carcinogénèse lorsque ces risques sont comparés aux techniques d'irradiation photons. Cependant l'action biologique du rayonnement proton (EBR ~ 1,1) est assez proche de celle des photons. Leurs paramètres de radiosensibilité intrinsèque et de radiosensibilité mutationnelle impliquent, pour un même dépôt de dose qu'en photons, les mêmes effets chroniques post-radiatifs ou néoplasiques. Un plan de traitement en protons imposera donc malgré ses caractéristiques balistiques avantageuses certains choix dosimétriques difficiles, résultat obligé d'un compromis entre risque chronique et risque carcinogène.

La complexité des modèles biologiques & physiologiques chez l'enfant et l'adulte jeune est telle que le compromis d'irradiation voulu par certains professionnels de santé en thérapie proton, à savoir pour un traitement un nombre total de 4-5 incidences d'irradiation, n'aboutira pas nécessairement aux effets escomptés. Le but de ce compromis est en effet (par approche simplificatrice) de ne pas trop diminuer le nombre de faisceaux, ce qui augmenterait les volumes d'isodoses intermédiaires et le risque de lésions et de complications chroniques ; de ne pas trop multiplier le nombre de faisceaux, ce qui augmenterait les volumes des basses isodoses et le risque néoplasique. Or le modèle se révèle beaucoup plus complexe et les liens doses-effets plus fluctuants, ce qui appellerait à un principe balistique moins rigide. Les effets de chaque niveau de dose sur les organes et les tissus sains environnants varient selon un comportement âge-, tissus-, organe- dépendant. La réponse carcinogène d'un organe à une même dose peut apparaître totalement contradictoire, variant en fait parallèlement à la cinétique de repopulation cellulaire en jeu à l'intérieur de l'organe irradié (plus la dynamique de prolifération est importante, et plus le risque est élevé et la réponse à la dose linéaire).

Chez l'enfant, la croissance asynchrone des différents tissues peut faire que dans un même volume irradié différents organes ne sont pas également sensibles ou pas au même moment. De plus leur sensibilité au risque carcinogène peut se déplacer dans l'échelle des doses. Ainsi, dans ces cas là, il peut apparaître très difficile d'obtenir un compromis qui réduise globalement le risque carcinogène.
Autre situation, si l'ensemble des tissus sains irradiés est en période d'activité lente (cela se traduit localement par l'absence temporaire de maturation), la multiplication des faisceaux au nombre de 4-5 est-elle le meilleur compromis vis à vis de l'impact réel des basses isodoses *vs* les isodoses intermédiaires ? La question reste entière.
En définitif si un compromis doit être trouvé, il variera selon la dose de prescription, la localisation tumorale et l'âge du patient.

L’utilisation de la précision millimétrique des protons ne fera pleinement sens que dans le cadre d’une connaissance approfondie des variations de sensibilité des tissus au cours du développement et de leur prise en compte dans les protocoles d’irradiation pédiatriques. La procédure thérapeutique devra ainsi définir, au delà d’une liste d’organes à risque et des seuils de doses limites (par niveaux de risque), les niveaux d’isodoses les plus à risque (néoplasie radio-induite) selon l’âge du patient pour l’ensemble des tissus de la sphère d’irradiation.

Bien entendu, l’existence de tels protocoles pédiatriques ne sera pas la panacée car les compromis et choix s’imposeront nécessairement. De ce point de vue, les ions carbone pourraient cependant offrir un certain intérêt. En effet les simulations réalisées dans ce travail ont permis de faire apparaître un effet qui serait particulier aux ions carbone, à savoir celui de la stérilisation cellulaire des cellules pré-malignes, à l’origine de la carcinogenèse radio-induite. En outre, cet effet se maintiendrait malgré tout accroissement de la cinétique de repopulation cellulaire dans les tissus et organes. Ceci permettrait (si cela se vérifiait) de diminuer drastiquement à dose équivalente le risque néoplasique chez l’enfant après irradiation par ions carbone *vs* les techniques photons et protons (hors avantage balistique des ions carbone). L’hypofractionnement semblerait accentuer encore plus cet avantage thérapeutique des ions carbone.
Concernant en outre les lésions chroniques, l’expérience japonaise rapporte chez l’adolescent un rapport contrôle tumoral – tolérance du traitement particulièrement bon. De plus, en cas de programme d’hypofractionnement leurs conclusions révèlent des niveaux de complication post-radique tout à fait *tolérables*.
Ainsi, si cet avantage des ions carbone se vérifie chez l’enfant et l’adulte jeune tant au niveau des complications chroniques que de la carcinogénèse radio-induite, l’on peut penser que les ions carbone seront une indication thérapeutique au traitement des cancers de l’enfant tant pour les tumeurs radiorésistantes que radiosensibles. Ils permettraient singulièrement une chute de la récidive tumorale, problème essentiel lors du traitement de l’enfant par rayonnements ionisants.

Postscript

Cette dernière partie est un ajout en forme de clin d'œil. Elle permet de sortir de l'aspect formel d'une présentation scientifique et prendre relâche. Il s'agit ici de dire les réponses ou l'ensemble des *desiderata* que je souhaiterais réglés dans un futur plus ou moins proche (si réellement ça se révèle être possible).

Il faudrait un protocole d'irradiation incluant une procédure thérapeutique décrivant, selon le type de particule[18] ou de rayonnement, selon l'âge du patient[19] au cours du traitement , selon le sexe du patient[20], selon la localisation tumorale et les organes & structures à risques environnants, s'il y a lieu selon les déficiences génétiques du patient, les effets volumes-isodoses *versus* complications aiguës, chroniques et carcinogéniques. Le protocole devrait inclure une procédure claire précisant un ordre d'importance pondérant chacun de ces risques de sorte à établir le meilleur des compromis parmi les nombreux choix possibles.
Ou plus *simple* encore… un protocole standardisé imposant à peu de choses près un design dosimétrique (ou un certain nombre d'*incidences possibles fortement conseillées*) selon la pathologie considérée.

Pour cela il faudrait entre *autres* :

- Connaître l'impact exact de chaque type d'irradiation sur la maturation des tissus & organes et leur radioprotection. Pour exemple, quel est l'effet du rayonnement carbone sur le processus de myélinogenèse – synaptogenèse ? Change-t-il la dynamique d'épaississement – amincissement de l'épaisseur corticale chez l'enfant (dynamique en relation avec le QI) ? Les protons sont-ils plus indiqués que les carbones dans le souci de préservation du processus de développement cérébral *postnatal* ? Les carbones permettent-ils, par leur meilleur design dosimétrique, une meilleure radioprotection de ces structures en maturation ?
- Une clarification des connaissances physiologiques et anatomiques en pédiatrie. S'il était possible d'obtenir une *cartographie* précise et exploitable des aires anatomiques en maturation & développement de telle sorte à éviter toutes ces zones de croissance sensibles à la dysplasie radique de même qu'à l'occurrence néoplasique radio-induite (phénomène d'*induction/prolifération* des cellules mutées). Et ceci, bien sûr en fonction de l'âge…

S'il était possible de construire un logiciel permettant de calculer pour chacun des plans de traitement dessinés le risque carcinogénique (selon le type de particule utilisée).
Pour cela il faudrait établir un ensemble assez conséquent de données radiobiologiques, fonction des niveaux d'énergie des particules et du type de tissus traversés. Ces données devraient inclure les paramètres biologiques de radiosensibilité intrinsèque[21] (courbe de survie) et de radiosensibilité mutationnelle[22] (malignité radio-induite) pour un large panel de cellules représentatives de la zone anatomique irradiée. Ce logiciel incrémenterait ces données radiobiologiques selon les modèles mathématiques & biologiques existants pour donner des valeurs de risque relatif ou même absolu.

[18] Energies spécifiées.
[19] Petite enfance, enfance, puberté, adolescence, adulte jeune, adulte.
[20] Exemple des cancers de la thyroïde où l'incidence de la carcinogénèse est plus grande est plus grande chez les filles après menstruation que chez les garçons.
[21] Paramètres $\{\alpha,\beta\}$ de l'article 3.
[22] Paramètres $\{\gamma,\delta\}$ de l'article 3.

Pour donner plus spécifiquement des valeurs du risque selon l'âge il faudrait établir précisément les tables de valeurs des paramètres de cinétique de développement & repopulation[23] pour l'ensemble des organes irradiés. Ils pourraient être donnés par tranche d'âge et tissus & organes. De plus il serait nécessaire de définir et d'obtenir pour chaque patient des critères informatifs de l'état de maturation atteint par le patient à traiter.

Bien entendu tout ceci demanderait un travail d'investigation considérable mais toute réponse précise et sérieuse d'un risque quantifié (de manière absolue ou relatif) de complication aiguë, de lésion chronique ou de néoplasie radio-induite ne pourra se faire que sur une base de données biologiques, physiologiques, anatomiques et épidémiologiques fiable et importante (quantitativement). La recherche fondamentale sur l'ensemble de ces sujets, de même qu'un travail de recoupement de la bibliographie se révèlent indispensables.

[23] Paramètres $\{\lambda \,\&\, r\}$ de l'article 3.

Références :

[1] http://etoile.univ-lyon1.fr
[2] http://www.gsi.de
[3] http://www.tera.it/ise.cgi

[4] A. Mazal, S. Delacroix, J. Arianer, F. Clapier, C. Nauraye, M. Louis, J. C. Rosenwald, A. Bridier, J. L. Habrand. La protonthérapie : bases physiques et technologiques. *Bull. Cancer. Radiother*. 1996 ; 83 : 230-246.

[5] Elizabeth R. Sowell, Paul M. Thompson, Kevin D. Tessner, and Arthur W. Toga. Mapping continued brain growth and gray matter density reduction in dorsal frontal cortex: inverse relationships during postadolescent brain maturation. *The Journal of Neuroscience*. 2001; *21*(22):8819–8829.

[6] Halperin EC, Constine LS, Tarbell NJ, Kun LE. Pediatric radiation oncology, 1994 (2nd edn). New York: Raven Press. Chapter 19 – Section: Influence of the developmental stage of the target organ on its sensitivity to therapy.

[7] Jannoun, L., Bloom, H.J.. Long-term psychological effects in children treated for intracranial tumors. *Int J Radiat Oncol Biol Phys.* 1990;18(4):747-53.

[8] Shaw P., Greenstein D., Lerch J., Clasen L., Lenroot R., Gogtay N., Evans A., Rapoport J. and GieddJ. Intellectual ability and cortical development in children and adolescents. *Nature*. 2006;440 : 676-679.

[9] Durston, S., Tottenham, N.T., Thomas, K.M., Davidson, M.C., Eigsti, I.M., Yang, Y., Ulug, A.M., Casey, B.J. Differential Patterns of Striatal Activation in Young Children with and without ADHD. *BIOL PSYCHIATRY*. 2003;53:871–878.

[10] Berquin, Patrick. Le trouble déficitaire d'attention avec hyperactivité: aspects neurofonctionnels. *Pediatrica*. 2005 ;Vol. 16 No. 6.

[11] Copeland, D.R., deMoor, C., Moore III, B.D. and Ater, J.L. Neurocognitive Development of Children After a Cerebellar Tumor in Infancy: A Longitudinal Study. *J Clin Oncol*. 1999;17:3476-3486.

[12] Schatz J, Hale S, Myerson J: Cerebellar contribution to linguistic processing efficiency revealed by focal damage. *J Int Neuropsychol Soc*. 1998; 4:491-501.

[13] Loganovsky KN, Loganovskaja TK. At Issue: Schizophrenia spectrum disorders in persons exposed to ionizing radiation as a result of the Chernobyl accident. Schizophrenia Bull. 2000;26(4):751–773.

[14] DurstonD., Tottenham N.T., Thomas K.M., Davidson M.C., Eigsti I-M, Yang Y., Ulug A.M., and Casey B.J. Differential Patterns of Striatal Activation in Young Children with and without ADHD. Biol Psychiatry 2003;53:871–878.

MEMORANDUM

***Quatre configurations de salle* :**

- *salle A*: traitement couché et irradiation par un faisceau horizontal fixe;
- *salle B* : salle 1 + faisceau vertical;
- *salle C* : salle 1 + traitement assis;
- *salle D* : traitement couché et irradiation par un bras isocentrique.

Définition des *index de conformation* :

Index de couverture RTOG : **Coverage-RTOG = Imin/IR**	Imin : Isodose minimale entourant la tumeur IR : Isodose de référence
Index d'homogénéité RTOG : **HI = Imax/IR**	Imax : Isodose maximale dans la tumeur IR : Isodose de référence
Index de conformation RTOG : **CI RTOG = VIR/VT**	VIR : Volume de l'isodose de référence VT : Volume tumoral
Facteur volumique de Couverture Lésionnel (FCV) : **TC = VTIR/VT**	VTIR : Volume tumoral couvert par l'isodose de référence VT : Volume tumoral
Facteur de conformation Tissus Sains : **CI = VTIR/VIR**	VTIR : Volume tumoral couvert par l'isodose de référence VIR : Volume de l'isodose de référence